Acta morphologica et anthropologica 26 (1–2)

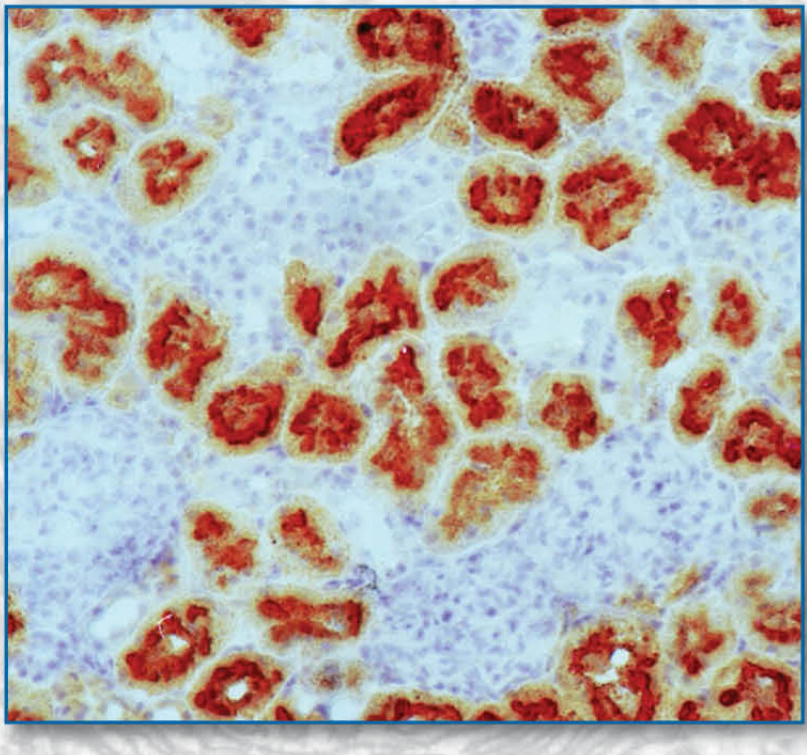

Prof. Marin Drinov Publishing House
of Bulgarian Academy of Sciences

Acta morphologica et anthropologica

is the continuation of Acta cytobiologica et morphologica

Editor-in-Chief: Prof. Nina Atanassova
e-mail: ninaatanassova@yahoo.com; ninaatanassova@bas.bg
+359 2 979 2342
Deputy Editor-in-Chief: Prof. Dimitar Kadiysky
e-mail: dkadiysky@yahoo.com; dimkad@bas.bg
+359 2 979 2311
Executive Secretary: Assoc. Prof. Y. Gluhcheva
e-mail: ygluhcheva@hotmail.com
+359 2 979 2344

Editorial Correspondence
Institute of Experimental Morphology, Pathology and Anthropology with Museum
Bulgarian Academy of Sciences
Acta morphologica et anthropologica
Acad. Georgi Bonchev Str., Bl. 25
1113 Sofia, Bulgaria
E-mail: ygluhcheva@hotmail.com; iempam@bas.bg
Tel.: +359 2 979 2311

Издаването на настоящия том 26, книжки 1 и 2 е осъществено с финансовата подкрепа на Фонд „Научни изследвания“

Настоящият том се посвещава на 150 годишнината от създаването на БАН

Prof. Marin Drinov Publishing House of Bulgarian Academy of Sciences
Bulgaria, 1113 Sofia, Acad. Georgi Bonchev Str., Bl. 6

Graphic designer Veronika Tomcheva
Format 70×100/16 Printed sheets 8.25

Printing Office of Prof. Marin Drinov Publishing House of Bulgarian Academy of Sciences
Bulgaria, 1113 Sofia, Acad. Georgi Bonchev Str., Bl. 5

ISSN 1311-8773 (print)
ISSN 2535-0811 (online)

Acta morphologica et anthropologica

26
(1-2)

26 (1-2) ● Sofia ● 2019
Institute of Experimental Morphology, Pathology and Anthropology with Museum
Bulgarian Anatomical Society

Contents

Morphology

Anthropology and Anatomy

Review Articles

Institute of Experimental Morphology, Pathology and Anthropology with Museum
Bulgarian Anatomical Society

Acta morphologica et anthropologica, 26 (1-2)
Sofia ● 2019

Morphology

Practical Use of Immunochistochemical Investigation in Diagnosis, Differential Diagnosis, Grading and Staging of Urothelial Carcinomas of Urinary Bladder

Veselin Belovezhdov[1], Maria Koleva[1], Dorian Dikov[1,2]*

[1] Department of General and Clinical Pathology, Medical University - Plovdiv, Plovdiv, Bulgaria
[2] Service d'Anatomie et Cytologie Pathologiques, Grand Hospital de l'Est Francilien Jossigny, France

***** Corresponding author e-mail: vesbel@abv.bg

Abstract

Urothelial carcinomas are the most common type of bladder tumors. They are the subject of a number of invasive and surgical interventions with a diagnostic and / or therapeutic purpose. In most cases their diagnosis is not a problem for the pathologist but there are also those when histological judgment is difficult and an immunohistochemical investigation is required. It may be useful in determining tumors with low differentiation, in situ carcinomas, in differential diagnosis, and assessment of invasion in order to correct staging and grading of the neoplasm.

Key words: urothelial carcinoma, urinary bladder, immunohistochemical investigation.

Introduction

Urothelial tumors represent 80% of bladder tumors. The most common malignances among them are carcinomas [2]. Diagnosis of urothelial carcinomas (UC) does not require immunohistochemical (IHC) investigation. But in everyday practice there are cases that demand such investigation and pathologist needs to be able to interpret the result accurately in order to make the correct diagnosis.

In the past years IHC become a routine method in the pathology units. It is used in differential diagnosis of many tumours. In other cases histopathological diagnoses are considered as incomplete if there is no phenotypic assessment of the morphological type of the neoplasm. This is important for lung and breast cancers in relation with

their subsequent therapy. Such investigations also take place in the diagnosis of UC. For these reasons, as well as the lack of sufficient information in the literature, the aim of this article is to highlight the possibilities of IHC in diagnosis of urothelial cancer of bladder.

Materials and Methods

Biopsy cases were selected from the daily practice associated with the routine diagnostics of bladder materials obtained from the urology units of University Hospital "St. George", Plovdiv and Grand Hospital de l'Est Francilien Jossigny, France.

Immunohistochemistry for cytokeratin (CK) 7, CK 20, Prostate Specific Antigen (PSA), p504S (Alpha-methylacyl-CoA racemase – AMACR), CDX2, p53 and Ki-67 was performed on 4–5μm formalin-fixed, paraffin-embedded tissue sections that were cut from the TMAs. The immunostainings are made in DAKO "AutostainerLink 48" under routine procedure.

Results and Discussion

Modern European criteria and protocols [1, 2, 5], as well as our own experience, take place in the development of the current study which is dedicated to the use of IHC in the diagnostics of the UC.

The use of IHC for diagnosis, of urothelial bladder carcinomas is required in the following cases [2, 6]:

I. For diagnosis and differential diagnosis (DD) of UC.

II. For grading and staging of invasive UC.

III. For diagnosis and DD of noninvasive urothelial tumors with flat appearance.

I. The use of IHC in diagnosis and DD of UC of the bladder.

The normal immune phenotype of the urothelium as well as the tumor cells of the UC is GATA3 (+), p63 (+), CK 7 (+), (**Fig. 1**), CK AE1/AE3 (+), CK 20 (+/-)p (**Fig. 2**) independently of the stage and grading of carcinoma.

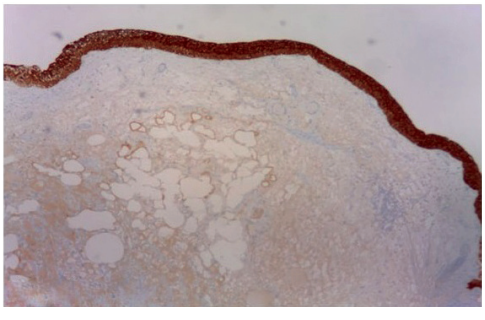

Fig. 1. CK 7, normal mucose. × 50

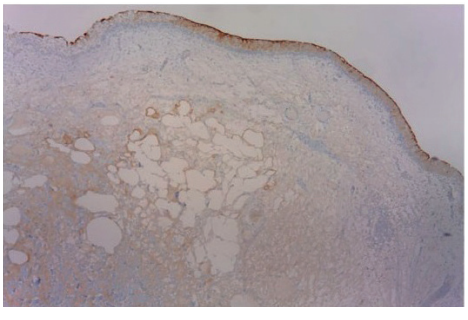

Fig. 2. CK 20, normal mucose. × 50

Commonly use of IHC may be necessary in:

1. DD of urothelial bladder carcinoma with prostate carcinoma:

a) in the cases of endovesical papillary type tumor located near the bladder neck in a patient treated from prostate adenocarcinoma;

b) in poorly differentiated adenocarcinoma of the prostate gland, spreading into the bladder neck. In these cases it should be considered that prostate adenocarcinoma is PSA (+), p504S (AMACR) (+) (**Figs. 3–5**), GATA3 (-), CK 7 (-).

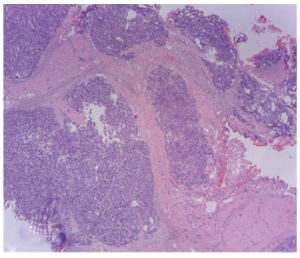

Fig. 3. Prostate adenocarcinoma, Hematoxylin-Eosin. × 50

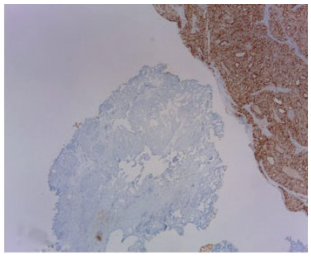

Fig. 4. Prostate adenocarcinoma, p504 S (AMACR). × 50

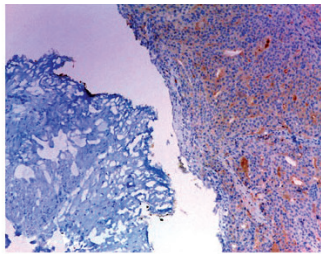

Fig. 5. Prostate adenocarcinoma, PSA. × 100

2. In bladder tumor presented by spindle cells, where the diagnostic problem is whether it is a sarcomatoid carcinoma, leiomyosarcoma or myofibroblast proliferation. Sarcomatoid carcinoma expresses the epithelial markers CK AE1/AE3, CK7, EMA, while leiomyosarcoma and myofibroblast tumors are negative and have positive expression for muscle and connective tissue markers – actin, caldesmon, desmin.

3. Bladder tumor with glandular architecture; in these cases, the dilemma is whether it is a UC with glandular structure or an adenocarcinoma – a primary bladder adenocarcinoma or secondary adenocarcinoma, originating from the adjacent organs (prostate, colon, endometrium). Primary bladder adenocarcinoma is most often of intestinal type and is CK 20 (+), CEA (+) but is CDX2 (-) in contrast to colorectal carcinoma; the latter have positive expression of CK20 (+) and CDX2 (+) (**Figs. 6–8**); beta-catenin is also a useful marker in these cases, it shows a positive nuclear staining in the colorectal adenocarcinoma and also a positive but membrane staining in the primary bladder adenocarcinoma;

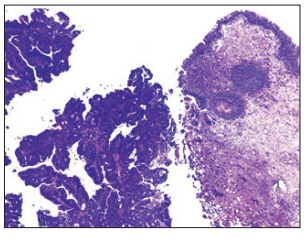

Fig. 6. Colorectal adenocarcinoma, Hematoxylin-Eosin. × 50,

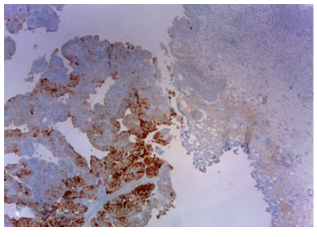

Fig. 7. Colorectal adenocarcinoma, CK 20. × 50

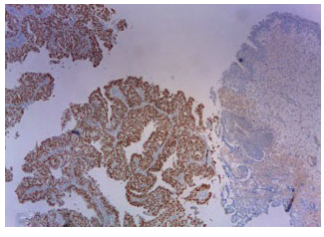

Fig. 8. Colorectal adenocarcinoma, CDX-2. × 50

4. Undifferentiated bladder tumor; in these cases, a melanoma must be excluded because is S100 pr. (+), HMB 45 (+) and Melan-A (+) and secondly rhabdomyosarcoma that express myogenin (+) and desmin (+); UC is negative for the listed markers but have possitive expression for GATA3, CK 7 and p63.

II. The use of IHC in staging and grading of bladder invasive UC.

1. Staging.

The common between clinical and pathological assessment of bladder UC is that they are divided into non-invasive and invasive.

The difference is that for urologists, the invasiveness criteria are determined by tumor muscle infiltration (from pT2 to pT4), while for the pathologist the invasiveness of urothelial tumor begins when the basal membrane and mucosal chorion is infiltrated (from pT1 to pT4) [6]. This difference has its therapeutic logic and explanation. The unfavorable prognosis of invasive UC requires to be treated with cysto-prostatectomy whenever it's possible, with or without chemotherapy (adjuvant or non-adjuvant).

In other words, the visualization of a muscle layer in biopsy specimen or in transurethral resection (TUR) of bladder cancer is a key moment responsible for taking a strategic therapeutic decision.

The presence of an initial tumor infiltration in lamina propria in a UC (pT1) can be visualized using cytokeratins (CK AE1/AE3 or CK7). Isolated single or small groups of cytokeratin-positive cells are observed in superficial lamina propria, which is particularly important for TUR material [1].

In pathology practice, the visualization of a muscle layer is not always an easy task. Especially when there are artefacts caused by electrocoagulation or because the TUR material is cross-cut. In these cases the use of IHC is appropriate. Smooth-muscle actin (SMA) is a useful marker. It is positive in the bladder musculature (superficial and deep) and helps the assessment of the tumor infiltration in it. To proof the latter is possible if there are cytokeratin positive (CK AE1 / AE3) elements, indicating their epithelial origin. The ideal option is to use more specific muscle marker – smoothelin, which has positive expression in the muscular fibres of detrusor (muscularis propria) and is negative in the fine muscle bundles – muscularis mucosae of lamina propria [4]. Unfortunately this variant is expensive and difficult to apply.

Sometimes, when there is a suspicion for tumor vascular invasion, endothelium markers may also be used. The most commonly used markers are D2-40 (podoplanin) which have a positive expression of lymph capillary endothelium or CD 31, which is expressed in endothelial cells of blood vessels [2]; the latter are well-stained by CD 34, as our experience shows.

2. Grading.

In cases where the morphology of a UC is not typical and the pathologist hesitates whether the UC is of low or high malignancy, it is recommended to use Ki 67 – a proliferative marker that is positive in over 20% and is positive in the upper cell lines in a high grade lesions.

III. The use of IHC in diagnosis and DD of noninvasive bladder UC with flat appearance.

In these cases, it is mostly about urothelial carcinoma in situ (UCIS) (pTis), which is defined as a flat, non-papillary urothelial proliferation with different thickness, that is made up by cytologically malignant cells [2]. Histological criteria for diagnosis of UCIS (architectural disorganization of tumor urothelium, cellular atypism, mitosis) are sometimes insufficient, and diagnosis is not easy, especially when there is a differential diagnosis with a wide range of bladder mucosal lesions that are characterized by reactive urothelial atypia; or in small-size materials; cross-cut materials or in electrocoagulated tissues.

DD of UCIS with other flat mucosal lesions [2, 3, 5] :

– *urothelial proliferation with uncertain malignant potential;*
– *urothelial dysplasia;*
– *reactive urothelial atypia (inflammatory, after treatment);*
– *urothelial hyperplasia without dysplasia.*

In these cases the pathologist use IHC. It is recommended to be done a panel of several markers performed on consecutive serial histological sections [2]:

1. Ki 67 (proliferative marker) – two major differences in the proliferative index of the UC are observed, as opposed to benign flat lesions - there is nuclear staining in over 20% of tumor cells throughout the whole thickness of the mucosal proliferation; in reactive urothelial atypia IHC signal for Ki 67 is with basal localization (**Fig. 9, Fig. 10**).

2. CK 20 – in normal and non-tumor urothelial mucosa, the expression of this marker is restricted to the superficial layer of cells, whereas in the UCIS, the expression is of the so-called aberrant type, i.e. in the entire thickness of the epithelium (**Fig. 11**). In reactive urothelial atypia, the IHC signal is localized only in the superficial umbrella cells.

3. p53 – it is observed a diffuse expression of the marker through the entire thickness of proliferation and in all tumor cells (60% of the UCIS cases) (**Fig. 12**).

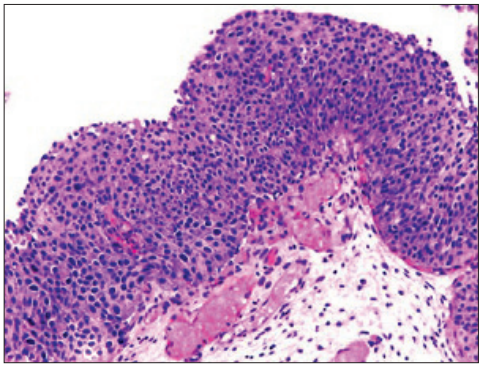

Fig. 9. Carcinoma in situ, Hematoxylin-Eosin. × 200

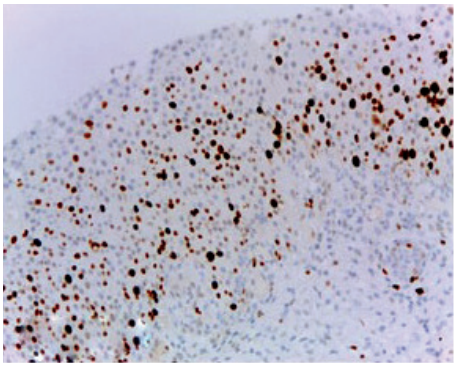

Fig.10. Carcinoma in situ, Ki 67. × 200

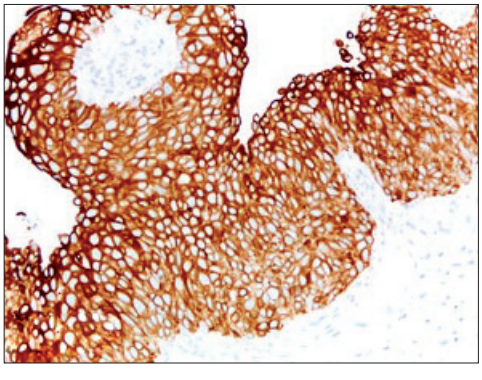

Fig. 11. Carcinoma in situ, CK 20. × 200

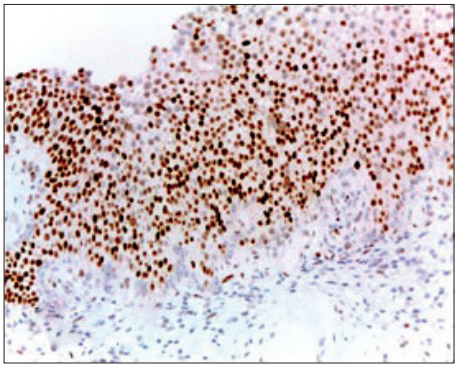

Fig. 12. Carcinoma in situ, p53. × 200

Conclusion

IHC investigation is not used in UCs as often as in other tumors, but in some cases it finds its application. Such are those with problems with differential diagnosis or grading and staging of the tumor, as well as the assessment of the presence of UCIS. Knowing the possibilities of IHC is a prerequisite for an adequate diagnosis.

References

1. **Epstein, J., M. Amin, V. Reuter.** Staging of bladder cancer – In: *Biopsy interpretation of the bladder*, Philadelphia, Wolters Kluwer/Lippincott Wiliams & Wilkins, (Second edition), 2010, 96-123.
2. **Grignon, D. J.** Tumors of the urinary bladder. – In: *Urological Pathology* (Eds. M. B. Amin, D. J. Grignon, J. R. Strigley, J. N. Eble), Philadelphia, Wolters Kluwer/Lippincott Wiliams & Wilkins, 2014, 340-360.
3. **Javier, A., Arias-Stella III, A. Shah, N. Gupta, S. Williamson.** CK20 and p53 immunohistochemical staining patterns in urinary bladder specimens with equivocal atypia. – *Arch .Pathol. Lab. Med.,* **142**, 2018, 64-69.
4. **McKenney, J. K, S. Desai, C. Cohen, M. B Amin.** Discriminatory immunohistochemical staining of urothelial carcinoma in situ and non-neoplastic urothelium: an analysis of cytokeratin 20, p53, and CD44 antigens. – *Am. J. Surg. Pathol.,* **25**(**8**), 2001, 1074-8.
5. **Moch, H., P. Humphrey, T. Ulbright, V. Reuter.** WHO classification of tumours of the urinary system and male genital organs. Fourth edition, Volume 8, 2017, IARC WHO Classification of Tumours, WHO Press
6. **Sibony, M., Y. Allory.** Tumors of the bladder and other lesions. EPU Uropathologie, Academie Internationale de Pathology DF, 9-10 February, 2012, Paris. [in French]

Institute of Experimental Morphology, Pathology and Anthropology with Museum
Bulgarian Anatomical Society

Acta morphologica et anthropologica, 26 (1-2)
Sofia ● 2019

Age-related Changes in Rat Thymus Connective Tissue Influenced by Aronia Melanocarpa

Elena Daskalova[1], Slavi Delchev[1], Lyudmila Vladimirova-Kitova[2], Petko Denev[3,4], Stefka Valcheva-Kuzmanova[5], Spas Kitov[6], Marin Kanarev[6]

[1] Deparment of Anatomy, Histology and Embryology, Faculty of Medicine, Medical University – Plovdiv, Plovdiv, Bulgaria
[2] Clinic of Cardiology, Faculty of Medicine, Medical University – Plovdiv, Plovdiv Bulgaria
[3] Laboratory of Biologically Active Substances, Institute of Organic Chemistry with Centre of Phytochemistry, Bulgarian Academy of Sciences, Plovdiv, Bulgaria.
[4] ITC-Innovative-Technological Centre Ltd., Plovdiv, Bulgaria.
[5] Department of Pharmacology and Clinical Pharmacology and Therapeutics, Faculty of Medicine, Medical University Prof. Dr. Paraskev Stoyanov, Varna, Bulgaria
[6] Student of medicine, Faculty of Medicine, Medical University – Plovdiv, Plovdiv, Bulgaria

* Corresponding author e-mail: eli_das@abv.bg

The purpose of this study is to determine the influence of Aronia melanocarpa (AM) on macrophage and mast cell quantity and collagen fibres distribution in age-related tissue remodeling of rat thymus. Two control groups, young (CY) – 2 month-old and mature (CO) – 12 month-old, have been put on a standard diet. The rats in the experimental group (A) received 10 *ml/kg* AM juice daily. Histological, immunohistochemical, morphometric and statistical assays were performed. Supplementation with juice from AM resulted in a significant decrease in the amount of collagen fibres, the number of mast cells in interlobular connective tissue and the number of CD68 positive cells in the medulla of rat thymus. Our results show for the first time the effect of AM on the age remodelling of connective tissue in the thymus. These results support the beneficial potential of the nutrient treatment of age-related diseases.

Key words: Aging, thymus, stromal elements, Aronia melanocarpa, rats

Introduction

Aging is a continuous and slow process compromising the morphofunctional characteristics of different organs and systems both in humans and in animals [14]. Chronic, low-grade, systemic inflammation is the primary risk factor for major human chronic diseases, including cardiovascular disorders, cancer, type 2 diabetes and neurodegenerative disease. Increased production of inflammatory mediators which accompanies this process is referred to as "inflammaging"[8].

Regression of the thymus leads to a decline in naive T cells output modifying the composition of the peripheral T cells pool and altering T cells' phenotype and function.

These changes are believed to contribute significantly towards the clinical features of immunosenescence [14].

With age, the thymus suffers changes in its architecture, losing a clear demarcation between cortex and medullary regions, which is related to lymphocyte cell death. Other changes observed in the aging thymus include a decrease in the number and activity of thymic epithelial cells, reducing growth factors production. Moreover, there is a progressive increase of collagen and adipose tissue deposition in the capsule and septa regions. A large corpus of evidence supports the notion that the stromal population in the thymus is a primary target of age-associated thymic dysfunction [2].

Mast cells (MCs) are strategically located at host/environment interfaces and also populate connective tissue in association with blood and lymphatic vessels and nerves. In the last few years literature data has clearly shown that the function of MCs is not limited to acting as first line of defence against invading pathogens or as effector cells in allergy. MCs play a critical role in tissue remodelling, tissue matrix turnover and renewal [15]. In the thymus, MCs are localized in the connective tissue of the capsule and interlobular septa, and inside the thymic lobules. MCs synthesize and release a large panel of growth factors and cytokines, including interleukin (IL) IL-1, IL-2, IL-3, IL-4, IL-6, TNFα, granulocyte-monocyte colony stimulating factors (GM-CSF), and nerve growth factor (NGF), which stimulate thymocyte and thymic epithelial cell functions. In human and chicken thymus, MCs are restricted to the medulla and to connective tissue septa and their number increases in the adult thymus when compared to a foetal thymus [15].

Macrophages are a type of thymic stromal cell involved in phagocytosis, antigen presentation and production of cytokines, which influence T cells proliferation and maturation [10].

Certain plants and spices containing flavonoids have been used for thousands of years in traditional Eastern medicine. Moreover, the inhibitory action on inflammatory cells, especially mast cells, appears to surpass any other clinically available compound. Evidence suggests that only activated cells are susceptible to the modulating effects of flavonoids. The stimulated activities of numerous cell types, including mast cells, basophils, neutrophils, eosinophils, T and B lymphocytes, macrophages, platelets and others, can be influenced by particular flavonoids [9]. Flavonoids are powerful antioxidants and anti-allergic nutrients which inhibit the release of chemical mediators, synthesis of Th2 type cytokines, such as IL-4, and CD40 ligand expression by high-affinity immunoglobulin E (IgE) receptor-expressing cells, such as mast cells and basophils [17]. The anthocyanin fruit AM is ranked first in its antioxidant potential as confirmed by several different methods. A number of *in vitro* and i*n vivo* studies have demonstrated the wide range of applications of the juice extracts or the dry substance of the fruits of AM, as anti-inflammatory, anti-mutagenic, anti-cancerogenic, lipidlowering, antidiabetic, antihypertensive, hepatoprotective, immunomodulatory effects, etc.[4].

Scientific literature provides only limited data on the effect of its application on aging and in particular on the age-related thymus changes.

Aim

The purpose of this study is to determine the influence of AM on macrophages and MCs quantity and collagen fibres distribution in relation with the age-related tissue remodelling of rat thymus.

Material and Methods

The study included 18 male Wistar rats, 12 of them – 9 months of age with initial body weight 350g ± 50; and 6 animals aged 2 months with body weight 100g ± 10. The animals were provided by and bred in the vivarium of the Medical University-Plovdiv under standard laboratory conditions. The rats were divided into 3 groups. Two control groups, defined as young (CY) – 2 month-old and mature (CO) – 12 month-old, have been put on a standard diet and tap water ad libitum. The rats in the experimental group (A) were age matched to the mature controls and received AM juice diluted 1:1 in drinking water in dose 10ml/kg. The experiment lasted for 90 days. The functional beverage from AM fruits was supplied by „Vitanea" Ltd and ITC – Innovative-Technological Centre Ltd., Plovdiv, Bulgaria.

Table 1. Anthocyanin and polyphenol content and antioxidant activity of Aronia melanocarpa juice. Data from the Innovative-Technological Centre Ltd.

	Antocyanins (mg/l)	Polyphenols (mg/l)	ORAC (μmol TE/l)
Aronia 100%	57	4772	55307

The experimental protocol was approved by the Committee on Ethical Treatment of Animals from the Bulgarian Agency for Food Safety (№102/10.07.2014). All animals received humane care in compliance with the "Principles of laboratory animal care" formulated by the National Society for Medical Research and the "Guide for the care and use of laboratory animals" prepared by the National Institute of Health (NIH publication No. 86-23, revised 1996). At the end of the experimental period the animals were euthanized with i.m. Ketamin (90 mg/kg) + Xilazine (10mg/kg). The whole thymus was dissected and was fixed in 10% neutral formalin for further histological examination. Thymus samples were subjected to routine paraffin embedding, cutting and staining with Toluidine blue and Azan (Heidenchain).

Immunoreaction for CD68 was performed using an automated Leica BOND-MAX system. Tissue sections of 4 μm thickness were incubated with mouse anti CD68 (ready to use) monoclonal antibody (Leica Biosystems Newcastle Ltd, United Kingdom).

The areas for morphometric analysis were the interlobular septa of the thymus on tissue sections of 4 μm thickness. On the Azan stained slices a measurement of the relative distribution of the collagen fibers in the interlobular thymic septa per unit area was performed. Slices with Toluidine bluestaining were used to determine the mean distribution of mast cells per unit area, by counting only the mast cells, located in the territory of the interlobular septa. Slices with CD68 immunoreaction were used to determine the mean distribution of CD68 positive cells per unit area, by separately counting the CD68 positive cells in medulla and cortex of the thymus. In all three studies five slices per animal were examined. The measurements were done with the help of software "DP – Soft" 3.2, Olympus, Japan. Microphotographs were performed with Nikon Microphot SA microscope (Japan), combined with Camedia-5050Z digital camera (Olympus, Japan).

Statistical analysis was performed using SPSS software (version 18.0). All data were presented as means ± standard error of mean (SEM) and analysed by one-way ANOVA, followed by Tukey's post hoc test. $P < 0.05$ was considered as statistically significant.

Results

The Azan-stained collagen fibres of the interlobular septa were blue in contrast to the red colour of the thymus parenchyma. In the young control group (CY), the amount of connective tissue in the septa was scarce in contrast to the adult controls (CO) in which septal and perivascular enlargement and the presence of adipose tissue were observed in addition to its increased amount. In the Aronia group (A), the septa were narrower and adipose tissue was almost absent (**Fig. 1**).

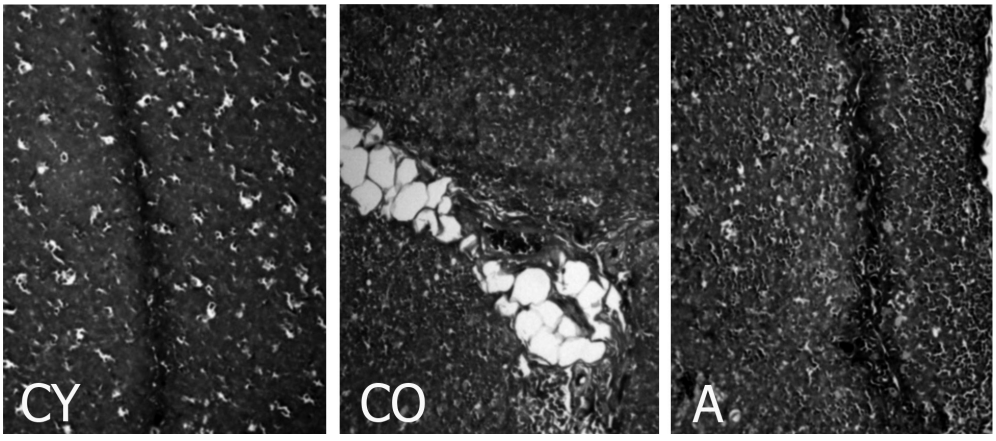

Fig. 1. Histological assay of thymus. Azan (Heidenhain) staining (x 200). Young controls (CY), mature controls (CO), AM supplemented group (A)

Toluidine blue-stained deep purple metachromatic granules were used as a hallmark of mast cells (**Fig. 2**).

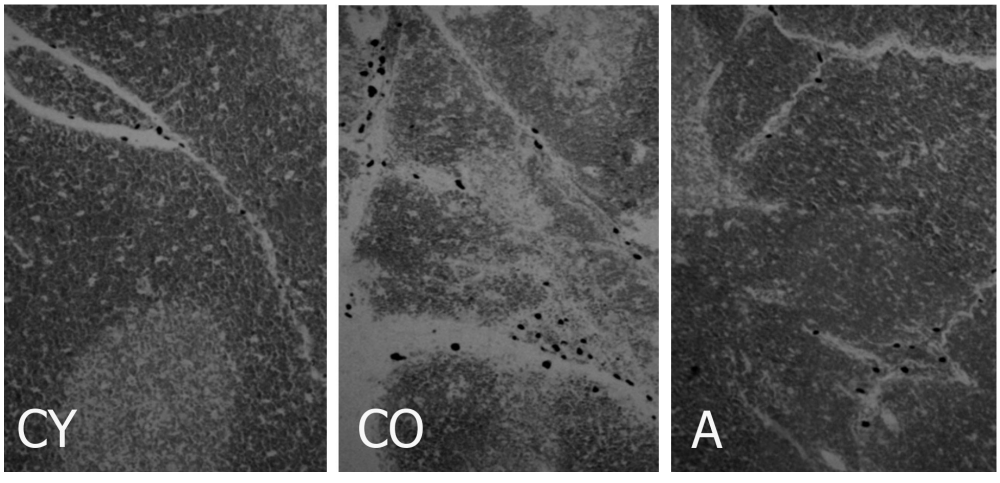

Fig. 2. Histological assay of thymus. Toluidine bluestaining (×100).Young controls (CY), mature controls (CO), AM supplemented group (A)

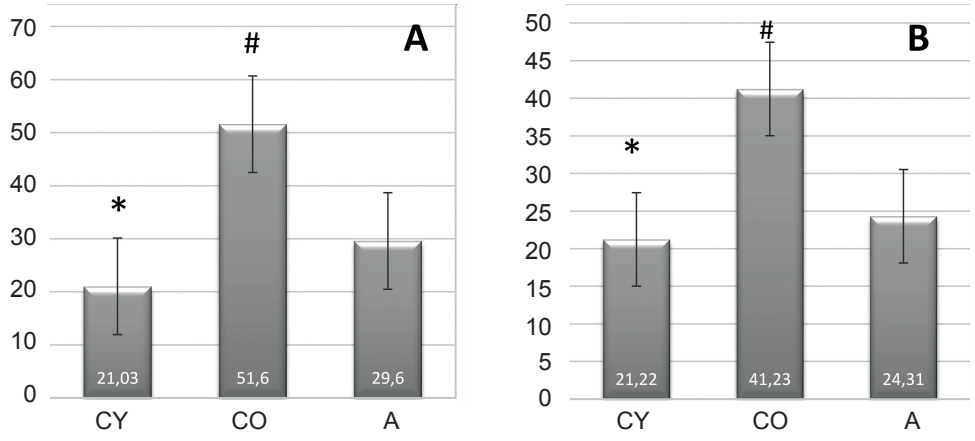

Fig. 3. Results from morphometric analysis: A: Relative distribution of connective tissue in thymus septa, * CY v/s CO, ($p<0.05$), # CO v/s A, ($p<0.05$).B: Mean distribution of mast cells in thymic septa. * CY v/s CO, ($p<0.05$), #CO v/s A, ($p<0.05$).

The morphometric evaluation demonstrated that the MCs number increased significantly in adult thymus compared with young thymus (**Fig. 3 B**). As a result of the supplementation, the number of mast cells has decreased significantly in the experimental group (A) compared to the mature controls (CO). Decrease of the amount of collagen connective tissue in the interlobular thymus septa corresponds with the lower number of MCs (**Fig. 3 A**).

Fig. 4 demonstrates CD68 positive cells with the cytoplasm of a dark-brown color. The immunohistochemical reaction represents macrophages on the background of the hematoxilin countrastained thymocyte nuclei.

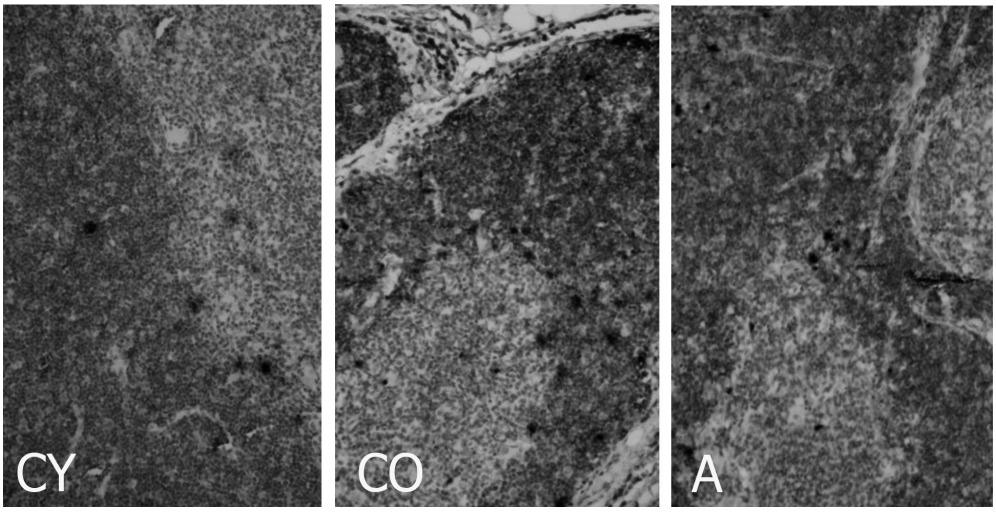

Fig. 4. CD68 immunoreaction in rat thymus (x 400).Young controls (CY), mature controls (CO), AM supplemented group (A)

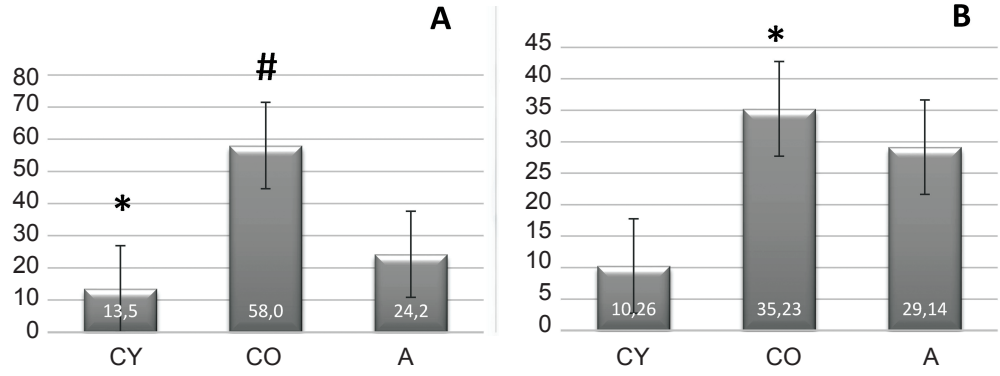

Fig. 5. Mean distribution of CD68 immunopositive cells in thymus. A: CD68 in thymic medulla *CY v/s CO, ($p<0.05$)#CO v/s A, ($p<0.05$) B: CD68 in thymic cortex *CO v/s CY, ($p<0.05$)

The morphometric evaluation demonstrated that the number of CD68 immunopositive cells in thymic medulla increased significantly in adult thymus compared with young thymus (**Fig. 5A**). As a result of the supplementation, the number of CD68 immunopositive cells has decreased significantly in the experimental group (A) compared to the mature controls (CO), ($p<0.05$).

In adult controls thymic cortex (CO), (**Fig. 5 B**) the number of CD68 immunopositive cells has increased significantly compared to young controls (CY), ($p<0.05$).The group of AM supplemented animals (A) showed a decreased number of CD68 immunopositive cells in thymic cortex, but differences with adult controls (CO) didn't reach significance.

Discussion

Our results showed that the MCs number has increased significantly in an adult thymus compared to a young thymus and coincide with the studies of other authors [13]. The decrease in the amount of collagen connective tissue in the interlobular thymus septa of the supplemented group (A) corresponds with the lower number of MCs in the same group. According to Langhi et al. [11] the mast cells have the ability to secrete pro-inflammatory cytokines and affect the activity of macrophages even without signs of degranulation, thus sustaining minimal levels of inflammation that lead to fibrosis. Pal et al. [12] in their study discovered that in the mesenteric lymph nodes the number of mast cells increased significantly with age while their function worsened which resulted in an increase in the oxidative stress in aged mesenteric tissue. In his study Gruber [7] demonstrated that mast cells interact with fibroblasts which changes their activity thus affecting extracellular fibrosis. Mechanistic links between aging, thymic adiposity, and thymic atrophy have been revealed by recent works showing that lipotoxic "danger-associated molecular patterns" (DAMPs), such as ceramide and free cholesterol, increase with aging [3, 19], and can initiate NLRP3 inflammasome signaling and IL-1β production in thymic myeloid cells [19]. These studies suggest that lipotoxic DAMPs inhibit thymus function via IL-1β signaling in thymic epithelial cells [19]. In experimental models of inflammation Borissova [1] and Valcheva-Kuzmanova [18] demonstrated the anti-inflammatory effect of flavonoids present in the juice from AM. Ghante et al. [5] in an experiment with plant extracts from Randia dumetorum (RD) fruits rich in al-

kaloids, flavonoids, polyphenols etc. proved that the bronchorelaxant potential of RD fruit extracts is well supported by an anti-inflammatory effect, stabilization of mast cell membranes and scavenging of different free radicals. In his study Shirley [16] showed that resveratrol at low concentrations exerts its anti-inflammatory properties by preferentially targeting the arachidonic acid pathway.

Our results showed for the first time that supplementation with AM juice leads to a significant decrease in the amount of collagen fibres, the number of mast cells in interlobular connective tissue and the number of CD68 positive cells in thymic medulla in rat thymus.

Conclusion

The decrease in the amount of collagen fibres, the number of mast cells in interlobular connective tissue and the number of CD68 positive cells in thymic medulla demonstrate that a functional drink of AM may counteract age-matched thymic connective tissue remodelling. These results support the beneficial potential of the nutrient treatment of age-related diseases.

Acknowledgements: This work was funded by Grant No DN 09/20/21.12.2016 from the Bulgarian National Science Fund.

References

1. **Borissova, P., S.Valcheva, A. Belcheva.** Antiinflammatory effect of flavonoids in the natural juice from Aronia melanocarpa, rutin and rutin-magnesium complex on an experimental model of inflammation induced by histamine and serotonin. – *Acta Physiol. Pharmacol. Bulg.,* **20** (**1**), 1994, 25-30.
2. **Cepeda, S., A. Griffith.** Thymic stromal cells: Roles in atrophy and age-associated dysfunctionof the thymus. – *Exp. Gerontol.,* **105**, 2018, 113-117.
3. **de Mello-Coelho, V., R. G. Cutler, A. Bunbury, A. Tammara, M. P Mattson, D. D. Taub.** Age-associated alterations in the levels of cytotoxic lipid molecular species and oxidative stress in the murine thymus are reduced by growth hormone treatment. – *Mech. Ageing Dev.,* **167**, 2017, 46-55.
4. **Denev, P., Ch. Kratchanov, M. Ciz, A. Lojek, M. Kratchanova.** Bioavailability and antioxidant activity of black chokeberry (aroniamelanocarpa) polyphenols: in vitro and in vivo evidences and possible mechanisms of action: a review. – *Compr. Rev. Food Sci. F.,* **11**(**5**), 2012, 471-489.
5. **Ghante, M., K. Bhusari, N. Duragkar, N. Jain, A. Warokar.** Bronchorelaxant, mast cell stabilizing, anti-inflammatory and antioxidant activity of Randia dumetorum (Retz.) lamk. extracts. Acta Pol. Pharm. – *Drug Research,* **69**(**3**), 2012, 465-474.
6. **Griffith, A. V., M. Fallahi, T. Venables, H. T. Petrie.** Persistent degenerative changes in thymic organ function revealed by an inducible model of organ regrowth. – *Aging Cell.,* **11**, 2012, 169-177.
7. **Gruber, B. L.** Mast cells in the pathogenesis of fibrosis. – *Curr. Rheumatol. Rep.,* **5**(**2**), 2003, 147-153.
8. **Isobe, K., N. Nishio,T. Hasegawa.** Immunological aspects of age-related diseases. – *World J. Biol. Chem.,* **8**(**2**), 2017, 129-137.
9. **Middleton, E. Jr., C. Kandaswami, T. C. Theoharides.** The effects of plant flavonoids on mammalian cells: implications for inflammation, heart disease, and cancer. – *Pharmacol. Rev.,* **52**(**4**), 2000, 673-751.
10. **Milićević, N.M., Z. Milićević, M. Colic, S. Mujović.** Ultrastructural study of macrophages in the rat thymus, with special reference to the cortico-medullary zone. – *J. Anat.,* **150**, 1987, 89-98.
11. **Langhi, L., G. Andrade, L. Shimabukuro.** Lipid-laden multilocular cells in the aging thymus are phenotypically heterogeneous. – PLoS ONE, 10(10), 2015. https://doi.org/10.1371/journal.pone.0141516
12. **Pal, S., C. Meininger, A. Gashev.** Aged lymphatic vessels and mast cells in perilymphatic tissues. – *Int. J. Mol. Sci.,* **18**, 2017, 965.

13. **Raica, M., A. M. Cimpean, B. Nico, D. Guidolin, D. Ribatti.** A comparative study of the spatial distribution of mast cells and microvessels in the foetal, adult human thymus and thymoma. – *Int. J. Exp. Path.,* **91**, 2010, 17-23.
14. **Rezzani, R., L. Nardo, G. Favero, M. Peroni, L. Rodella.** Thymus and aging: morphological, radiological and functional overview. – *Age (Dordr.),* **36**, 2014, 313-351.
15. **Ribatti, D., E. Crivellato.** The role of mast cell in tissue morphogenesis. Thymus, duodenum, and mammary gland as examples. – *Exp. Cell Res.,* **341**, 2016, 105-109.
16. **Shirley, D., C. McHale, G. Gomez.** Resveratrol preferentially inhibits IgE-dependent PGD2 biosynthesis but enhances TNF production from human skin mast cells. – *Biochim. Biophys. Acta,* **1860**(**4**), 2016, 678-685.
17. **Tanaka, T, R. Takahashi.** Flavonoids and Asthma. – *Nutrients,* **5**, 2013, 2128-2143.
18. **Valcheva-Kuzmanova, S., A. Kuzmanov, V. Kuzmanova, M. Tzaneva.** Aronia melanocarpa fruit juice ameliorates the symptoms of inflammatory bowel disease in TNBS-induced colitis in rats. – *Food Chem Toxicol.,* **113**, 2018, 33-39.
19. **Youm, Y. H., T. D. Kanneganti, B. Vandanmagsar, X. Zhu, A. Ravussin, A. Adijiang, J. S. Owen, M. J. Thomas, J. Francis, J. S. Parks, V.D. Dixit.** The Nlrp3 inflammasome promotes age-related thymic demise and immunosenescence. – *Cell Rep.,* **1**, 2012, 56-68.

Institute of Experimental Morphology, Pathology and Anthropology with Museum
Bulgarian Anatomical Society

Acta morphologica et anthropologica, 26 (1-2)
Sofia ● 2019

Germ Cell Marker DDX4 (Vasa) Transiently Accumulates in Balbiani Body of Early Mouse Oocytes

Valentina Hadzhinesheva, Maya Markova, Stefka Delimitreva, Irina Chakarova, Venera Nikolova, Ralitsa Zhivkova*

Department of Biology, Medical Faculty, Medical University of Sofia, 2 Zdrave Street, 1431 Sofia, Bulgaria

* Corresponding author e-mail: mayamarkov@gmail.com

Abstract

RNA helicase DDX4 (Vasa) is a marker of germ cells. There is controversy about its intracellular distribution in early oocytes, reported by different authors to be uniform throughout the cytoplasm in mice or transiently associated with the oocyte-specific complex of organelles known as Balbiani body in humans. We performed immunohistochemical localization of DDX4 in sections from neonatal mouse ovaria. Prophase I oocytes from 1-day old mice showed reaction in a perinuclear aggregate, while in dictyate oocytes from 2-day old mice the reaction had diffuse staining throughout the cytoplasm. These results indicate that DDX4 is associated with the Balbiani body in early oogenesis of both mice and humans, and suggest that the Balbiani body in mammals may be a site of storage and regulation of mRNA as in other vertebrates.

Key words: DDX4, Vasa, oocytes, Balbiani body, meiosis

Introduction

RNA helicases are enzymes participating in splicing of primary transcripts, biogenesis of ribosomes, initiation of translation and other processes requiring changes in RNA secondary structure. The cytoplasm of mammalian germ cells at all stages of differentiation contains an RNA helicase known as DDX4 (Dead-box helicase 4) or Vasa after its homolog in *Drosophila*. It is not present in somatic cells and is regarded as a germ cell marker [7, 8]. There are reports that DDX4 keeps the germ cell genome stable by inhibiting the expression and propagation of retrotransposons [5]. Despite the apparent functional importance of this protein for germ cells, there is still controversy about its intracellular localization in immature oocytes. Uniform distribution of DDX4 has been described in early mouse oocytes [6], while in human oocytes, it has been found concentrated in the Balbiani body in primordial follicles and spread over wider areas of cytoplasm in primary follicles [1]. The Balbiani body is a perinuclear aggregate of membrane organelles (endoplasmic reticulum, Golgi cisternae and mitochondria) observed in early oocytes and in non-mam-

malian vertebrates related to polarity determination during oogenesis [3]. To examine the intracellular distribution of DDX4 protein in early mammalian oocytes, we localized it immunohistochemically in ovarian sections from newborn mice.

Materials and Methods

Experiments were performed in compliance with the European Union and Bulgarian legislature concerning use of animals as research objects. Tissue processing and immunocytochemistry was carried out as described before [4]. Briefly, ovaria of newborn female BALB/c mice were isolated, fixed and paraffin embedded at the first and second day after birth. Sections were prepared, mounted on slides, deparaffinized and rehydrated. Then immunofluorescent detection of DDX4 was performed on them using rabbit DDX4-specific primary antibody diluted 1:40 (Quartett, Germany) and FITC-labeled secondary antibody diluted 1:80 (Sigma – Aldrich, Germany). Chromatin was counterstained by Hoechst 33258. The result was observed and documented using Leica TSC SPE laser scanning confocal microscope.

Results

In ovaria of one-day old mice, oocytes were surrounded by few, irregularly positioned somatic cells. Oocyte nuclei were characterized by presence of condensed meiotic chromosomes. Antibodies against DDX4 produced a bright localized reaction in oocytes, staining a perinuclear aggregation (**Fig. 1**).

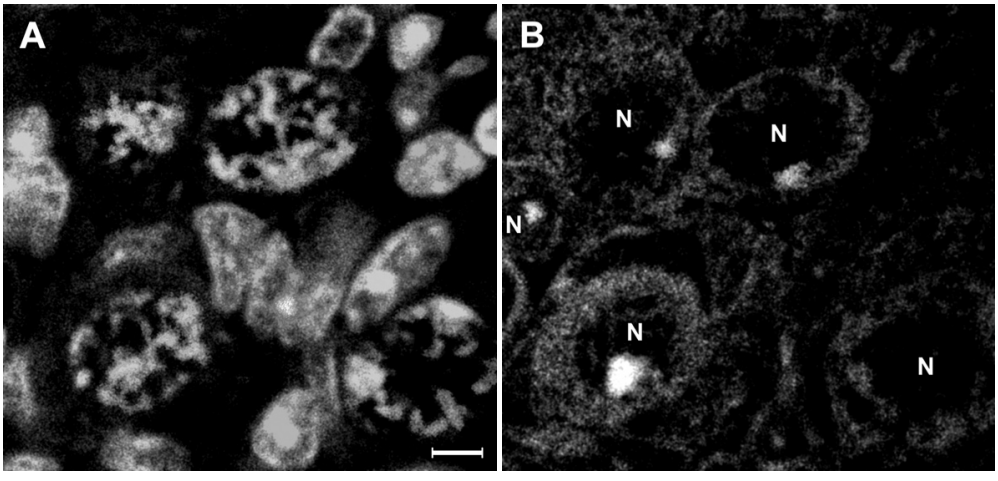

Fig. 1. Staining of a section from 1-day old mouse ovary for chromatin (**A**) and DDX4 (**B**). N, oocyte nuclei. Bar = 5 μm.

In ovaria of two-day old mice, well-formed primordial follicles were observed, with elongated somatic cells surrounding the oocytes. Oocyte nuclei had homogeneous appearance of chromatin corresponding to the first meiotic arrest in dictyate. The positive reaction for DDX4 protein was finely distributed in the oocyte cytoplasm (**Fig. 2**).

Somatic cells were negative for DDX4 in all ovarian samples.

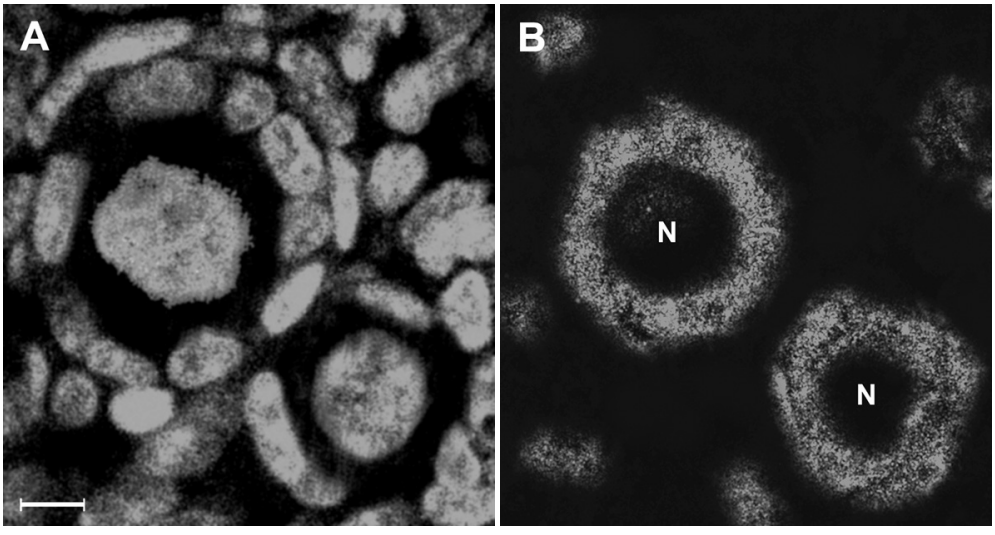

Fig. 2. Staining of a section from 2-day old mouse ovary for chromatin (**A**) and DDX4 (**B**). N, oocyte nuclei. Bar = 5 μm.

Discussion

This study was carried out on newborn mouse ovaria because in mice, prophase I of meiosis is still ongoing by the time of birth, and oocytes are arrested in dictyate only on the 2nd or 3rd day of postnatal life [2]. Comparing the reaction for DDX4 in ovaria of one-day versus two-day old newborn mice allowed us to trace the dynamics of DDX4 during late meiotic prophase I and transition to dictyate. The different appearance of chromatin (condensed in meiotic chromosomes in one-day old ovaria vs. homogenous in two-day old ovaria) and the cellular organization of ovaria (recognizable primordial follicles only in the two-day old group) confirmed that oocyte differentiation stage differed between the two sets of samples: ongoing prophase I in 1-day-old mice versus dictyate in 2-day-old ones.

There is controversy about the distribution of DDX4 in early mammalian oogenesis: uniform throughout the cytoplasm in fetal and neonatal mouse oocytes [6] or associated with the Balbiani body in human oocytes from primordial follicles and dispersing in oocytes from primary follicles [1]. More data are needed to clarify this discrepancy. Our finding of DDX4 in neonatal mouse oocytes concentrated in a large perinuclear cluster before dispersing in the cytoplasm suggests that in both mice and humans it is a component of the Balbiani body during prophase I. Messenger RNAs have been detected in the Balbiani body of fishes and amphibians but so far not in mammals [3]. The transient perinuclear concentration of the RNA-associated enzyme DDX4 revealed in this study makes it likely that the Balbiani body in mammals may be a site of storage and regulation of mRNA as in other vertebrates.

Conclusions

The germ-cell specific RNA helicase DDX4 colocalizes with Balbiani body in prophase I mouse oocytes before dispersing in the cytoplasm at dictyate. This result suggests that mammalian Balbiani body may have a function to accumulate and regulate mRNA.

Acknowledgements: We thank Assoc. Prof. Pavel Rashev and Assoc. Prof. Milena Mourjeva from the Institute of Biology and Immunology of Reproduction at the Bulgarian Academy of Sciences for valuable help in providing the specimens and documenting the results. This work was supported by the Bulgarian Ministry of Education and Science uder the National Program for Research "Young Scientists and Postdoctoral Students".

References

1. **Albamonte, M. I., M. S. Albamonte, I. Stella, L. Zuccardi, A. D. Vitullo**. The infant and pubertal human ovary: Balbiani's body-associated VASA expression, immunohistochemical detection of apoptosis-related BCL2 and BAX proteins, and DNA fragmentation. – *Hum. Reprod.,* **28**, 2013, 698-706.
2. **Chen, Y., W. N. Jefferson, R. R. Newbold, E. Padilla-Banks, M. E. Pepling.** Estradiol, progesterone, and genistein inhibit oocyte nest breakdown and primordial follicle assembly in the neonatal mouse ovary in vitro and in vivo. – *Endocrinology,* **148**, 2007, 3580-3590.
3. **Hadzhinesheva, V., V. Nikolova, I. Chakarova, S. Delimitreva, M. Markova, R. Zhivkova.** Mammalian Balbiani body as a sign of ancestral oocyte asymmetry: review. – *Acta Morphol. Anthropol.,* **22**, 2015, 159-162.
4. **Hadzhinesheva, V. P., I. V. Chakarova, S. M. Delimitreva, M. D. Markova, V. P. Nikolova, M. S. Mourdjeva, P. I. Rashev, R. S. Zhivkova.** Centriolar satellites associate with condensed chromatin in early mouse oocytes and undergo redistribution during transition to dictyate. – *Biotechnol. Biotechnol. Equip.,* **2018**, DOI: 10.1080/13102818.2018.1541761.
5. **Hadziselimovic, F., N. O. Hadziselimovic, P. Demougin, G. Krey, E. J. Oakeley.** Deficient expression of genes involved in the endogenous defense system against transposons in cryptorchid boys with impaired mini-puberty. – *Sex Dev.,* **5**, 2011, 287-293.
6. **Pepling, M. E., J. E. Wilhelm, A. L. O'Hara, G. W. Gephardt, A. C. Spradling.** Mouse oocytes within germ cell cysts and primordial follicles contain a Balbiani body. – *Proc. Natl. Acad. Sci. USA,* **104**, 2007, 187-192.
7. **Song, K., W. Ma, C. Huang, J. Ding, D. Cui, M. Zhang.** Expression pattern of mouse vasa homologue (MVH) in the ovaries of C57BL/6 female mice. – *Med. Sci. Monit.,* **22**, 2016, 2656-2663.
8. **Stoop, H., F. Honecker, M. Cools, R. de Krijger, C. Bokemeyer, L. H. Looijenga.** Differentiation and development of human female germ cells during prenatal gonadogenesis: an immunohistochemical study. – *Hum. Reprod.,* **20**, 2005, 1466-1476.

Institute of Experimental Morphology, Pathology and Anthropology with Museum
Bulgarian Anatomical Society

Acta morphologica et anthropologica, 26 (1-2)
Sofia ● 2019

Morphological Characterization of Erythrodermic Mycosis Fungoides

Vessel Kantardjiev[1], Simona Davidovska[1], Valentina Broshtilova[1], Mary Gantcheva[2]*

[1] *Department of Dermatology and Venereology, Military Medical academy, Sofia, Bulgaria*
[2] *Institute of Experimental Morphology, Pathology and Anthropology with Museum, Bulgarian Academy of Sciences, Sofia, Bulgaria*

* Corresponding author e-mail: mary_gant@yahoo.com

Abstract

Mycosis fungoides (MF) is the most common variant of primary cutaneous T-cell lymphoma (CTCL). CTCLs constitute 65% of all cutaneous lymphoid malignancies, of which 50% are patients with MF. The erythrodermic variant of MF, a malignancy of mature, skin homing, clonal T lymphocytes, is a very rare clinical sub type that usually presents in mid- to late adulthood. We report a case of a 70-year-old man with intractable progressive erythroderma of a 2 year-duration, accompanied by severe persistent pruritus. Upon histological and immunohistochemical diagnosis, the most provocative challenge was ruling out leukemization confirming Sezary syndrome. A short critical overview of literature sources disputing this rightful verification is herein highlighted.

Key words: mycosis fungoides, erythroderma, Sezary syndrome

Introduction

Mycosis fungoides is the most common type of cutaneous T-cell lymphoma. MF is a primary cutaneous mature T-cell epidermotropic non-Hodgkin lymphoma [4]. It is considered a low-grade malignancy initially presenting in the skin, however, it can be aggressive and spread to lymph nodes, blood, and other organs, such as the liver, spleen, and gastrointestinal tract. Clinical features of MF include presence of progressive skin lesions such as patches, plaques, papules, tumor, erythroderma. The prognosis worsens in late stages.

Case report

A 70-year-old man was afflicted with large confluent erythematous pruritic patches with scaling dated back from 15 years. They gradually increased in size and number, mostly in the last 2 years, involving over 90% of his body surface area. There was no lymphadenopathy or hepatosplenomegaly. The patient had received previous topical corticosteroid treatment for chronic atopic dermatitis with no beneficial effect. His medical history was notable for hypertension and hypothyroidism.

On dermatological examination, diffuse, erythematous and scaly lesions were present on the trunk, arms, legs and face. A clinical diagnosis of MF was made, and multiple skin biopsies were taken from different sites. On histopathological examination the hematoxylin and eosin-stained section of the skin showed variable acanthosis, epidermotropism of atypical lymphocytes (characteristic "haloed cells") without spongiosis (**Figs. 1, 2**). On immunohistochemisty, lymphocytic infiltrate was positive for T-cell marker CD4 and to a much lesser extent for CD8 (**Figs. 3, 4**). Peripheral blood flow cytometry analysis showed a normal CD4/CD8 ratio (<10) and the Sezary cells were less than 5%, with the absolute number being 183 cells/mm3 (<1000 cells/mm3). Bone marrow aspiration cytology, chest X-ray and abdominal ultrasound exam appeared normal.

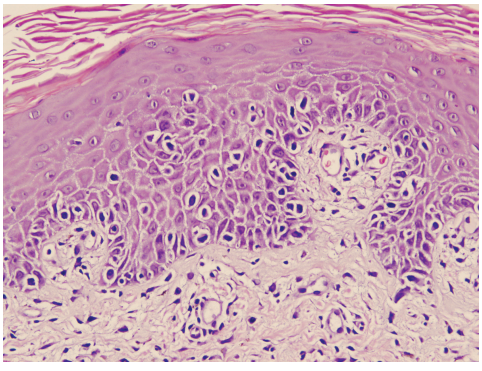

Fig. 1. Hyperkeratosis, acanthosis, epidermotropic atypical lymphoid cells in the low portion of the epidermis. (Hematoxylin-Eosin, × 200)

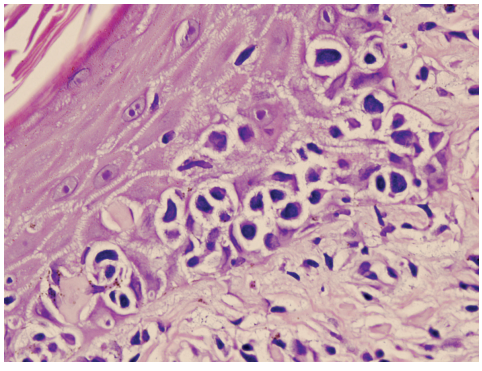

Fig.2. Pautrier's microabscesses. (Hematoxylin-Eosin, × 400)

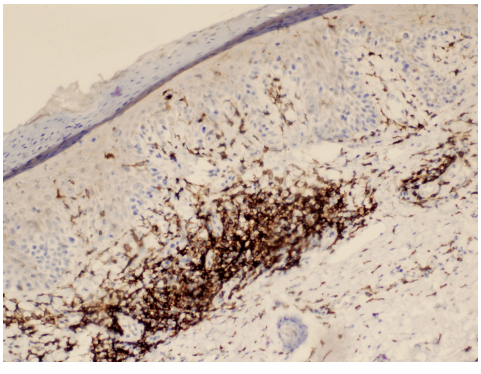

Fig. 3. CD4+ lymphoid cells. (× 400)

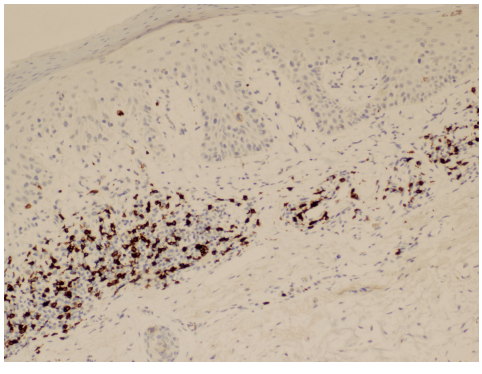

Fig. 4. CD8+ lymphoid cells. (× 400)

The patient's findings were consistent with an erythrodermic variant of MF, stage IIIA (T4N0M0B0) according to the ISCL/EORTC revised classification system.

Psoralen plus UVA therapy and IFN-alpha 2a (3 MIU SC 3 times weekly) resulted in partial clearance of lesions.

Discussion

Mycosis fungoides and Syndroma Sezary are the most common types of cutaneous T-cell lymphomas. MF is a malignancy of mature, skin homing, clonal T lymphocytes [9]. Sezary syndrome (SS) is an erythrodermic and leukemic variant of CTCL. It is defined by the triad of erythroderma, generalized lymphadenopathy and the presence of neoplastic T cells (Sezary cells) in the skin, lymph nodes and peripheral blood [7]. According to EORTC/WHO classification, a case of SS must demonstrate one or more of the following criteria: an absolute Sezary count of > 1000 cells/mm^3, a CD4/CD8 ratio of >10, T-cell clonality in the peripheral blood by flow cytometry, or a chromosomal abnormal T-cell clone [5]. The lack of monoclonal atypical lymphoid invasion in the peripheral blood ruled out SS and categorized our patient as an erythrodermic MF.

The erythrodermic MF variant was originally described in 1892 [8]. MF usually affects mid-aged adults with a slight male preference (2:1) [6]. The etiology and the pathogenic mechanisms involved in the development and step-wise progression of MF are largely unknown. Genetic, environmental and immunologic factors have been considered [3]. The diagnosis is based on standard histopathological findings, showing small cerebriform lymphoid cells that solitary or in groups (Pautrier's microabscesses) invade the lower portion of the epidermis. Usually those cells express CD4+/CD7- immunohistochemical profile. Interestingly, the invasive lymphoid population may transform into lower differentiated, more aggressive in biological behavior subtypes (CD30+ anaplastic T cells). Therefore, regular clinical and histological monitoring is essential in all MF cases.

Skin-directed therapies are preferred in early MF stages [2]. Topical corticosteroids, retinoids (bexarotene) or chemotherapeutic agents (nitrogen mustard), psoralen plus UVA phototherapy, and total skin electron beam irradiation (TSEB) are among the most effective treatment options. Systemic therapy is strictly preserved for advanced disease. Conventional chemotherapy (methotrexate, doxorubicin, vincristine), oral retinoids, IFN-alpha, alemtuzumab (monoclonal antibody), and histone deacetylase inhibitors such as Vorinostat and Romidepsin are the most common treatment of choice [1]. Ruling out SS utilizes better prognosis and a less aggressive treatment approach. The combined interferon – systemic photochemotherapy regimen initiated in our case proved beneficial, leading to partial clearing of the skin lesions.

Conclusion

Physicians should have a high index of suspicion for primary cutaneous lymphoid proliferation in any patient with therapy-resistant persistent pruritus. MF should be ruled out in patients with long-standing erythematous papules and plaques, progressing from confluent patches to generalized exfoliative dermatitis (erythroderma). Chronic erythroderma with atypical epidermotropic lymphoid cells, arranged in Pautrier's microabscesses and obscuring the dermal-epidermal junction is compatible with mycosis fungoides. The lack of peripheral blood monoclonal lymphoid cell inva-

sion ruled out SS, verifying erythrodermic MF. Regular follow-up visits and repeated skin biopsies are required to monitor the progression of MF to SS for better patient survival and outcome.

References

1. **Belousova, I., V. Khairutdinov, A. Bessalova, D. Kazakov.** Mycosis fungoides manifesting as giant cell lichenoid dermatitis. – *Am. J. Dermatopathol.,* **40**, 2018, 283-285.
2. **Brazzelli, V., N. Rivetti, G. Croci, G. Barbarini, C. Vassallo, M. Paulli, G. Borroni.** Long-term remission of erythrodermic mycosis fungoides after persistent control of hepatitis B infection. – *J. Eur. Acad. Dermatol. Venereol.,* **31**, 2017, 108-110.
3. **Chaudharry, S., C. Bansal, U. Ranga, K. Singh.** Erythrodermic mycosis fungoides with hypereosinophilic syndrome: a rare presentation. – *Ecancermedicalscience,* **7**, 2013, 337.
4. **Goyal, T., A. Varshney.** A rare presentation of erythrodermic mycosis fungoides. – *Cutis,* **89**, 2012, 229-232.
5. **Jawed, S., P. Myskowski, S. Horwitz, A. Moskowitz, C. Querfeld.** Primary cutaneous T-cell lymphoma (mycosis fungoides and Sézary syndrome): part I. Diagnosis: clinical and histopathologic features and new molecular and biologic markers. – *J. Am. Acad. Dermatol.,* **70**, 2014, 221-222.
6. **Megna, M., A. Sidikov, D. Zaslavsky, I. Chuprov, E. Timoshchuk, U. Egorova, J.Wenzel, R. Nasyrov.** The role of histological presentation in erythroderma. – *Int. J. Dermatol.,* **56**, 2017, 400-404.
7. **Olsen, E., E. Vonderheid, N. Pimpinelli.** Revisions to the staging and classification of mycosis fungoides and Sezary syndrome: a proposal of the International Society for Cutaneous Lymphomas (ISCL) and the cutaneous lymphoma task force of the European Organization of Research and Treatment of Cancer (EORTC). – *Blood,* **110**, 2007, 1713-1722.
8. **Vonderheid, E. C.** On the diagnosis of erythrodermic cutaneous T-cell lymphoma. – *J. Cutan. Pathol.,* **33**, 2006, 27-42.
9. **Vonderheid, E., G. Burg, M. Duvic, P. Heald, L. Laroche, E. Olsen, M. Pittelkow, R. Russell-Jones, M. Takigawa, R. Willemze.** Update on erythrodermic cutaneous T-cell lymphoma: report of the International Society for Cutaneous Lymphomas. – *J. Am. Acad. Dermatol.,* **46**, 2002, 95-106.

Institute of Experimental Morphology, Pathology and Anthropology with Museum
Bulgarian Anatomical Society

Acta morphologica et anthropologica, 26 (1-2)
Sofia ● 2019

Study of Amyloid Precursor Protein Developmental Changes in Homogenate, Membrane and Soluble Fractions Derived from Rat Brain, Skeletal Muscle, Kidney and Liver

Ludmil Kirazov, Evgeni Kirazov*

Institute of Experimental Morphology, Pathology and Anthropology with Museum, Bulgarian Academy of Sciencs, Sofia, Bulgaria

* Corresponding author e-mail: lkirazov@yahoo.com

In previous studies we have shown marked changes in the amyloid precursor protein (APP) expression during the period of synaptic contact formation, indicating an important role of APP in the synaptogenetic process. In the present study we investigated the changes in APP expression during ontogenesis at protein level in homogenate, membrane and soluble fractions from rat brain in order to obtain further data on the changes of APP processing/secretion. We also followed up the changes of the content of APP in skeletal muscle, kidney and liver.

The results show an increased expression of APP during synaptogenesis in brain. In the other organs a clear tendency of change in the content of APP is observed only in skeletal muscle. The lack of changes in postnatal development in kidney and liver confirms the hypothesis that the secretion of APP is a brain/nervous tissue-specific process.

Key words: amyloid precursor protein, ontogenetic changes, expression, peripheral organs

Introduction

Alzheimer's disease (AD) is the most common degenerative disease of the human brain and causes about 50% of dementias. It is generally accepted that APP is the centerpiece of the etiology of AD. APP is an integral membrane glycoprotein and contains the amino acid sequence of the amyloid beta peptide (Aβ). In the healthy brain APP is processed by an enzyme called alpha secretase, which cuts within the sequence of Aβ. As a result a large extracellular portion of APP is secreted into the intercellular space. There is also an alternative route of degradation via beta and gamma secretases that act at the ends of Aβ. In the diseased brain the balance between the secretases is disturbed and increased amounts of intact Aβ are formed, which is available for deposition in the senile plaques – the basic morphological hallmark of AD. Because senile plaques are

only observed in the brain, the interest in the metabolizing of APP and the role of its metabolites in the brain is enormous.

Despite the intensive research there is still no clarity about the physiological role of APP and its derivatives/metabolites. APP is believed to play the role of receptor as well as to participate in cell adhesion processes in embryonic tissue. Intact APP and its secreted forms can participate in cellular growth, cell-cell interactions, neurite outgrowth, synapse formation and maintenance, neuroprotection, homeostasis, blood coagulation and interact with receptors (e.g. p75 neurotrophin receptor [3]). APP can act in gene regulation through the cleaved C-terminal domain which translocates to the nucleus and activates gene transcription. On the other hand, Aβ has a neurotoxic effect [9] and leads to the loss of synapses [for reviews see 2, 4, 12, 13].

APP is expressed to a considerable extent in peripheral tissues and organs, however, the deposition of Aβ in senile plaques is specific to the brain alone. Very little is known about the role of APP and its derivatives in peripheral organs.

Interestingly, Maarouf et al. [11] observed that in AD patients there is an abnormal degradation of APP in the liver and hypothesize that this can contribute to the development of the disease.

In this study we followed up the changes of APP at the protein level in the homogenates, the membrane and soluble fractions prepared from brain, skeletal muscle, liver and kidney of rats during ontogenesis, starting at embryonic day (ED) 16 through to postnatal day (PD) 90. A comparative analysis of the results would help to clarify the role of APP metabolism in the brain and other organs.

Materials and Methods

The monoclonal Anti-APP A4 Antibody, clone 22C11 was purchased from Sigma Aldrich (Merck), Germany. All other reagents were commercial products of highest purity.

Pregnant Wistar rats were sacrificed on ED16. The fetuses were rapidly removed and brain, skeletal muscle and liver were dissected. For postnatal studies the brain, skeletal muscle, kidney and liver of Wistar rats at ages 1, 4, 7, 14, 20, 30, 60 and 90PD were rapidly removed.

The organs were carefully homogenized and the homogenates (H) were centrifuged at 100 000 × g for 1h at 4°C to yield the pelleted membrane fraction (P) and the soluble fraction (S).

Protein content was estimated by the method of Folin and Lowry as described earlier [6].

The proteins of the three fractions were separated by sodiumdodecylsulphate-polyacrylamide gel electrophoresis (SDS-PAGE) on 0.75 mm thick 12% slab gels. The protein load was 15 µg of protein per well. Western blotting and visualization of immunoreactive bands was performed as described [8]. The quantification of grey values of the immunoreactive bands was performed by densitometric scanning using a computer assisted imaging device and the 1D Image AnalysisSoftware from KODAK – EDAS 290. We have previously shown that the grey values produced by the visualization of immunoreactive bands are linearly dependent on the amount of protein loaded on the gel [7]. Electrophoretic separation of H, P and S fractions of the studied organs derived from different ages were blotted together to allow direct quantitative comparison of the age-related changes of APP levels.

The data represented on the figures are the means of two experiments, each performed in duplicate. The standard deviations did not exceed 15%.

Results and Discussion

The monoclonal antibody 22C11 employed in this study binds to an epitope in the N-terminal portion of the APP molecule, i.e. it recognizes both the intact APP molecules as well as the metabolites, obtained as a result of the activity of the proteases acting at the C-terminal. These comprise the secreted forms of APP which are found in the soluble fraction.

The changes in the levels of APP, assayed in the homogenates, membrane and soluble fractions from rat brain during the studied ontogenetic period are shown on **Fig. 1.** A clear-cut maximum in all fractions is evident during the period of vigorous synaptogenesis between PD1 and PD14, suggesting an essential role of APP in the process of targeting and establishing the synaptic contacts. This is accentuated by an increased secretion of APP metabolites during and after the onset of synaptic activity.

A comparative analysis of the distribution of protein and APP between the membrane and soluble fractions is presented on **Fig. 2.** Following the period of active synaptogenesis the amount of protein in the membrane fraction increases from some 53% to 72%, while the concentration of APP remains grossly unchanged, reflecting a decrease of APP content as a fraction of membrane protein. On the other hand the amount of protein in the soluble fraction decreases from some 47% to 38% and the amount of APP remains almost unchanged, suggesting that after synaptogenesis there is an increase of APP as percentage of the soluble fraction protein content. This is a further indication that the secretion of APP is under neurotransmitter control, since synapses have now been established and fully functional, confirming the view that it's processing is under neurotransmitter control [10].

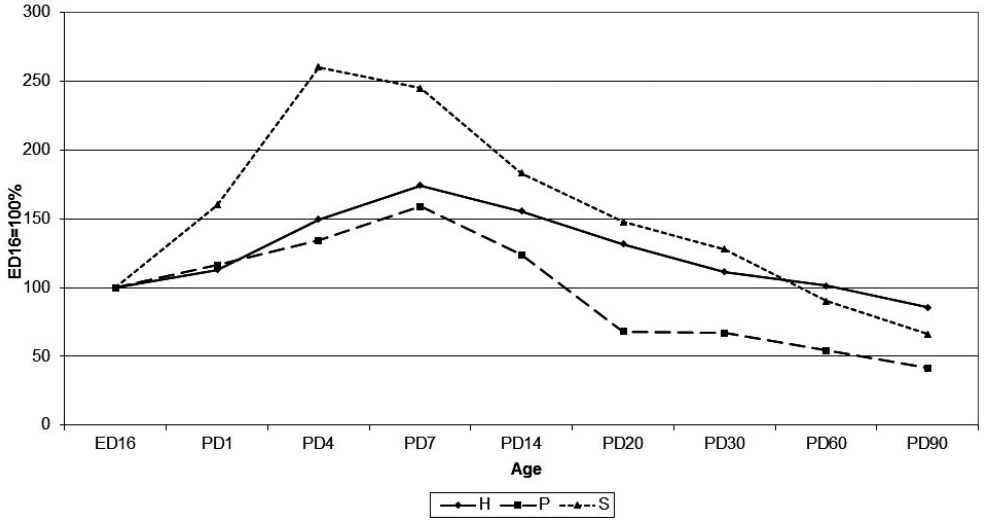

Fig.1. Age-related changes in APP level in rat brain H, P and S fractions. The data are calculated as grey values/μg protein and the value at ED16 is taken as 100%. The data are the means of two experiments, each performed in duplicate. The standard deviations did not exceed 15%.

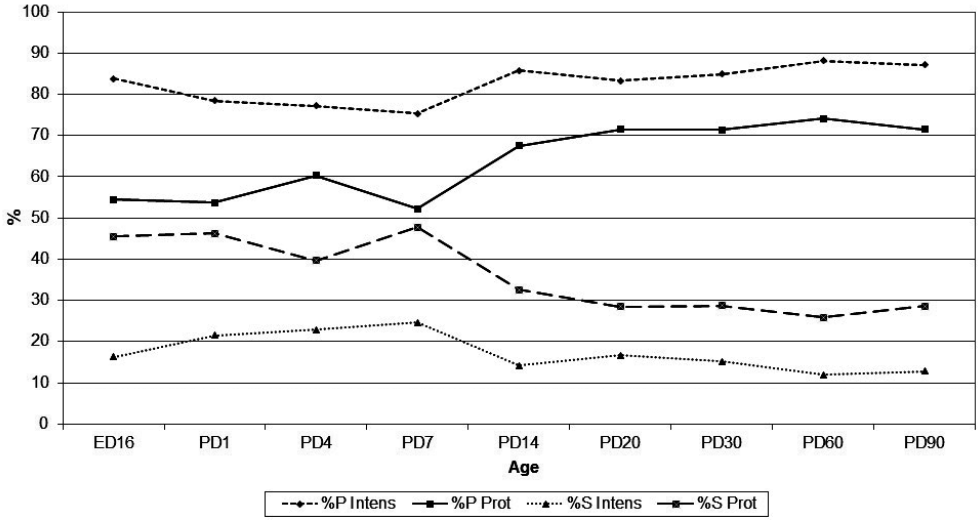

Fig. 2. Distribution (%) of protein and APP (grey values) between P and S fractions from rat brain during ontogenesis. The data are the means of two experiments, each performed in duplicate. The standard deviations did not exceed 15%.

A well-defined change of APP expression during the studied period was observed in skeletal muscle. After an initial high level of APP in embryonic muscle there is a decrease towards PD1 (**Fig. 3**). This change is most probably due to the participation of APP in the process of formation and consolidation of the neuromuscular junctions [15]. This suggestion is supported by histochemical studies, revealing the abundance of APP in the cytoplasm of myotubes at 16ED and an ensuing progressive concentration at the neuromuscular junction at birth [1, 14]. The continuous decline after PD1 to PD14 (**Fig. 3**) most probably reflects the process of elimination of synapses. At birth nearly all muscle fibers are polyneuronaly innervated. During the next two weeks the multiple innervation disappears until each muscle fiber is innervated by only one axon [5].

It has also been suggested that atypical processing of APP plays a role in the etiology of amyotrophic lateral sclerosis, a neurodegenerative muscle disease [16].

Examining the course of APP change in homogenates from kidney and liver we did not find any pronounced changes during ontogenesis (**Fig. 4**). The changes of APP in the membrane and soluble fractions follow the same course as these in homogenate. From the results shown in this figure it is also evident that APP is expressed to a much higher extent in the brain as compared to the other organs studied.

Conclusions

On the basis of our findings we can conclude that: a) The expression and procession/secretion of APP in brain during ontogenesis has unique features; b) The secretion of APP is a brain/nervous tissue-specific process; c) APP is expressed predominantly in the brain where its concentration exceeds several fold this in the other organs.

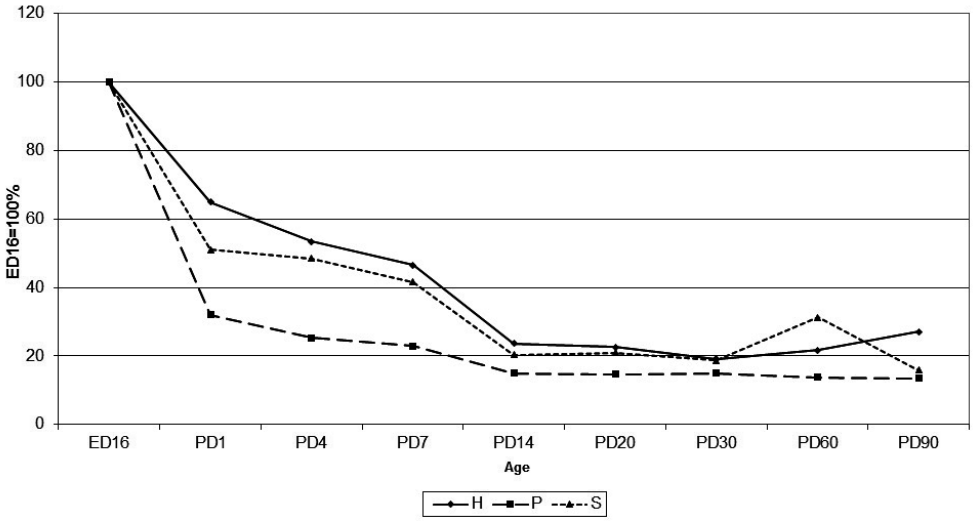

Fig. 3. Developmental changes of APP in H, P and S fractions from skeletal muscle. The data are calculated as grey values/µg protein and the value at ED16 is taken as 100%. The data are the means of two experiments, each performed in duplicate. The standard deviations did not exceed 15%.

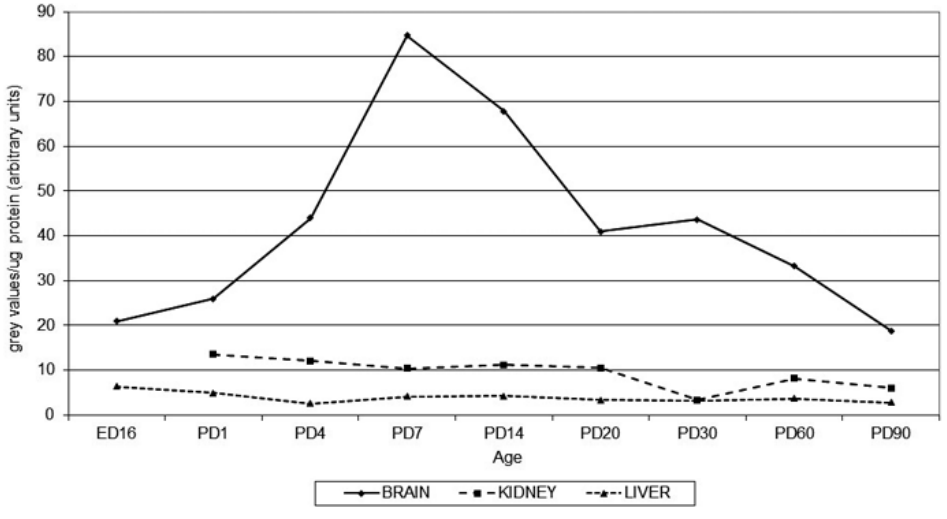

Fig. 4. Developmental changes of APP in H fractions from rat brain, kidney and liver. The data are expressed as arbitrary units, calculated on a grey values/µg protein basis.The data are the means of two experiments, each performed in duplicate. The standard deviations did not exceed 15%.

References

1. **Akaaboune, M., B. Alliquant, H. Farza, K. Roy, R. Magoul, M. Fiszman, B. W. Festoff, D. Hantai.** Developmental regulation of amyloid precursor protein at the neuromuscular junction in mouse skeletal muscle. – *Mol. Cell. Neurosci.,* **15**(**4**), 2000, 355-367.
2. **Dawkins, E., D. H. Small.** Insights into the physiological function of the β-amyloid precursor protein: beyond Azlheimer's disease. – *J. Neurochem.,* **129**(**5**), 2014, 756-769.
3. **Hasebe, N., Y. Fujita, M. Ueno, K. Yoshimura, Y. Fujino, T. Yamashita.** Soluble b-amyloid precursor protein alpha binds to p75 neurotrophin receptor to promote neurite outgrowth. – *PlOS ONE,* **8**(**12**), 2013, e82321.
4. **Kant, R. v. d., L. S. B. Goldstein.** Cellular functions of the amyloid precursor protein from development to dementia. – *Dev. Cell,* **32**, 2015, 502-515.
5. **Kasthuri, N., J. W. Lichtman.** The role of neuronal identity in synaptic competition. – *Nature,* **424**, 2003, 426-430.
6. **Kirazov, L., L. Venkov, E. Kirazov.** A comparison of the Lowry and the Bradford protein assays as applied for protein estimation of membrane-containing fractions. – *Anal. Biochem.,* **208**, 1993, 44-48.
7. **Kirazov, L., T. Loeffler, R. Schliebs, V. Bigl.** Glutamate-stimulated secretion of amyloid precursor protein from cortical rat brain slices. – *Neurochem. Int.,* **30**, 1997, 557-563.
8. **Kirazov, E., L. Kirazov, V. Bigl, R. Schliebs.** Ontogenetic changes in protein level of amyloid precursor protein (APP) in growth cones and synaptosomes from rat brain and prenatal expression pattern of APP mRNA isoforms in developing rat embryo. – *Int. J. Dev. Neurosci.,* **19**, 2001, 287-296.
9. **Kirazov, E., L. Kirazov, L. Venkov, E. Vassileva, S. Stuewe, D. G. Weiss.** Studies on the effects of the amyloidogenicA-ß-peptide on the electrical activity of neuronal networks cultured on microelectrode arrays. – *Acta morphol. anthropol.,* **7**, 2002, 9-16.
10. **Kirazov, L. P., E. P. Kirazov, C. L. Naydenov, V. I. Mitev.** Model systems and approaches to the study of the metabolism of Alzheimer's amyloid precursor protein. – *Acta morphol. anthropol.,* **21**, 2015, 55-61.
11. **Maarouf, C. L., J. E. Walker, L. I. Sue, B. N. Dugger, T. G. Beach, G. E. Serrano.** Impaired hepatic amyloid-beta degradation in Alzheimer's disease. – *PLOS ONE,* **13**(**9**), 2018, e0203659.
12. **Mueller, U. C., T. Deller, M. Korte.** Not just amyloid: physiological functions of the amyloid precursor protein family. – *Nat. Rev. Neurosci.,* **18**, 2017, 281-298.
13. **Nalivaeva, N. N., A. J. Turner.** The amyloid precursor protein: a biochemical enigma in brain development, function and disease. – *FEBS Lett.,* **587**, 2013, 2046-2054.
14. **Puig, K. L., C. K. Combs.** Expression and function of APP and its metabolites outside the central nervous system. – *Exp. Gerontol.,* **48**(**7**), 2013, 608-611.
15. **Wang, P., G. Yang, D. R. Mosier, P. Chang, T. Zaidi, Y. D. Gong, N. M. Zhao, B. Dominguez, K. F. Lee, W. B. Gan, H. Zheng.** Defective neuromuscular synapses in mice lacking amyloid precursor protein (APP) and APP-like protein 2. – *J. Neurosci.,* **25**, 2005, 1219-1225.
16. **Yang, H.** Enhanced β-secretase processing of amyloid precursor protein in the skeletal muscle of ALS animal models. – *bioRxiv*, **352401**; 2018, doi: https://doi.org/10.1101/352401.

Institute of Experimental Morphology, Pathology and Anthropology with Museum
Bulgarian Anatomical Society

Acta morphologica et anthropologica, 26 (1-2)
Sofia ● 2019

Expression of GHS-R1 in the Stomach of Male and Female Rats after High-Fat, High-Carbohydrate Diet

Nadya Penkova[1], Petar Hrischev[2], Katerina Georgieva[2], Pepa Atanassova[1]*

[1] Department of Anatomy, Histology and Embryology, Medical University-Plovdiv, Bulgaria;
[2] Department of Physiology, Medical University-Plovdiv, Bulgaria

* Corresponding author e-mail: nadja_penkova@abv.bg

The aim of our work was to investigate the expression of ghrelin receptor (GHS-R1) in the stomach of dietary-manipulated rats by high-fat-high-carbohydrate-diet (HFHCD). Wistar rats (5 male, 5 female) were fed HFHCD for 16 weeks. Control rats (5 male, 5 female) were fed with standard rat chew for the same period of time. Metabolic control was determined by measuring body weight gain and BMI. Immunohistochemical study was performed on the stomach of both groups with primary ghrelin receptor GHS-R1 antibody. Results: We found positive expression of GHS-R1 in the stomach fundus and antral glandular cells of the experimental rats. The reaction had moderate and high intensity in single and clusters of cells. HFHCD activates the expression of GHS-R1 in the gastric mucosa in both sexes.GHS-R1 presence indicates the ability of ghrelin to affect the secretory activity of the ghrelin-producing cells in paracrine/autocrine way and allow for autonomous regulation of gastric secretion, different from other hormonal and nerve pathways.

Key words: ghrelin, GHS-R1, stomach, high-fat-high-carbohydrate diet, rats

Introduction

The involvement of ghrelin in the pathogenetic mechanisms of obesity is intensively studied but still not evaluated in details [19]. The ghrelin secretion depends on humoral factors such as blood glucose levels or insulin secretion, respectively; as well as external factors – the composition of the ingested nutrients. The hormonal regulation of the ghrelin secretion is affected by a number of circulating and gastrointestinal hormones [4,23,25]. Intravenous administration of glucagon caused transient increases of ghrelin levels and this effect was shown to be mediated by glucagon receptors on ghrelin cells [14]. De la Cour et al. found that epinephrine, norepinephrine, endothelin, and secretin stimulated ghrelin release [8]. GHS-R1A is a mature polypeptide expressed in brain and some peripheral tissues, GHS-R1B is an immature polypeptide [1,5,11,16]. Kitazawa et al. [15] reported of presence of GHS-R1 in gastrointestinal tract of rat and guinea pig.There is an evidence for an endocrine/paracrine role for ghrelin in the reproductive tissues [17]. Ghrelin and GHS-R1 have been found to regulate the proliferation of cancer cells in astrocytoma and glioblastoma by an autocrine/paracrine mechanism [9,18]. Some authors explore the potential functional role of ghrelin and its receptor in hormone-dependent cancers, such as

prostate and breast cancer [12]. There are fine autoregulatory mechanisms, performed by the autocrine/paracrine effect of ghrelin on the ghrelin-producing cells themselves in the stomach [10,22]. It is concluded that ghrelin may affect gastrointestinal motility via specific ghrelin receptors [20]. Obesity and insulin resistance may play an important role in the release of ghrelin [24]. Obesity selectively impairs the stimulatory effect of a caseinhydrolyaste on ghrelin release in the fundus [26].

The aim of our work is to investigate the immunohistochemical (IHC) expression of ghrelin receptor GHS-R1 in the stomach of dietetic manipulated male and female rats by high-fat-high-carbohydrate diet.

Materials and Methods

Male and female Wistar rats (5 male, 5 female)were fed with high-fat-high-carbohydrate diet (HFHCD) for 16 weeks. Control male and female rats (5 male, 5 female) were fed a normal diet for the same period of time. Metabolic control was determined by measuring body weight and BMI. Two-way ANOVA statistic analysis was used.Immunohistochemical study was performed on the stomach of the both groups with primary ghrelin receptor antibody (goat polyclonal antibody GHS-R1: sc-10351 – Santa Cruz Biotechnology USA). GHS-R1, was diluted in PBS in 1:100 ratio. We used a semi-quantitative evaluation method for the obtained results. We accept the presence of expression of the primary antibody as a positive result, and as a negative – the lack of its expression. Positive reaction for GHS-R1 was reported in the presence of fine brown granulation in the cell cytoplasm. The specificity of immunohistochemical reactions was confirmed by negative controls in which the specific antibodies are substituted with a buffer (PBS). In them there was a complete lack of a product of the respective reaction. Observation and photo documentation of microscopic preparations were performed with digital photo microscopic camera of a light microscope "Olympus BX51".

Results

Metabolic control. The obtained results showed that from the beginning of the study until the 11th week there were no significant differences in the body weight of the animals. From the 12th week until the end of the experiment the HFHCD had a significant main effect on the body weight ($P<0.05$). At the end of the experiment the dietary-manipulated (male and female) rats had higher body weight in comparison with the controls (357.33 ± 12.24 g vs 320.42 ± 12.24 g, $P<0.05$) (**Fig. 1.**). At the end of the experiment dietary-manipulated rats had a higher BMI as compared to the control rats (0.69 ± 0.02 g·cm-² vs 0.63 ± 0.02 g·cm-², $P < 0.01$).

Immunohistochemical expression of GHS-R1 in the stomach.The immunohistochemical response for GHS-R1in the stomach of the rat control group was negative (**Fig.2.A.**). The glands in the stomach mucosa showed typical characteristics. There was no expression of GHS-R1 in the different types of cells - parietal, chief, foveolar, as well as in the enteroendocrine cells (**Fig. 2.B.**). In the experimental groups of animals, we detected a positive immunohistochemical reaction for ghrelin receptor GHS-R1. We observed fine brown granules in the cytoplasm of some cells from gastric glands (**Fig. 3A**). Some of the GHS-R1-positive cells were located in groups along the tubular glands of the stomach body (**Fig. 3.B**). In the transverse sections of the gastric glands the expression engaged the basal parts of the cells (**Fig. 4.A**). The larger number of GHS-R1-positive cells had a moderate intensity of the immunohistochemical reaction. Some cells with high intensity of the immunohistochemical reaction were also observed (**Fig. 4.B**).

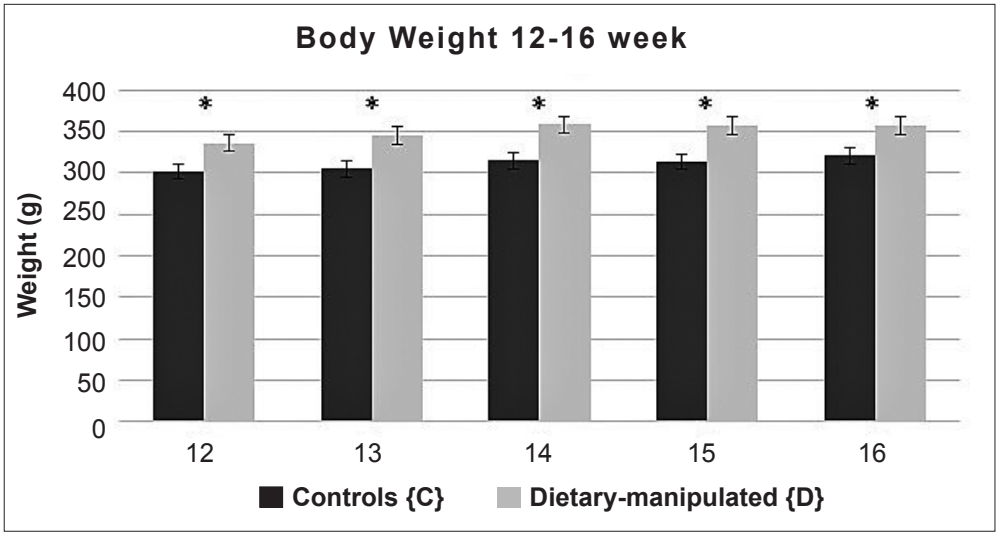

Fig. 1. Weight (g) of dietary-manipulated and control groups from the 12th week until the end of the experiment. *P<0.05, dietary-manipulated vs controls.

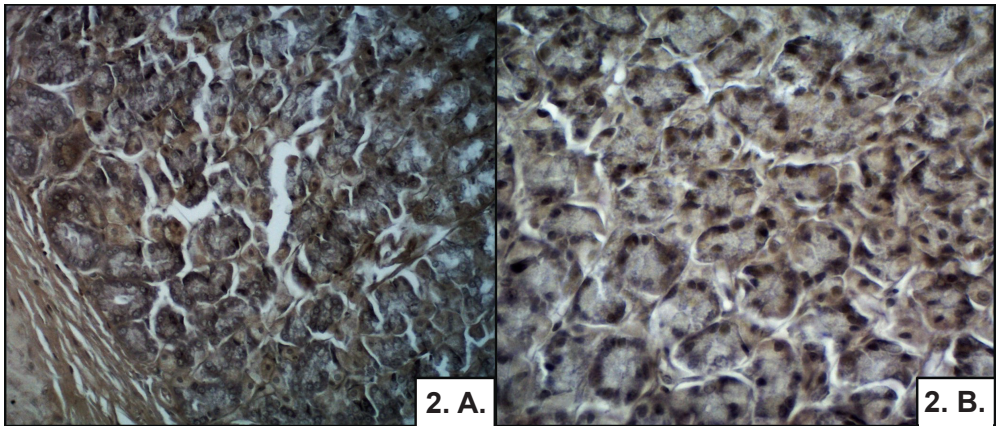

Fig. 2. Control group. IHC reaction for GHS-R1. A. Female rats. Stomach – body. Negative IHC reaction for GHS-R1 in fundic glands. Magn. × 200. B. Male rats. Stomach – body. Cross-section of fundic glands without expression of GHS-R1 in the different cell types. Magn. × 400.

Discussion

We report for the first time of influence of HFHCD on the expression of ghrelin receptor in the stomach of rats of both sexes. In our study the rats from the experimental groups subjected to a long-term HFHC diet demonstrated obesity with significant differences in body weight and BMI compared to the animals of the control groups.We detected presence of expression of GHS-R1 in the stomach body and antrum of the experimental rats, while the reaction for the receptor in the control groups was negative. Some authors report for GHS-R1 expression in the gastrointestinal tract of rat but this expression is located in

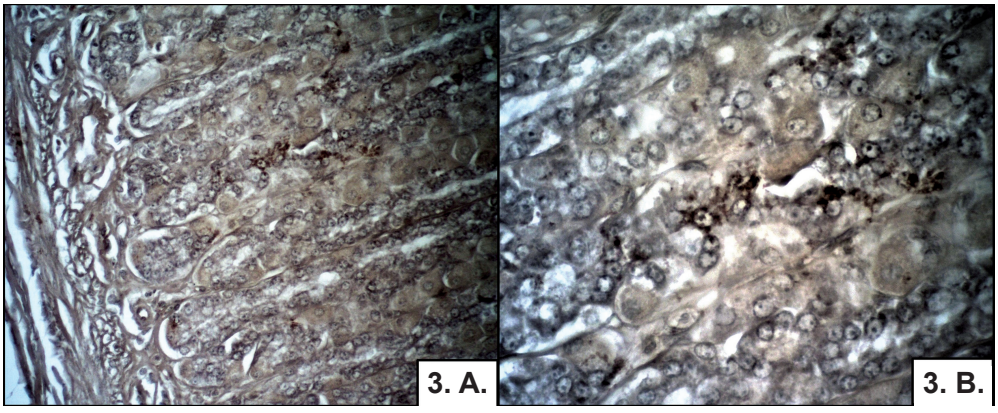

Fig. 3. Experimental group. IHC reaction for GHS-R1. A. Female rats. Stomach – body. GHS-R1-positive cells cells in the fundic glands with moderate intensity of the reaction. Magn. × 200. B. Female rats. Stomach – body. A group of GHS-R1-positive cells in the fundic glands. Magn. × 400.

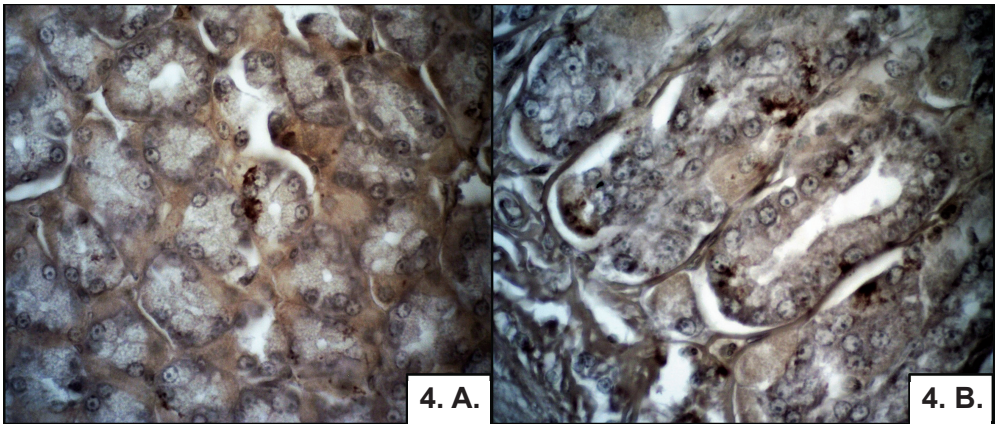

Fig. 4. Experimental group. IHC reaction for GHS-R1. A. Male rats. Stomach - body. Single GHS-R1-positive cells in the fundic glands. Expression of GHS-R1 in the basal part of the cells. Magn. × 400. B. Male rats. Stomach – anthrum. GHS-R1-positive cells in the pyloric glands with moderate to high intensity of the reaction. Magn. × 400.

the smooth muscle cells of the wall [15]. The GHS-R1 positive expression in the gastric mucosa showed that ghrelin could have an endocrine and paracrine effect on the cellsin the gastric glands. Ghrelin could affect in an autocrine/paracrine way the ghrelin-producing cells themselves. Changes in expression level and/or cell density are supposed to be accompanied with a consumption of high HFHCD. Feeding a HFHCD might affect the expression of fatty acid receptors or the number of lipid sensing cells as well as ghrelin-producing cell populations.

The long-term intake of dietary fat is supposed to be associated with adaptive reactions of the organism and it is assumptive that this is particularly true for fat responsive epithelial cells in the mucosa of the gastrointestinal tract [27]. May be HFHCD is also associated with similar adaptive reactions through the ghrelin-producing cells in the gas-

tric glands via the activation of the ghrelin receptors. Whether these changes are a consequence of the direct exposure to high fats and carbohydrates in the luminal content or a physiological response to them in the body remains elusive. Ghrelin shows orexigenic effect through its action on the hypothalamic appetite-regulating pathways, while in the periphery it increases adipose tissue accumulation [2]. In contrast to other forms of obesity, patients with Prader-Willi syndrome display reduced visceral adiposity and high levels of ghrelin [21]. Peripheral ghrelin induces a depot-specific increase in white adipose tissue mass by GHS-R1A-mediated lipolysis [7]. Although the precise mechanisms governing the export of free fatty acids from adipocytes remain to be elucidated [3,13]. Some authors concluded that exposure to ghrelin appears to induce adipocyte hypertrophy by enhancing lipid retention in responsive adipocytes [7]. Ghrelin can exert its effects in the regulation of feeding behavior and energy homeostasis and through systemic or autocrine/paracrine actions [6,22].

Conclusion

The HFHCD applied to male and female rats activates the expression of ghrelin receptor GHS-R1 in the gastric mucosa. These results imply that the diet leads to significant changes in the cellular repertoire of the stomach mucosa. GHS-R1 presence in the gastric mucosa cells indicates the ability of ghrelin to affect the secretory activity of the ghrelin-producing cells in both paracrine and autocrine way. Auto/paracrine action of ghrelin allows autonomous regulation of gastric secretion, different from other hormonal and nerve pathways. This possibility makes the stomach adaptive to the excessive conditions such as HFHCD.

Acknowledgements: The study was funded by the Medical University of Plovdiv (Project № SDP 09 / 2015).

References

1. **Albarrán-Zeckler, R. G., R. G. Smith.** The ghrelin receptors (GHS-R1a and GHS-R1b). – *Endocr. Dev.,* **25**, 2013, 5-15.
2. **Álvarez-Castro, P., L. Pena, F. Cordido.** Ghrelin in obesity, physiological and pharmacological considerations. – *Mini Rev. Med. Chem.,* **13**, 2013, 541-552.
3. **Bonen, A., A. Chabowski, J. J. Luiken, J. F. Glatz.** Is membrane transport of FFA mediated by lipid, protein, or both? Mechanisms and regulation of protein-mediated cellular fatty acid uptake: molecular, biochemical, and physiological evidence. – *Physiology (Bethesda),* **22**, 2007, 15-29.
4. **Broglio, F., Pv. Koetsveld, A. Benso, C. Gottero, F. Prodam, M. Papotti, G. Muccioli, C. Gauna, L. Hofland, R. Deghenghi, E. Arvat, A. J. Van Der Lely, E. Ghigo.** Ghrelin secretion is inhibited by either somatostatin or cortistatin in humans. – *J. Clin. Endocrinol. Metab.,* **87**, 2002, 4829-4832.
5. **Callaghan, B., J. B. Furness.** Novel and conventional receptors for ghrelin, desacyl-ghrelin, and pharmacologically related compounds. – *Pharmacol. Rev.,* **66**, 2014, 984-1001.
6. **Castañeda, T. R., J. Tong, R. Datta, M. Culler, M. H. Tschöp.** Ghrelin in the regulation of body weight and metabolism. – *Front. Neuroendocrinol.,* **31**, 2010, 44-60.
7. **Davies, J. S., P, Kotokorpi, S. R. Eccles, S.K. Barnes, P. F. Tokarczuk, S. K. Allen, H. S. Whitworth, I. A. Guschina, B. A. Evans, A. Mode, J. M. Zigman, T. Wells.** Ghrelin induces abdominal obesity via GHS-R-dependent lipid retention. – *Mol. Endocrinol.,* **23**, 2009, 914-924.
8. **De la Cour, C. D., P. Norlén, R. Håkanson.** Secretion of ghrelin from rat stomach ghrelin cells in response to local microinfusion of candidate messenger compounds: a microdialysis study. – *Regul. Pept.,* **143**, 2007, 118-126.

9. **Dixit, V. D., A. T. Weeraratna, H. Yang, D. Bertak, A. Cooper-Jenkins, G. J. Riggins, C. G. Eberhart, D. D. Taub.** Ghrelin and the growth hormone secretagogue receptor constitute a novel autocrine pathway in astrocytoma motility. – *J. Biol. Chem.,* **281**, 2006, 16681-16690.
10. **Higgins, S. C., M. Gueorguiev, M. Korbonits.** Ghrelin, the peripheral hunger hormone. – *Ann. Med.,* **39**, 2007, 116-136.
11. **Howard, A. D., S. D. Feighner, D. f. Cully, J. P. Arena, P. A. Liberator, C. I. Rosenblum M. Hamelin, D. L. Hreniuk, O. C. Palyha, J. Anderson, P. S. Paress, C. Diaz, M. Chou, K. K. Liu, K. K. McKee, S. S. Pong, L. Y. Chaung, A. Elbrecht, M. Dashkevicz, R. Heavens, M. Rigby, D. J. Sirinathsinghji, D. C. Dean, D. G. Melillo, A. A. Patchett, R. Nargund, P. R. Griffin, J. A. DeMartino, S. K. Gupta, J. M. Schaeffer, R. G. Smith, L. H. Van der Ploeg.** A receptor in pituitary and hypothalamus that functions in growth hormone release. – *Science,* **273**, 1996, 974-977.
12. **Jeffery, P. L., A. C. Herington, L. K. Chopin.** The potential autocrine/paracrine roles of ghrelin and its receptor in hormone-dependent cancer. – *Cytokine Growth Factor Rev.,* **14**, 2003, 113-122.
13. **Kampf, J. P., A. M. Kleinfeld.** Is membrane transport of FFA mediated by lipid, protein, or both? An unknown protein mediates free fatty acid transport across the adipocyte plasma membrane. – *Physiology (Bethesda),* **22**, 2007, 7-14.
14. **Katayama, T., S. Shimamoto, H. Oda, K. Nakahara, K. Kangawa, N. Murakami.** Glucagon receptor expression and glucagon stimulation of ghrelin secretion in rat stomach. – *Biochem. Biophys. Res. Commun.,* **357**, 2007, 865-870.
15. **Kitazawa T, T. Nakamura, A. Saeki, H. Teraoka, T. Hiraga, H. Kaiya.** Molecular identification of ghrelin receptor (GHS-R1a) and its functional role in the gastrointestinal tract of the guinea-pig. – *Peptides,* **32**, 2011, 1876-1886.
16. **Laviano, A., A. Molfino, S. Rianda, F. Rossi Fanelli.** T he growth hormone secretagogue receptor (Ghs-R). – *Curr. Pharm. Des.,* **18**, 2012, 4749-4754.
17. **Miller, D. W., J. L. Harrison, Y. A. Brown, U. Doyle, A. Lindsay, C. L. Adam, R. G. Lea.** Immunohistochemical evidence for an endocrine/paracrine role for ghrelin in the reproductive tissues of sheep. – *Reprod. Biol. Endocrinol.,* **3**, 2005, 60.
18. **Okada, Y., Y. Sugita, K.Ohshima, M. Morioka, S. Komaki, J. Miyoshi, H. Abe.** Signaling of ghrelin and its functional receptor, the growth hormone secretagogue receptor, promote tumor growth in glioblastomas. – *Neuropathology,* **36**, 2016, 535-543.
19. **Papandreou, D., C. Karavolias, F. Arvaniti, E. Kafeza, F. Sidawi.** Fasting. Ghrelin Levels Are Decreased in Obese Subjects and Are Significantly Related With Insulin Resistance and Body Mass Index. – *Open Access Maced. J. Med. Sci.,* **5**, 2017, 699-702.
20. **Peeters, T. L.** Central and peripheral mechanisms by which ghrelin regulates gut motility. – *J. Physiol. Pharmacol.,* **54**, 2003, 95-103.
21. **Scerif, M., A. P. Goldstone, M. Korbonits.** Ghrelin in obesity and endocrine diseases. – *Mol. Cell. Endocrinol.,* **340**, 2011, 15-25.
22. **Shiiya, T., M. Nakazato, M. Mizuta, Y. Date, M. S. Mondal, M. Tanaka, S. Nozoe, H, Hosoda, K. Kangawa, S. Matsukura.** Plasma ghrelin levels in lean and obese humans and the effect of glucose on ghrelin secretion. – *J. Clin. Endocrinol.Metab.,* **87**, 2002, 240-244.
23. **Shimada, M., Y. Date, M. S. Mondal, K. Toshinai, T. Shimbara, K. Fukunaga, N. Murakami, M. Miyazato, K. Kangawa, H. Yoshimatsu, H. Matsuo, M. Nakazato.** Somatostatin suppresses ghrelin secretion from the rat stomach. – *Biochem. Biophys. Res. Commun.,* **302**, 2003, 520-525.
24. **Stylianou, C., A. Galli-Tsinopoulou, D. Farmakiotis, I. Rousso, M. Karamouzis, G. Koliakos, S. Nousia-Arvanitakis.** Ghrelin and leptin levels in obese adolescents. Relationship with body fat and insulin resistance. – *Hormones (Athens),* **6**, 2007, 295-303.
25. **Tan, T. M., M. Vanderpump, B. Khoo, M. Patterson, M. A. Ghatei, A. P. Goldstone.** Somatostatin infusion lowers plasma ghrelin without reducing appetite in adults with Prader-Willi syndrome. – *J. Clin. Endocrinol. Metab.,* **89**, 2004, 4162-4165.
26. **Vancleef, L., T. Thijs, F. Baert, L. J. Ceulemans, E. Canovai, Q. Wang, S. Steensels, A. Segers, R. Farré , J. Pirenne, M. Lannoo, J. Tack, I. Depoortere.** Obesity Impairs Oligopeptide/Amino Acid-Induced Ghrelin Release and Smooth Muscle Contractions in the Human Proximal Stomach. – *Mol. Nutr. Food Res.,* **62**, 2018. doi: 10.1002/mnfr.201700804.
27. **Widmayer, P., H. Goldschmid, H. Henkel, M. Küper, A. Königsrainer, H. Breer.** High fat feeding affects the number of GPR120 cells and enteroendocrine cells in the mouse stomach. – *Front. Physiol.,* **6**, 2015, 53.

Institute of Experimental Morphology, Pathology and Anthropology with Museum
Bulgarian Anatomical Society

Acta morphologica et anthropologica, 26 (1-2)
Sofia ● 2019

Brain Morphological Changes in Immature Mice after Perinatal Exposure to Cobalt Chloride

Emilia Petrova[1], Yordanka Gluhcheva[1], Ekaterina Pavlova[1], Ivelin Vladov[1], Alexey A. Tinkov[2], Yulia V. Zaitseva[2], Anatoly V. Skalny[2]*

[1] *Institute of Experimental Morphology, Pathology and Anthropology with Museum – Bulgarian Academy of Sciences, Sofia, Bulgaria*
[2] *P. G. Demidov Yaroslavl State University, Yaroslavl, Russia*

* Corresponding author e-mail: emiliapetrova@abv.bg

Abstract

Over the last years, human activities have considerably increased the levels of cobalt (Co) in the environment. Cobalt overexposure is associated with serious health risks, especially in children. The aim of the present study was to examine the effects of perinatal Co treatment on the brain morphology in immature mice. Eighteen-day-old mice were subjected to cobalt chloride ($CoCl_2$) exposure 2-3 days prior to birth and during the postnatal period. The histopathological studies revealed substantial cerebral and cerebellar damage with features of neuronal necrosis compared to the age-matched healthy controls. In the cerebrum, the neurons, glial cells and the neuropil were affected, as well the Purkinje cells in the cerebellum.
The results are indicative of the enhanced susceptibility of the immature brain to the exposure of cobalt. They contribute to the elucidation of the neurotoxic potential of the metal and the related health risks in newborns and infants, especially in regions with cobalt pollution.

Key words: cobalt chloride, immature mouse brain, morphological changes

Introduction

Cobalt is a naturally-occurring trace element with a wide range of industrial and medical applications. It is essential to mammals and, being a key component of vitamin B12, cobalt is necessary for a variety of biological processes. Nevertheless, the inorganic form of the metal is toxic and excessive levels can induce various adverse health effects. The intense anthropogenic activities utilizing cobalt and its compounds result in extensive environmental pollution and human exposure. In daily life, humans are exposed to Co through inhalation, drinking water and food. Occupational exposure is also considered as an important route of uptake, as well as internal exposure through cobalt containing implants [11].

Cobalt toxicity has been documented in animal and human studies. The available literature data indicate that cobalt has also a neurotoxic potential. It has been shown

that Co can induce neural cell death, neurotransmitter deficits and inhibition of the synaptic transmission, reactive oxygen species generation and behavioural alterations [2]. Though, there are scanty data for the effects of perinatal Co exposure during late prenatal and early postnatal period on brain morphology of the offspring. According to Garoui et al. [4], their study has evaluated for the first time cerebral and cerebellar damages induced by Co treatment during late pregnancy and early postnatal periods in rats. The present study was undertaken to investigate the brain morphological changes in suckling mice after perinatal cobalt chloride exposure.

Material and Methods

Animal model

Mature ICR mice were purchased from the Experimental and breeding base for laboratory animals (EBBLA) - Slivnitza, Bulgaria, and left to acclimatize for a week prior to the initiation of experiment. Animals were maintained in the Institute's animal breeding facility at 23±2°C and 12:12 h light/dark cycle in individual standard hard-bottom polypropylene cages. The mice were fed a standard diet and had access to food ad libitum with strong control of the feeding regime. Pregnant mice were subjected to a daily dose of 75 mg/kg body weight cobalt chloride ($CoCl_2 \times 6H_2O$) 2-3 days before they gave birth and treatment continued until day 18 after delivery. The compound was dissolved and administrated with drinking tap water. The suckling pups were sacrificed by decapitation after etherization on day 18. Brains were excised, weighed and processed for histological studies. Age-matched mice obtaining regular tap water were used as a control group.

The experimental design was carried out in accordance with guidelines EU Directive 2010/63/EU for animal experiments.

Histological analysis

Brains from control and Co-exposed mice were fixed in Bouin fixative for 24 h and paraffin-embedded. Briefly, after fixation, the samples were dehydrated in a graded series of ethanol, cleared with xylene, impregnated in molten paraffin, embedded in fresh molten paraffin and sectioned into 5-μm thickness sections using a microtome. Subsequently, the sections were stained with hematoxylin and eosin (HE) and observed on a light microscope Leica DM 5000B (Leica Microsystems, USA).

Results

Our observations in controls showed normal architecture of the cerebral and cerebellar cortex. Studies on cerebral samples demonstrated intact neurons with round nuclei, centrally located within the perikaryon, and prominent nucleoli (**Fig. 1 a, b**). Morphologically normal glial cells and brain capillaries were also observed.

The cerebellar cortex was composed of three layers: the deep granular layer, the Purkinje cell layer and the superficial molecular layer (**Fig. 2 a, b**). The Purkinje cells (PC) were well differentiated and arranged in a single row of large neurons with pear-shaped perikaryon and large nucleus. A single binucleate PC in the granular layer was also observed, as well a few mononucleate PC with the same heterotopic location.

Perinatal exposure of suckling mice to cobalt chloride resulted in substantial brain morphological changes compared to the untreated control animals. The changes

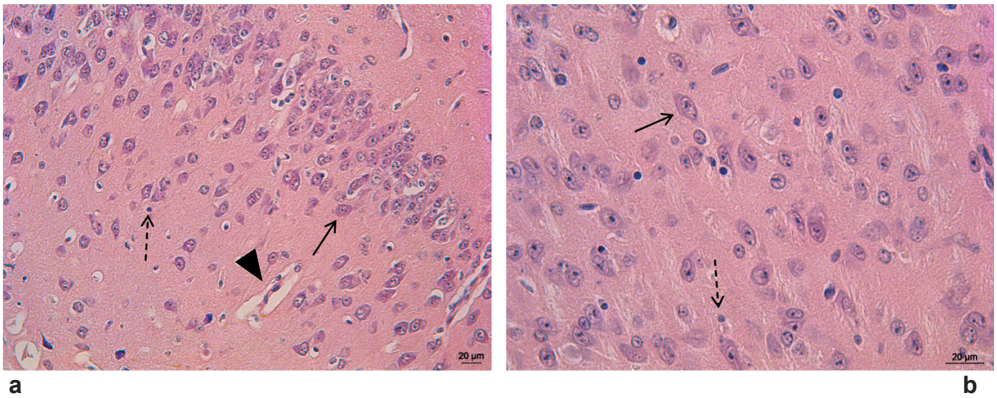

Fig. 1. Light microphotograph of the cerebral cortex of 18-day-old mice, hematoxylin-eosin staining. Untreated control, 200× (a), 400× (b): neurons (arrow) with normal nuclei, normal glial cells (dash arrow) and blood vessels (arrowhead).

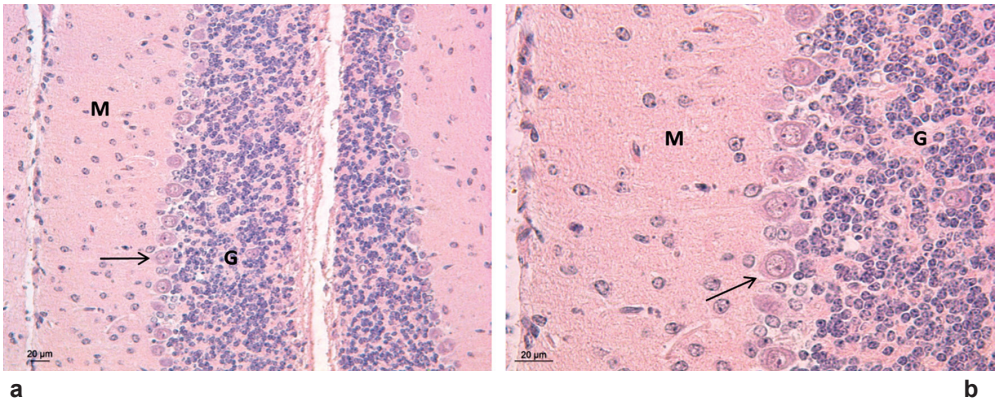

Fig. 2. Light microphotograph of the cerebellar cortex of 18-day-old mice, hematoxylin-eosin staining. Untreated control, 200× (a), 400× (b): different layers of the cerebellar cortex: molecular layer (M), Purkinje cell layer (arrow) and granular layer (G).

were accompanied by a significant decrease in the body weight of Co-exposed mice ($p<0.0002$). In contrast, brain weight index, calculated as organ-to-body weight ratio, was significantly increased by ~32.8% ($p<0.0001$) compared to the untreated age-matched control animals.

Histopathological studies in Co-treated mice demonstrated damaged cerebral and cerebellar cortices with features of neuronal necrosis compared to the untreated controls. In the cerebrum, abnormal basophilic neurons with atrophic shrunken perikarya and darkly stained pyknotic nuclei were present (**Fig. 1 c, d**). Prominent perineuronal and periglial spaces, as well as enlarged perivascular spaces and blood vessels with reactive endothelial cells were also observed. The neuropil appeared vacuolated.

In the cerebellum, along with the intact PC with distinctly stained nucleus, shrunken and darkly stained necrotic PC with enlarged pericellular spaces were found

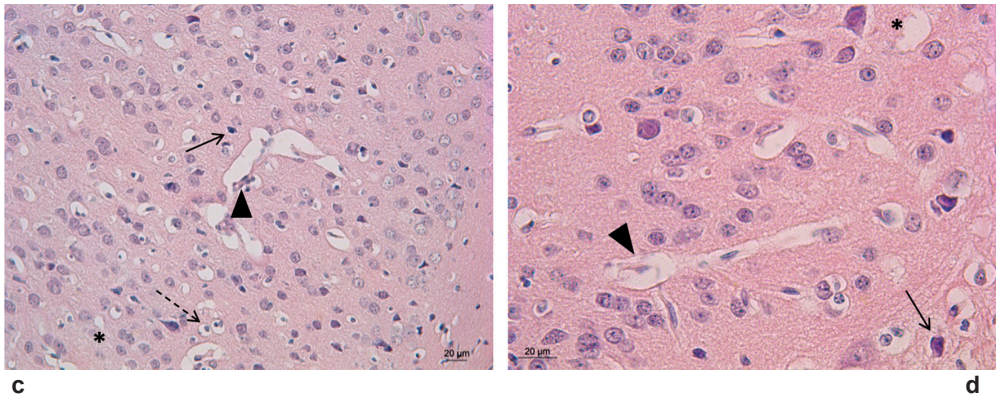

Fig. 1. Light microphotograph of the cerebral cortex of 18-day-old mice, hematoxylin-eosin staining. $CoCl_2$-exposed mice, 200× (c), 400× (d): neuronal necrosis characterized by many shrunken, darkly stained pyknotic neurons (arrow) with prominent perineuronal spaces; enlarged periglial spaces (dash arrow); dilated perivascular spaces and reactive endothelial cells (arrowhead) and vacuolation (asterisk).

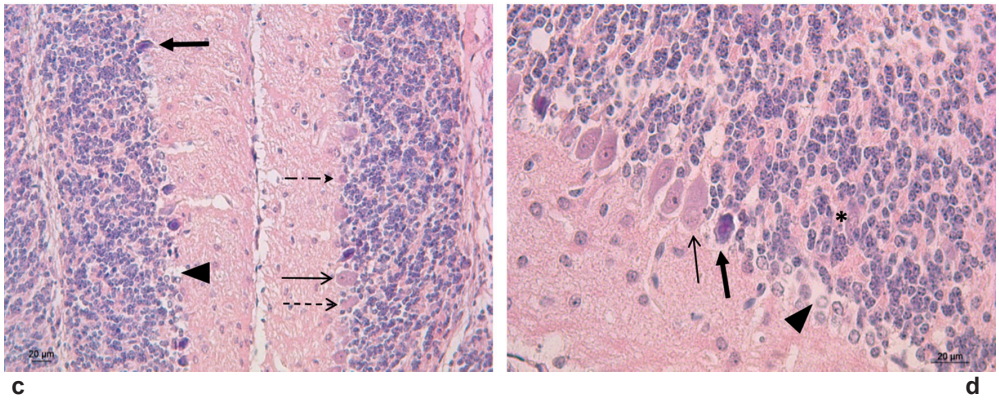

Fig. 2. Light microphotograph of the cerebellar cortex of 18-day-old mice, hematoxylin-eosin staining. $CoCl_2$-exposed mice, 200× (c), 400× (d): pyknotic PC (thick arrow), autolytic PC (dash arrow), PC with irregular shape (dash-dot arrow), loss of PC (arrowhead), binucleate PC (thin arrow), heterotopic PC in the granular layer (asterisk).

(**Fig. 2 c, d**). Some autolytic PC lacking nuclear staining and fading out of cytoplasm were observed. Our findings also demonstrated PC with irregular shape, loss of PC, a few binucleate PC, as well as PC in the granular layer.

Discussion

The results of the present study reveal that perinatal exposure of mice to $CoCl_2$ during late prenatal and early postnatal period affects the weight and the architecture of their brains. It is known that the developing central nervous system (CNS) is most sensitive to the influence of environmental factors namely throughout gestation and during the neonatal period. Moreover, the cerebellum is considered more vulnerable to neurotoxic agents than other brain regions [4, 5] and this is well demonstrated by our histopathological findings.

Besides neurotoxic, $CoCl_2$ is known as a hypoxia-mimicking agent which activates hypoxia-mediated signaling pathways. It is the most frequently used agent in both *in vivo* and *in vitro* experimental models for inducing chemical hypoxia [16]. Cobalt ions can substitute the iron ions in prolyl hydroxylases, the key enzymes in the regulation of oxygen homeostasis and the response to hypoxia. Thus, the enzyme activity is inhibited, leading to the accumulation of hypoxia-inducible factor-1α.

Our findings for significantly lower body weight of mice born to mothers exposed to $CoCl_2$ are in agreement with the results obtained in hypoxia models. For example, Minior et al. [14] and Tong et al. [19] demonstrate that chronic hypoxia during late pregnancy caused a significant reduction in the body weight of rat pups. The authors also report reduced brain size, indicating a developmental retardation via the activation of cell death pathways. In fact, fetal and postnatal brain damage due to hypoxia is well documented and is reported to depend on the duration, intensity of oxygen deprivation and age of the fetus and the pup [12]. In contrast, we estimated increased brain weight and brain weight index in Co-exposed suckling mice. A similar tendency of brain weight increase is associated with cerebral edema in many neurological conditions (hemorrhagic stroke, ischemic stroke, traumatic brain injury, brain tumors, etc.) [7].

Cobalt is among the elements actively transported across the placenta and the breast milk, causing temporary or permanent brain injury in the offspring [4, 9]. In the present study, the histopathological manifestation of Co-induced brain damage in the suckling mice is well demonstrated. The changes include vacuolation in the neuropil and different neural cell types affected by the exposure. Some cortical neurons appeared shrunken with pyknotic nuclei and enlarged perineuronal spaces. Increased periglial and perivascular spaces were also observed, as well reactive capillary endothelial cells. Our findings are in agreement with the results of Mohamed et al. [15], obtained for the adult $CoCl_2$-exposed rat cerebrum. In contrast, the study of Garoui et al. [4] in $CoCl_2$-exposed suckling rats indicated a normal structure of the treated cerebrums.

The Purkinje cells in our study showed a heterogeneous pattern of changes. They appeared shrunken with pyknotic nucleus, autolytic with no nucleus and no distinct cellular morphology, irregular in shape. Areas with loss of PC were also observed. Similar findings in the cerebellum were reported by Garoui et al. [4]. Their study was performed on 14-day-old rats, and at this postnatal age, the cerebellar cortex is still consisted of four layers. The authors observe markedly developed external granular layer which is suggested to be an indication of a delayed migration of granular cells towards the molecular layer and the internal granular layer.

Our histological examination in $CoCl_2$-exposed suckling mice showed some PC present in the granular layer. Since we have found a single PC with this heterotopic location in the untreated mice, it may be due to defective migration that causes the Purkinje cells to end-up trapped in the white matter tracts or granular layer [10]. In the mice born to $CoCl_2$-treated mothers, Purkinje cells in the granular layer could be a result of the exposure, as the same heterotopic location has been reported following prenatal exposure to X-radiation [3].

Moreover, binucleate PC were observed both in control and Co-exposed suckling mice. It has been shown that under normal physiological conditions, although extremely rarely, migration and fusion of bone marrow-derived stem cells with neuronal cells, predominantly Purkinje cells, occurs [20]. Paltsyn and Komissarova [18] suggest that the appearance of the second nucleus is a form of physiological and reparative regeneration of Purkinje cells. Because of the low frequency of Purkinje cell fusion under normal physiological conditions, some authors hypothesize that its role is negligible and fusion is a transient event [8, 17]. Magrassi et al. [13] suggest that this cell fusion represents a physiological phenomenon to introduce young nuclei or functional genes in

aged or degenerating cells. In fact, binucleate PC are more frequently demonstrated in old and sick mammals, therefore their occurrence is considered a compensatory mechanism for the age-related or pathogenic loss of Purkinje cells. Inflammation and other pathological conditions in rodents and humans have been shown to promote migration and infiltration of bone marrow-derived stem cells to the site of brain injury [8]. Based on the above, the observed binucleate PC in $CoCl_2$-treated suckling mice in our study may be suggested as a sequel of the exposure to the toxic metal.

One of the major mechanisms of heavy metal toxicity is the generation of oxidative stress [6]. Garoui et al. [4] have demonstrated development of oxidative stress and impairment of defense systems even in the cerebrum and cerebellum of suckling pups born to Co-exposed pregnant and lactating rats.

The brain histopathological findings in the present investigation are not surprising since the developing CNS is extremely sensitive to disruption. The vulnerable period extends from the beginning of organogenesis to the postnatal period. Unlike humans, the cerebellum in rodents is relatively immature at birth and the postnatal period is characterized by intense neuronal proliferation, migration and differentiation [1]. Therefore, Co exposure during this critical period may have a deleterious impact on the structure and maturation of the brain.

Conclusions

Exposure of mice to CoCl2 during late prenatal and early postnatal period affects body and brain weight and provokes cerebral and cerebellar histopathological changes. Our data are indicative of the enhanced susceptibility of the immature brain to the exposure of cobalt. The results contribute to the elucidation of the neurotoxic potential of the metal and the related health risks in newborns and infants, especially in highly industrialized areas.

Acknowledgements: The study was supported by Grants No. DNTS/Russia 02/1/14.06.2018 from the Bulgarian National Science Fund and No. 18-54-18006 from the Russian Foundation for Basic Research.

References

1. **Biran, V., C. Verney, D. M. Ferriero.** Perinatal cerebellar injury in human and animal models. – *Neurol. Res. Int., 2012.* Available at http://dx.doi.org/10.1155/2012/858929.
2. **Catalani, S., M. C. Rizzetti, A. Padovani, P. Apostoli.** Neurotoxicity of cobalt. – *Hum. Exp. Toxicol.,* **31**(**5**), 2012, 421-437.
3. **Darmanto, W., M. Inouye, Y. Takagishi, M. Ogawa, K. Mikoshiba, Y. Murata.** Derangement of Purkinje cells in the rat cerebellum following prenatal exposure to X-irradiation: decreased Reelin level is a possible cause. – *J. Neuropathol. Exp. Neurol.,* **59**(**3**), 2000, 251-262.
4. **Garoui, E., I. Ben Amara, D. Driss, A. Elwej, S. E. Chaabouni, T. Boudawara, N. Zeghal.** Effects of cobalt on membrane ATPases, oxidant, and antioxidant values in the cerebrum and cerebellum of suckling rats. – *Biol. Trace Elem. Res.,* **154**, 2013, 387-395.
5. **Hasebe, M., I. Matsumoto, T. Imagawa, M. Uehara.** Effects of an anti-thyroid drug, methimazole, administration to rat dams on the cerebellar cortex development in their pups. – *Int. J. Dev. Neurosci.,* **26**, 2008, 409-414.
6. **Jomova, K., V. Marian.** Advances in metal-induced oxidative stress and human disease. – *Toxicology,* **283**, 2011, 65-87.
7. **Keep, R. F., Y. Hua, G. Xi.** Brain water content: a misunderstood measurement? – *Transl. Stroke Res.,* **3**(**2**), 2012, 263-265.

8. **Kemp, K., E. Gray, A. Wilkins, N. Scolding.** Purkinje cell fusion and binucleate heterokaryon formation in multiple sclerosis cerebellum. – *Brain,* **135**(**10**), 2012, 2962-2972.
9. **Kratchler, M., S. L. E. Rossipal, K. J. Irgolic.** Changes in the concentrations of trace elements in human milk during lactation. – *J. Trace Elem. Med. Biol.,* **12**, 1998, 159-176.
10. **Larouche, M., U. Beffert, J. Herz, R. Hawkes.** The Reelin receptors Apoer2 and Vldlr coordinate the patterning of Purkinje cell topography in the developing mouse cerebellum. – *PloS ONE,* **3**(**2**), 2008, e1653.
11. **Leyssens, L., B. Vinck, C. Van Der Straeten, F. Wuyts, L. Maes.** Cobalt toxicity in humans – A review of the potential sources and systemic health effects. – *Toxicology,* **387**, 2017, 43-56.
12. **Mach, M., M. Dubovický, J. Navarová, I. Brucknerová, E. Ujházy.** Experimental modeling of hypoxia in pregnancy and early postnatal life. – *Interdiscip. Toxicol.,* **2**(**1**), 2009, 28-32.
13. **Magrassi, L., P. Grimaldi, A. Ibatici, M. Corselli, L. Ciardelli, S. Castello, M. Podestà, F. Frassoni, F. Rossi.** Induction and survival of binucleated Purkinje neurons by selective damage and aging. – *J. Neurosci.,* **27**, 2007, 9885-9892.
14. **Minior, V. K., B. Levine, A. Ferber, S. Guller, M. Y. Divon.** Nucleated red blood cells as a marker of acute and chronic fetal hypoxia in a rat model. – *Rambam Maimonides Med. J.,* **8**(**2**), 2017, e0025.
15. **Mohamed, A. A. R., M. M. Metwally, S. R. Khalil, G. A. Salem, H. A. Ali.** Moringa oleifera extract attenuates the CoCl2 induced hypoxia of rat's brain: Expression pattern of HIF-1α, NF-kB, MAO and EPO. – *Biomed. Pharmacother.,* **109**, 2019, 1688-1697.
16. **Muñoz-Sánchez, J., M. E. Chánez-Cárdenas.** The use of cobalt chloride as a chemical hypoxia model. – *J. Appl. Toxicol.,* 2018, 1-15. Available at https://doi.org/10.1002/jat.3749.
17. **Nern, C., I. Wolff, J. Macas, J. von Randow, C. Scharenberg, J. Priller, S. Momma.** Fusion of hematopoietic cells with Purkinje neurons does not lead to stable heterokaryon formation under noninvasive conditions. – *J. Neurosci.,* **29**(**12**), 2009, 3799-3807.
18. **Paltsyn, A. A., S. V. Komissarova.** Binuclear Purkinje neurons. – *Patol. Fiziol. Eksp. Ter.,* **60**(**4**), 2016, 107-113 [in Russian].
19. **Tong, W., W. Chen, R. P. Ostrowski, Q. Ma, R. Souvenir, L. Zhang, J. H. Zhang, J. Tang.** Maternal hypoxia increases the activity of MMPs and decreases the expression of TIMPs in the brain of neonatal rats. – *Dev. Neurobiol.,* **70**(**3**), 2010, 182-194.
20. **Weimann, J. M., C. A. Charlton, T. R. Brazelton, R. C. Hackman, H. M. Blau.** Contribution of transplanted bone marrow cells to Purkinje neurons in human adult brains. – *Proc. Natl. Acad. Sci. USA,* **100**, 2003, 2088-2093.

Institute of Experimental Morphology, Pathology and Anthropology with Museum
Bulgarian Anatomical Society

Acta morphologica et anthropologica, 26 (1-2)
Sofia ● 2019

Newly Synthesized Polymer Hydrogels and Hydroxyapatite Nanoparticles (nHAP) for Biomedical Application: Histological and Biochemical Studies in Rats

Katerina Todorova[1], Veselin Nanev[1], Ivelin Vladov[1], Petar Dimitrov[1], Elena Vassileva[2], Elena Dyulgerova Taneva[3], Radosveta Vassileva[3], Margarita Gabrashanska[1]*

[1] *Institute of Experimental Morphology, Pathology and Anthropology with Museum, Bulgarian Academy of Sciences, Sofia, Bulgaria*
[2] *Laboratory on Structure and Properties of Polymers, Department of Pharmaceutical and Applied Organic Chemistry, Faculty of Chemistry and Pharmacy, Sofia University "St. Kl. Ohridski", Sofia, Bulgaria*
[3] *Dental Medicine Faculty, University of Medicine, Sofia, Bulgaria*

* Corresponding author e-mail: katerinagencheva@yahoo.com

Abstract

The development of biocompatible zwitterionicpolymers and polymer-reinforced calcium phosphate pastes and cements in combination with specific drugs, has been considered as a promising strategy in bone tissue engineering and dental medicine. The main purpose of this work was to evaluate the relationship between physicochemical and mechanical properties of newly synthesized polymer hydrogels and hydroxyapatite nanoparticles (nHAP) and their biocompatibility *in vivo*. Standard hematological, biochemical and histological laboratory tests with Wistar rats and statistical analysis of the data obtained were performed. The results from the histological, hematological and biochemical analyses revealed that all tested materials are characterized by good biocompatibility and biodegradation. No hard inflammatory effects were noticed, only slight foreign body reaction responses were observed. The histological findings made by us confirmed the acceptance of the implanted materials and the good tolerance to their componential compounds.

Key words: zwitterionic polymers, histological, hematological and biochemical tests

Introduction

Application and development of biocompatible zwitterionic polymers and composite polymer-reinforced calcium phosphate pastes and cements in combination with specific

drugs, have been considered as a promising strategy in biomedicine. In bone tissue engineering and dental medicine with beneficial effects are used calcium-phosphate (Ca-P) cements and pastes (hydroxyapatite (HA) (self-setting HA or brushite (dicalcium phosphate dihydrate (DCPD)) and collagen [2, 6]. Due to their good biocompatibility and extensive bone conductivity they are applied as substitutes in orthopedic and reconstructive surgery. These products possess certain limitations and studies investigate the development and the incorporation mainly in composed of polymer reinforced synthetic materials as an alternative strategy for biomaterials which mimic the extracellular matrix of bone tissue. Compounds with promising usage in surgery especially as an effective wound regeneration system are zwitterionic polymers due to their chemical structure resemble many naturally occurring substances. Polycarboxybetaines (PCB) are analogues to the betaine form of α-amino acids and have the lowest protein absorption found. Polysulfobetaines (PSB) have also a zwitterionic moiety but they do not have a naturally existing analogue. Zwitterionic polymers are able to absorb the excess of exudate and prevent bacteria adhesion and the formation of biofilms [3], useful in biomedical application.

The main purpose of this work was to study and evaluate the relationship between synthesis, boundary phase and mechanical properties of newly synthesized polymer hydrogels and hydroxyapatite nanoparticles (nHAP) on one hand and the biological response on the other hand, by applying modern methodologies, the results of which to serve as a scientific base for the design of a broad range of biomaterials. We focused in our survey on composite polymer-reinforced calcium phosphate pastes and poly (sulfobetaine and carboxybetainemethacrylate) (PSB, PCB) networks with promising addendum in wound dressing procedures,surgery and dental medicine.

Materials and Methods

Study on synthesis and properties

Synthesis of polymer-reinforced nanometric calcium phosphates /hydroxyapatite nanoparticles/ was performed for molar pulp coverage. For the synthesis of poly (sulfobetaine methacrylate) (PSB) and poly(carboxybetaine methacrylate) (PCB) networks substances (PSB in aqueous solution; PCB dissolved in ethylene glycol / ethanol / distilled water in a 3:1:1 ratio) were mixed with initiators $K_2S_2O_8$ or $Na_2S_2O_5$, $(NH_4)\ S_2O_8$ and the cross-linking agent PEGDA or N,N'-Methylenebisacrylamide with varying concentrations. The compound was homogenized and then allowed to cross-linking polymerization carried out at 60° for 6 – 15 hours. The resulting hydrogels were purified from the unreacted reagents by dipping them into a large amount of distilled water. The water was changed every day within 2 weeks as the waters were monitored with UV every day. Some of the prepared networks after drying, in order to obtain PSB + CaP, were immersed in a 0.6M $CaCl_2$ solution, where they stayed for 48 hours. The samples were washed with water and immersed in a 0.3M solution of K_2HPO_4. There the samples sank for a week, removing the crust from the precipitated calcium phosphates.

Physical, chemical and biochemical characterization of biomaterials was performed, mainly the prepared polymer networkswere studied, due to their specificity as swelling kinetics; rheological behavior; salt effect on the swelling behavior; their temperature sensitivity; swelling capacity in simulated body fluid and enzyme absorption concerning their in vitro collagenase and myeloperoxidase inhibitory activity and *ex vivo* inhibitory activity of hydrogels against collagenase in wound exudates. Standard investigation on calcium and zinc binding ability, bacterial growth inhibition and cytotoxicity were also evaluated, before applying in live organisms, in order to validate the stability and safety.

In vivo biocompatibility testing

Animal design and implantation of biomaterials

In vivo studies were performed in order to test the biological response of the polymer hydrogels and bruschite cements (HA). The tests were performed on experimental rats and the defects were introduced on soft tissues (subcutaneous, near the muscles application) and hard tissues (teeth).

All procedures were consistent with the definitions and recommendations for in vivo animal studies, designed to provide initial evidence of medical device safety, potential performance when used in a living system, and/or the biologic response to the device, in accordance with International Standard ISO 10993 -1:2009 for biological evaluation of medical devices and criteria for evaluation set out in ISO 7405:1997 conserving tissue and inflammatory reactions, and ISO 10003-6, 2007 Part 6- Tests for local effects after implantation. The animal usage was in accordance with the requirements and Regulation № 15/ 03.02.2006 regarding laboratory animals and animal welfare.

I A and I B *in vivo* experiments: 48 Wistar male rats were used in both experiments (24 animals in I A experiment and 24 – in I B experiment). The animals were divided into 6 groups (4 animals in each group in IA and the same scheme in IB experiment):

I A experiment – the 1st group consisted of animals without implantation, from the 2nd tothe 6th group – implantation of PSB networks with cross-linking agent PEGDA mol. % from 0,1 to 3 was performed.

I B experiment – animals from the 1st to the 3th group were implantated with PSB CaP networks, additionally immersed with $CaCl_2$ and K_2HPO_4.(PSP CaP), those from the 4th to the 6th –implantation with PCB networks was done.

An aseptic surgical procedure was used after standard ketamine &xylazine anesthesia in appropriate doses. Sterilized implants were inserted in the fossa poplitea near to the fascial superficies of biceps femoral muscle and m. semitendinosus. After 12 weeks of evaluation period all animals were humanely euthanized. To enable access to the subcutaneous space and implants were made incisions full thickness through the skin and surrounding muscle tissues.

In the II *in vivo* experiment: 4 Wistar male rats were used with molar implantation of hydroxyapatite nanoparticles according to standard dentistry procedures.

A new procedure was developed for creating initial artificial caries of intact teeth (incisors and molars) in a gel medium with lactic acid and in a collagen gel with acrylic and metacrylic acids, resulting in enamel defects. The created initial artificial caries is subjected to subsequent remineralization with the hybrid hydroxyapatite materials obtained. A model for direct pulp coverage on test animals was created by inducing tertiary dentinogenesis. An aseptically procedure was used after standard ketamine and xylazine anesthesia of rats in appropriate doses. Sterilized implants were inserted in the pulp cavity. After 8 weeks of evaluation period all animals were humanely euthanized. Materials from teeth were processed for histology.

Standard hematological and biochemical laboratory tests were performed on blood and serum parameters. The markers of bone metabolism (total alkaline phosphatase (TAP) activity and bone alkaline phosphatase (BAP), calcium (Ca), phosphorus (P), as well as markers of potential hepatotoxicity (aspartate aminotransferase and alanine aminotransferase activity (ASAT, ALAT) etc. were measured on semi-automated biochemical analyser BC-88A (MINDRAY, China), hematological indicators were determined on hematological analyzer BC 2800 (MINDRAY, China).

Ca and P content in soft tissues was determined by a standard atomic absorption method.

The element content changes in soft tissues around the implants are an important early indicator of biochemical homeostasis and some parameters of the body's reactivity to the implants.

Statistical analysis of the results

The statistical analysis of the data were be made by GraphPADInStat, Software, USA and using one-way ANOVA, followed by Bonferroni's post hoc test. The results were presented as $x\sim \pm$ S.E.M. Statistical significance was marked as follows: *** $P<0.001$.

Histological procedures for light microscopy.

After surgical excision tissue samples (10/10/10mm in size) with introduced implants were routinely fixed in 10% buffered formalin, rinsed in water and placed in 8% formic acid for demineralization. After dehydration in graded ethanol and xylene clearing, materials were embedded in paraffin. Tissue sections (3-5 μm thick) were stained in hematoxylin and eosin (H&E) and examined by a light microscope (Leica DM 5000B, Wetzlar, Germany).

The sections were examined standardly for the presence of a fibrous capsule and its thickness, newly formed vessels, foreign body reaction and occurrence of various types of inflammatory cells. Evaluation system of three categories was used to measure the microscopic observations. The inflammatory reactions were scored according to the following criteria (ISO_7405):

No reaction or slight reaction: Fibrous capsule formation and absence of inflammatory cells or presence of a fibrous capsule formation with few lymphocytes and plasmocytes.

Moderate reaction: Fibrous capsule formation with the presence of macrophages (MA), polymorphonuclear leukocytes (PMNL), lymphocytes, and plasmocytes.

Severe reaction: Presence of large accumulations of PMNL, lymphocytes, plasmocytes, macrophages, foreign-body giant cells, and congested capillaries.

Results and Discussion

The results from the histological, hematological and biochemical analyses revealed that all tested materials are characterized by good biocompatibility andgood biodegradation; they do not cause hard inflammatory effects, and induce only slight foreign body reaction responses.

Ca and ALP levels (**Figs. 1, 2**) were slightly elevated in PSB CaP group (**Fig. 3**) compared to the controls and the other experimental groups, while that of P (**Figs. 1, 3**) remained similar to that of other groups. It can be assumed that the increased activity of ALP was associated with upcoming processes of demineralization of the implant, containing Ca and the ability these networks to serve as donation capacity to the surrounding tissues, if used in bone defects implementation surgery. The values of the parameters in the other groups were similar and there was no evidence of deviations from the norm. Biochemical parameters suggest good biocompatibility of the new materials with the experimental model tissues.

The local mini-environment in soft tissues reflects and responds to implants. Immune environmental reactivity studies are the initial step to investigate the biocompatibility of materials as tissue substitutes.

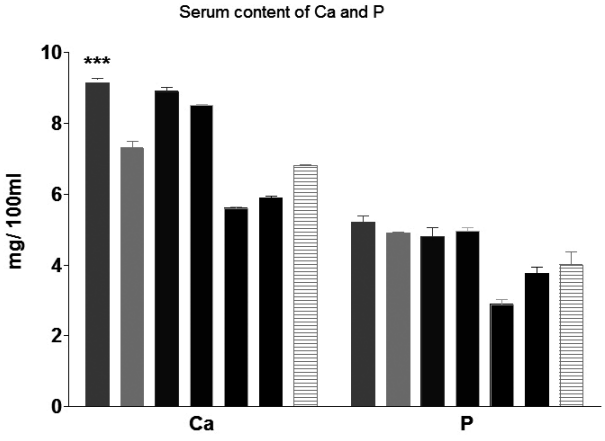

Fig. 1. Serum content of calcium (Ca) and phosphorus (P).

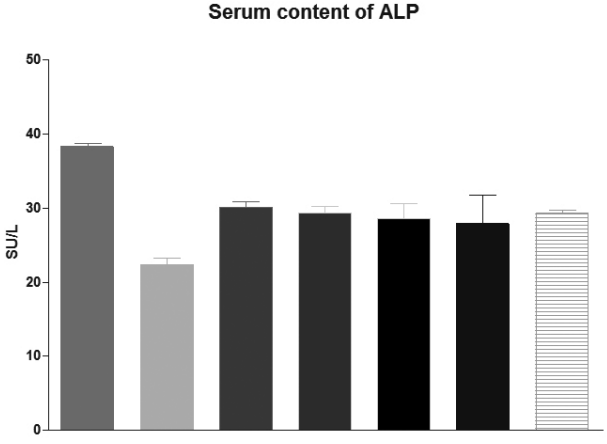

Fig.2. Serum content of alkaline phosphatase (ALP).

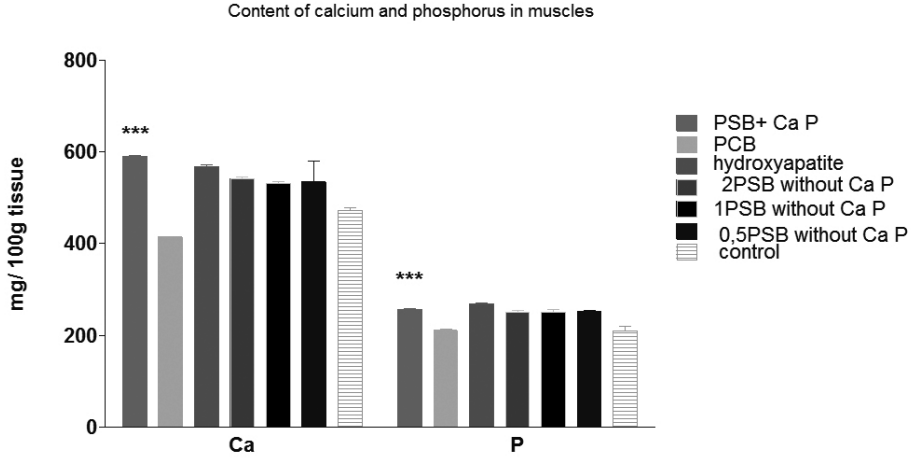

Fig. 3 Content of calcium (Ca) and phosphorus (P) in muscles

The histological aspects revealed regeneration- reparation processes around the introduced implants in soft tissues and in teeth. After the application in the muscle fascial space, a recovery of the surroundings was observed (**Fig.4 a,b**). Signs of a slight non-cellular edema were presented between loose fascial strands and hyalinization of some collagenous fibers was noticed. Newly formed capillaries perforating the nearby tissues and closely attached to the neoformative peripheral fibrous capsule were also found. Progressive fibroblast population and endothelial cells forming the intracapsularneovasculature were presented. As dominant early responders to biomaterial implantation tissue macrophages composing foreign body reactions were noticed. The lymphoplasmocytic reaction was negligible.

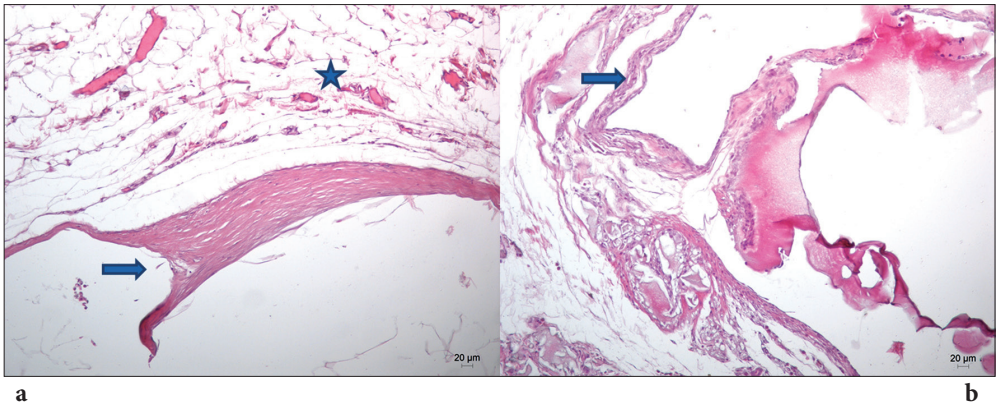

a **b**

Fig.4 a, b. Formation of a thin fibrous capsule (arrow) and newly formed capillaries (5-point star) peripherally to the neoformative fibrous tissues. H&E.

In terms of dental implants, a good general feeling was observed, and after feeding with soft food at the beginning, the animals moved seamlessly to solid, regular granular food. Histologically, filling of the pulp cavity with nanometric hydroxyapatite material, reflected in proliferation reaction of cementoblasts and cementocytes and production of non-cellular cement. This finding is connected with the response of the organism and is a healing reaction to the trauma processes during dental procedures. The main affirmative finding for positive tissue acceptance of the materials implanted was the intended proliferation of dentin producing odontoblasts, due to the hydroxyapatite stimulation, under the artificial defects created (**Fig. 5**). No signs of inflammatory dental granuloma were observed.

This biomedical evaluation assessed the used materials as not producing any adverse local or systemic effects. Histopathological signs of necrosis, calcification or residual effect or material intolerance were not evidential in selected areas of implantation. No signs of acute inflammation were noticed, only occasional lymphocytes and MA in some specimens. All materials had shown good biocompatibility and were assessed in first and second criteria of ISO_7405. The objective to validate the organism tolerance towards the used biomaterials as substitutional therapeutic agents was clearly resumed via histological and biochemical aspects of this study.

The histological findings made by us validated the acceptance of the polymer materials and the good tolerance to their componential compounds. Observation of biomaterial-tissue interfaces are important markers for the lifetime of the medical devices tested. Biomaterial surface properties play a crucial role in modulating the foreign body

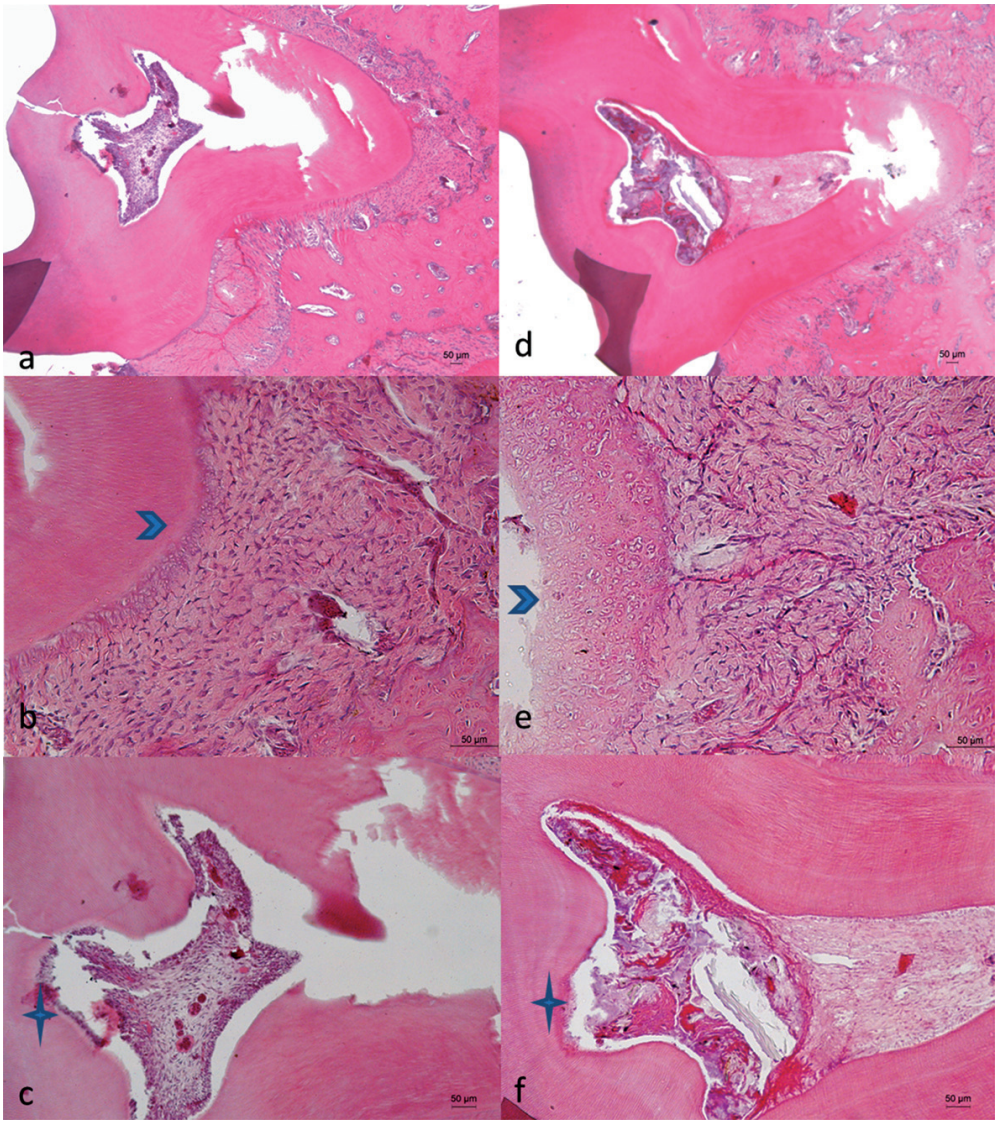

Fig. 5a, b, c. Intact tooth: odontoblasts (4-point star), layer of cellular and cell-free cement) (arrow head); d,e,f -Treated tooth, deposited material in the pulp, a small number of visible odontoblasts (4-point star), a proliferative reaction of the top layer of cellular and cell-free cement, protective response of root to trauma (arrow head). H&E.

reaction in the first several weeks following implantation of medical devices. Macrophage function in the body is to mediate degradation and phagocytosis of bioresorbable materials including foreign body reaction. These chronic inflammatory processes are essential in wound healing responses and may impact biocompatibility of implanted materials, their short- and long-term success in tissue engineering and regenerative medicine. Implantation *in vivo* always provokes cellular and tissue responses as stages in inflammatory and wound healing process, following application of biomaterials.

Moreover the formation of fibrous connective tissue around the implants is indicative of good tolerance by the surrounding tissues, according to [5] and [4] as well as the well-developed new vascularization.

Conclusions

- The biochemical and histological findings made by us confirm the acceptance of the implanted materials and the good tolerance to their component compounds.
- The observed processes of inflammation, proliferation and remodeling in the healing of wounds after implantation have their significance in studding biocompatibility and have a specific place in implantology.
- Surface properties of biomaterials play a crucial role in modulating the foreign reaction during the first few weeks after the implantation of medical devices, and are often an integral part of these processes [1, 7].
- The formation of a fibrous capsule and well-developed neoangiogenesis around the implants is indicative of good tolerance from the surrounding tissues [4, 5].

Acknowledgments: This work was financially supported by the Bulgarian Ministry of Education and Science under Project DFNI T02-5/2014-2017and by the Operational Programme "Science and Education for Smart Growth" 2014-2020, co-financed by the European Union through the European Structural and Investment Funds, Grant BG05M2OP001-2.009-0019-C01 from 02.06.2017.

References

1. **Anderson, J. M., A. Rodriguez, D. T. Chang.** Foreign body reaction to biomaterials. – *Semin. Immunol.,* **20**, 2008, 2, 86-100.
2. **Dorozhkin, S. V.** Calcium orthophosphates. – *J. Mater. Sci.,* **42**, 2007, 4, 1061-1095. doi:10.1007/s10853-006-1467-8
3. **Liu, P., G. Xu, D. Pranantyo, L. Q. Xu, K. G.Neoh, E. T. Kang.** pH-Sensitive Zwitterionic Polymer as an Antimicrobial Agent with Effective Bacterial Targeting. – *ACS Biomater Sci. Eng.,* **4**, 2017, 1, 40-46.
4. **Maher, W. P., R. L. Johnson, J. Hess, H. R. Steiman.** Biocompatibility of retrograde filling materials in the ferret canine Amalgam and IRM. – *Oral. Surg. Oral Med. Oral Pathol.,* **73**, 1992, 6, 738-745.
5. **Marcotte, L. R., J. Dowson, N. H. Rowe.** Apical healing with retrofilling materials amalgam and gutta-percha. – *J. Endod.,* **1**, 1975, 2, 63-65.
6. **Perez, R. A., H. W. Kim, M. P.Ginebra.** Polymeric additives to enhance the functional properties of calcium phosphate cements. – *J. Tissue Eng.,* **3**, 2012, 1, 2041731412439555. doi: 10.1177/2041731412439555.
7. **Sheikh, Z., P. J. Brooks, O. Barzilay, N. Fine, M. Glogauer.** Macrophages, foreign body giant cells and their response to implantable biomaterials. – *Materials,* **8**, 2015, 9, 5671-5701.

Institute of Experimental Morphology, Pathology and Anthropology with Museum
Bulgarian Anatomical Society

Acta morphologica et anthropologica, 26 (1-2)
Sofia ● 2019

Mast Cell Distribution in the Terminal Part of Porcine Ureter

Nikolay Tsandev[1], Angel Vodenicharov[1], Genadi Kostadinov[1], Ivaylo Stefanov[2]*

[1] *Department of Veterinary Anatomy, Histology and Embryology, Faculty of Veterinary Medicine, Trakia University of Stara Zagora, Bulgaria*
[2] *Department of Anatomy, Faculty of Medicine, Trakia University of Stara Zagora, Bulgaria*

*Corresponding author e-mail: drcandev@abv.bg

Abstract

The distribution of mast cells (MCs) in the terminal (intramural, intravesical) part of porcine ureter using toluidine blue staining was performed. It was established that in the *lamina propria mucosae* MCs were localized predominantly in the vicinity of blood vessels of the microcirculatory bed and rarely near the basal membrane of *lamina epithelialis mucosae*. In *tunica muscularis*, MCs were located mainly in the loose connective tissue around the blood vessels of the microcirculatory bed, as well as near the smooth muscle bundles. No statistical difference was estimated between number of Mcs/mm^2 in males and females in the *lamina propria mucosae*, while significant difference ($P<0.05$) was established between values in *tunica muscularis* comparing males and females. Statistical significant difference ($P<0.0001$) between values in *tunica muscularis* and *lamina propria* in each group of animals (in males and in females, respectively), was also found.

Key words: Mast cells, ureter-vesical junction, pig

Introdiction

The intramural part of ureter located within the dorsal urinary bladder wall, remains as independent organ among the bladder structures. It represents special anatomical, physiological and clinical interest, because that part like in man shows an anatomical narrowing in which urinary stones (ureteral calculi) could be retained. The latter sometimes provokes inflammation, spasm of musculature, particular or full obstruction, resulting in hydronephrosis or hydroureteronephrosis [1, 7].

That part of the ureter is responsible for protection of urine reflux from the bladder. The vesicoureteral reflux in combination with infection of the upper urinary tract and/or hydronephrosis bring often to kidney injuries [3].

Previous study convincingly demonstrated MCs localization in all layers of the extravesical parts of porcine ureter [10]. The evidence of some ligands as histamine

and vasoactive intestinal polypeptide (VIP) gave a reason to suggest that MCs take part not only in the maintenance of local homeostasis (microenvironment), but in the influence of smooth muscle motility as well. Recently, Lim et al. [2] confirmed that opinion, based on their results on isolated porcine distal ureter to 5-HT in young and old animals.

There is enough data that the swine is the most convenient animal model for performance of biomedical studies, results of which could be successfully interpreted and taken in mind for the human, including for the aims of xenotransplantation [4, 5, 6, 8, 9].

Materials and Methods

The intramural part of ureters from 6 males and 6 females 6-month-old pigs, 90 – 100 kg b. w. slaughtered for meat consumption according to Bulgarian laws were collected. Tissue pieces were immediately fixed in Carnoy's liquid for 24 h at room temperature, dehydrated in ascending ethanol lines, cleared in xylene and embedded in paraffin. After toluidine blue staining of 5 μm sections, only nucleated MCs expressing metachromasia were calculated on five serial sections of each organ (two fields with area of 1 mm^2 each per section). Data for density (number/mm^2) of MCs were estimated by Leica DM 1000 light microscope, digital camera Leica DFC 290 and software LAS V4.10.0 2016. The significance of difference (when $P < 0.05$) was assessed using one-way ANOVA.

Results

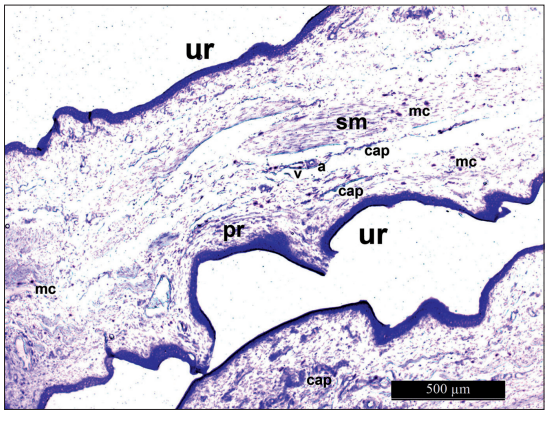

Fig. 1. Section through the terminal part of ureters (ur) into the urinary bladder wall of female pig mc – mast cells, sm – smooth muscle bundles, a – arteriola, v – venula and cap – capillaries of the microcirculatory bed. Toluidine blue staining. Bar = 500 μm.

MCs localization and density in both subepithelial connective tissue and muscle layer of intramural part of ureter were estimated. In the *lamina propria mucosae* MCs were observed predominantly in the vicinity of blood vessels of the microcirculatory bed and rarely near the basal membrane of *lamina epithelialis mucosae*. In *tunica muscularis*, MCs were located mainly in the loose connective tissue around the blood vessels of the microcirculatory bed, as well as near the smooth muscle bundles (**Figs.1, 2**). It should be noted that all of the observed mast cells showed well expressed γ-ma metachromasia.

It was detected a higher number of MCs in the muscle layer (86.60± 5.01 in males and 91.10±4.07 in females) compared to the mucosal propria in both males and females individuals (30.60±2.27 and 32.50±2.59, respectively) with $P < 0.0001$, (**Table 1**).The average number of mast cells in tunica muscularis was significantly higher in females than in males.

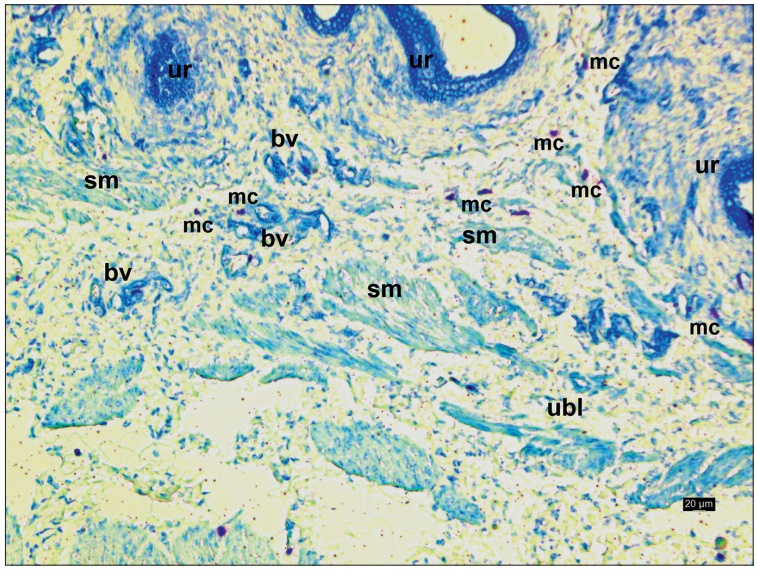

Fig. 2. Mast cells (mc) with expressed γ-ma metachromasia. ur –terminal part of male ureter, ubl – urinary bladder, sm – smoot muscle bundles. Toluidine blue staining. Bar = 10 µm.

Table 1. Distribution of mast cells (mm^2) in the terminal part of ureter's wall

Parameters	males	females
MCs number in: Lamina propria Min-max Tunica muscularis Min-max	 30.60±2.27 27-34 86.60±5.01**** **A** 78-93	 32.50±2.59 30-38 91.10±4.07**** 86-99

**** (P<0.0001) Statistical significant difference between values in *tunica muscularis and lamina propria* in each group of animals (in males and in females, respectively)
A (P<0.05) - Statistical significant difference between values in tunica muscularis comparing males and females
Min-max: minimal and maximal number of mast cells per mm^2 in each layer

Discussion

The current study presents original data about the distribution of mast cells in the wall of intramural part of the porcine ureter. The results allowed us to suggest that mast cells contribute not only in maintaining local microenvironment, but they are also important for the smooth muscle motility which is related to the regulation of urine flow via this part of the ureter.

Our previously study of MCs distribution in porcine abdominal part of the ureter showed that they are are located in all layers of this particular part of the ureter, but the highest number of them was estimated in the muscular sheet. Based on the results

of histo- and immunocytochemical investigation it was suggested that mast cells take important part not only in maintaining local homeostasis, but also in the motility of ureteral smooth muscle cells [10]. In addition, according to Lim et al. [2] mast cells presence in the ureter also play an important role in the regulation of ureteral motility via the release of mediators including histamine and 5-HT in inflammatory circumstances – it is possible that mast cell regulatory mechanisms occur via 5-HT receptor.

In general, the average number of mast cells found on mm^2 was a little higher in females than in males – 1.9-fold (lamina propria mucosae) and much more - 4.5-fold (tunica muscularis), respectively. The latter values also showed statistically significant difference. This fact is difficult to explain, but it could be presumed that the higher number of mast cells in the female ureteral muscle layer is related with more active participation in motility of smooth muscle cells and in keeping of local microenvironment in the intravesical part of the ureter.

Conclusion

This study presents original data about distribution of mast cells in the wall of the intramural part of the porcine ureter. The results allow us to suggest that mast cells contribute not only in maintaining local microenvironment but they are also important for the smooth muscle motility which is related to the regulation of urine flow via this part of the ureter.

References

1. **Vodenicharov, A., R. Leiser, M. Gulubova, T. Vlaykova**. Morphological and immunocytochemical investigations on mast cells in porcine ureter. – *Anat. Histol. Embryol.,* **34**, 2005, 343-349.
2. **Hess, B.** Pathophysiology, diagnosis and conservative therapy in calcium kidney calculi. – *Ther. Umsch.,* **60** (2), 2003, 79-87.
3. **Lim I., R. Chess-Williams, D. Sellers.** 5-HT2A receptor is the predominant receptor mediating contraction of the isolated porcine distal ureter to 5-HT in young and old animals. – *Eur. J. Pharmacol.,* **818**, 2018, 328-334.
4. **Roshani, H., N. F. Dabhoiwala, F. J. Verbeek, W. H. Lamers.** The functional anatomy of human ureterovesical junction. – *Anat. Rec.,* **245,**1996, 645-651.
5. **Swindle, M. M.** Swine as models in biomedical research. Ames, Iowa: Iowa State University Press, 1992, 54-67.
6. **Swindle, M. M., A. C. Smith, K. Laber-Laird, and L. Dungan.** Swine in Biomedical Research: Management and Models. – *ILAR news,* 1994, 1-5.
7. **Swindle, M. M., A. Makin, A. J. Herron, F. J. Clubb, K. S. Frazier.** Swine as a model inbiomedical research and toxicology testing. – *Vet. Pathol.,* **49**, 2, 2012, 344-356.
8. **Thomson, A. S., N. F. Dabhoiwala, F. J. Verbeek, W. H. Lamers.** The functional anatomy of ureterovesical junction. – *Br. J. Urol.,* **73**, 1994, 284-291.
9. **Tumbleson, M. E.** Swine in Biomedical Research, Vol. 1, Plenum Press, NewYork. 1986, 112-130.
10. **Tumbleson, M. E., Schook, L. B.** Advances in swine in biomedical research. Vols. 1-2, 1996, Plenum Press, New York, 423-451

Institute of Experimental Morphology, Pathology and Anthropology with Museum
Bulgarian Anatomical Society

Acta morphologica et anthropologica, 26 (1-2)
Sofia ● 2019

Inhibitory Effects of Plant Extracts on Postproline Cleaving Enzyme Activity in Human Breast Cancer Cells

Anelia Vasileva[1], Mashenka Dimitrova[2], Ivan Iliev[2], Donka Tasheva[3], Ivaylo Ivanov[1]*

[1] *Department of Medical Chemistry and Biochemistry, Medical University of Sofia, Sofia, Bulgaria*
[2] *Institute of Experimental Morphology, Pathology and Anthropology with Museum, Sofia, Bulgaria*
[3] *Faculty of Chemistry and Pharmacy, Sofia University "St. Kl. Ohridski", Sofia, Bulgaria*

* Corresponding author e-mail: mashadim@abv.bg

Effects of crude extracts from three herbs: *Rhaponticum carthamoides* (maral root), *Tanacetum vulgare* L. (tansy) and *Tribulus terrestris* L. (small caltrops) on the postproline-specific enzyme activity in the human triple negative breast carcinoma cell line MDA-MB-231were investigated. In all cases, a concentration-dependent inhibition was observed, with the degree of inhibition from *T. vulgare* L. being the highest. Different tansy extracts, also had a pronounced inhibitory dose-dependent effect on the enzyme activity in this cell line. The highest effect was observed using the ethyl acetate/aqueous extract from *Flores Tanaceti*. Since the proline specific enzymes are known to participate in different tumors growth, it could be concluded that the natural inhibitors from tansy have a potential to be used as therapeutic anti-cancer agents.

Key words: postproline-specific enzymes, *Tanacetum vulgare* L., *Tribulus terrestris* L., *Rhaponticum carthamoides*, MDA-MB-231cells

Introduction

Studies on the identification of proteolytic enzymes - markers of pathological processes, could lead to the development of innovative therapeutic strategies and agents. Those enzymes are known to be involved in the genesis and development of many types of tumors and are considered as potentially attractive therapeutic targets. Proline is an important amino acid in many biologically relevant polypeptide sequences. Its presence affects the peptide's interactions with other proteins and prevents their degradation by the most common proteases. Postproline proteases constitute a subset of serine proteases involved in the regulation of many signaling events and are emerging as promising therapeutic targets for prevalent diseases such as diabetes and cancer [14]. This protease subset belongs to the S9 family of serine peptidases and includes such diverse and important enzymes as prolyl oligopeptidase (POP; EC 3.4.21.26) [7], dipeptidyl peptidase

IV (DPP-IV, EC 3.4.14.5) [12] and fibroblast activation protein alpha (FAP, EC 3.4.21. B28) [6]. Increased activity levels of these enzymes are observed in various pathological conditions, including malignancies [2, 17]. Their inhibitors are potential therapeutic agents [13].

Plants produce a broad range of bioactive compounds via their secondary metabolism. These compounds elicit different effects on humans' and animals' organs and tissues. Recently, there is increasing interest towards substances of natural origin that are selective inhibitors of proline-specific enzymes. For example, it has been found that certain flavonoids and caffeoylquinic acids, as well as derivatives thereof, are POP inhibitors with good selectivity to DPP-IV [1, 5, 10, 11]. Some of the chemical constituents of *Rhaponticum carthamoides* (*Leuzea carthamoides*; maral root), *Tanacetum vulgare* L. (tansy) and *Tribulus terrestris* L. (small caltrops) are phenolic acids, flavonoids and their derivatives [3, 9, 18], which are potential inhibitors of these peptidases.

In the present study, the effect of the extracts from three herbs on the postproline-specific enzyme activity in the human tumor mammary gland cell line MDA-MB-231 was investigated. The IC_{50} values of inhibition from fractions were determined.

Materials and Methods

Chemicals and reagents. Ethyl acetate, diethyl ether, diisopropyl ether and hexane were from Fisher Chemical (UK). All reagents were of the highest purity available. The substrate Z-Gly-Pro-methyl coumaryl amide (Z-Gly-Pro-AMC) was from Bachem (Switzerland).

Plant extracts. The crude extracts of *T. terrestris* L. and *T. vulgare* L. and flowers of tansy were kindly provided by Vemo 99 Ltd (Sofia, Bulgaria). In the present study, we used a commercial extract from the roots of *R. carthamoides*.

Preparation of the ethyl acetate fraction from the crude extract (EACE). Twenty mL of water were added to 5 g of the powdered crude tansy extract while stirring. 6N HCl was then added in a dropwise manner until pH 3.0. Ethyl acetate (15 mL) was applied to the aqueous phase while stirring. The organic phase was separated and the aqueous phase was extracted with 10 mL ethyl acetate. The combined organic phases were filtered, washed with brine and dried by Na_2SO_4. Ethyl acetate was removed under vacuum and a small amount of diisopropyl ether was added. The formed dark yellow solid was filtered and dried out.

Preparation of dicyclohexylammonium salts fraction (DCHAS). Solid dicyclohexylammonium salts were obtained from the ethyl acetate extract, as follows: The volume of the ethyl acetate extract was reduced to 1/4 and dicyclohexylamine was added dropwise. The obtained precipitate was filtered, washed with diisopropyl ether and dried.

*Isolation of solid substance from diethyl ether/hexane (DEHS).*The filtrate obtained after the removal of dicyclohexylammonium salts was concentrated *in vacuo* to give a thick oily residue. Diethyl ether was added to this residue, followed by hexane, thus obtaining a dark yellow precipitate.

Preparation of ethyl acetate extract from Flores Tanaceti (EAFT). Sixteen mL of water and 48 mL ethyl acetate were added to 4 g of *Flores Tanaceti* while stirring. Then, 6N HCl was added dropwise until the aqueous phase reached a pH 3.0 and the mixture was stirred for an additional hour. Following filtration, the organic phase was separated and processed as above. Finally, diisopropyl ether was added and the obtained precipitate was filtered and dried.

Cell culturing. A permanent cell line was used – MDA-MB-231 (human tumor cells from triple negative mammary gland carcinoma). The cancer cells were cultured

in 75 cm^2 tissue culture flasks in Dulbecco's Modified Eagle's Medium – high glucose 4.5‰ (DMEM), supplemented with 10% fetal calf serum and antibiotics in usual concentrations. Cell culture was maintained at 37.5°C in a humidified atmosphere and 5% CO_2 until 95% confluence was achieved. The cells were harvested by a rubber policeman and homogenized using homogenizer MSE (England) in 5 mL 0.1 M phosphate buffer (pH 7.4) with 0.1 M NaCl and 1 mM EDTA.

Enzyme activity measurement. Enzyme activity in the cell homogenate was measured in the presence of 0.1 or 0.2 mg/mL extracts or fractions in 0.1 M phosphate buffer (pH 7.4), containing 0.1 M NaCl and 1 mM EDTA at 37°C using 80 μM fluorogenic substrate Z-Gly-Pro-AMC. Enzyme assays were carried out in 96-well plates, in a multifunctional spectrofluorimeter Varioscan Fluorescence at 360 nm excitation and 460 nm emission every 3 minutes. The software program EnzFitter V2 was used for data processing. The enzyme activity was determined from the initial rate of the reaction.

IC_{50} determination. Enzyme activity in homogenate of cell line MDA-MB-231 was measured in the presence of different concentrations (5, 10, 15, 20, 25, 37.5 и 50 μg/mL) from highest activity fraction in 0.1 M phosphate buffer (pH 7.4), containing 0.1 M NaCl and 1 mM EDTA using 80 μM fluorogenic substrate Z-Gly-Pro-AMC at 37°C.

Column chromatography. The crude extract of *T. vulgare* was fractionated with chromatography system Grace Davison Purification (USA) Reveleris® Flash System. Chromatographic separation was performed on a Claricep C_{18} column (Bonna-Angela), 80 g, particle size 20-45 μm and pore size 100Å, ELSD detector: isopropanol, UV wavelength irradiation (UV1: 254 nm and UV2: 325 nm) using the following mobile phases: A: water and B: acetonitrile, at a flow rate of 40 mL/min and gradient (62 min): 0% B for 2 min, 23% B for 50 min, 90% B for 3 min, hold 90% B for 4 min and 0% B for 3 min.

Results and Discussion

The effect of the crude extracts from *R. carthamoides*, *T. terrestris* L. and *T. vulgare* L. on postproline-specific enzyme activity on the human cell line MDA-MB-231 was studied using the nonspecific fluorogenic substrate Z-Gly-Pro-AMC for post-proline cleaving enzymes. The tested extracts were with concentrations 0.1 mg/mL and 0.2 mg/mL respectively. In all three extracts, concentration-dependent inhibition was observed (**Fig. 1**). Degree of inhibition at concentration 0.1 mg/mL in the cell homogenates were 0.26 (*R. carthamoides)*, 0.32 (*T. terrestris*L.) and 0.40 (*T. vulgare* L.). The lowest degree of inhibition at concentration 0.2 mg/mL was observed for *R. carthamoides* (0.37) and the highest for *T. vulgare* L. (0.61). In view of the obtained results it can be concluded that crude extract of *T. vulgare* L. has the highest inhibitory effect on the enzymes' activity in breast cancer cells homogenates.

Cell line MDA-MB-231 (triple negative human mammary gland carcinoma) is usually used as a negative control for FAP, since it is known to lack this enzyme activity [4, 8]. The tansy extract inhibited mildly recombinant DPP-IV, specifying a high selectivity of the natural tansy inhibitors to the postproline endopeptidase activity. On the other hand, the MDA-MB-231 cell line is POP-positive [16], indicating that an inhibition of POP-activity was observed in our study.

Using the LC-HRMS method, we determined the major nonvolatile compounds in the extract of tansy. In the crude extract of tansy we detected the presence of 3-caffeoylquinic acid, 5-caffeoylquinic (chlorogenic) acid, 3,4-, 3,5- and 4,5-dicaffeoylquinic acids, O-glucuronides of apigenin, luteolin and quercetin and O-hexosides of luteolin and quercetin [15].

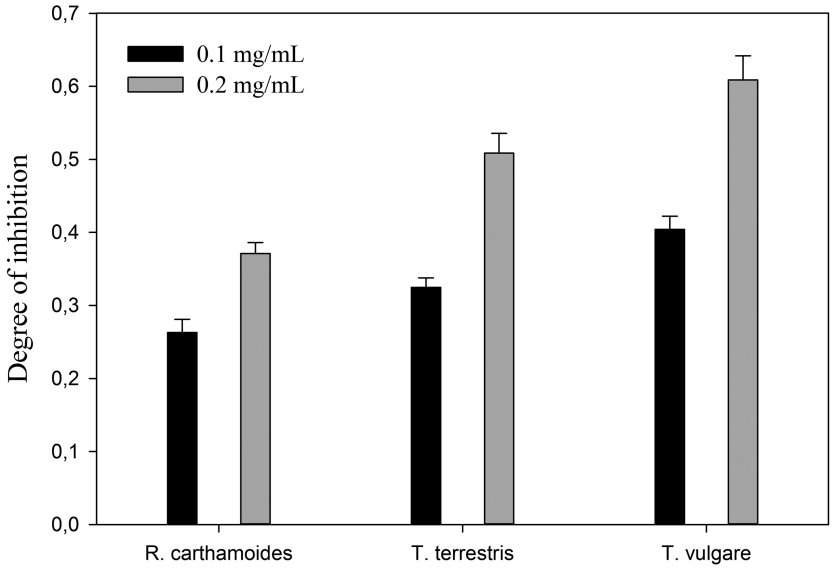

Fig. 1. The degree of inhibition of the postproline-specific enzymes' activity from the crude plant extracts in homogenates ofMDA-MB-231 human cells.

Further on, the crude extract was partitioned between water and ethyl acetate and the effect of the aqueous and organic fractions on postproline-specific enzyme activity in the homogenates of MDA-MB-231 cell line were investigated. Ethyl acetate fraction exhibited a higher activity (0.68 degree of inhibition at concentration 0.1 mg/mL and 0.83 at 0.2 mg/mL respectively) (**Fig. 2**) as compared to the crude extract (**Fig. 1**). On the other hand, aqueous fraction showed a very low activity.

From these data, we can assume that some of the above compounds are effective inhibitors of postproline endopeptidase activity, i.e. POPs activity. Dicyclohexylamine was added to the ethyl acetate fraction, whereby a precipitate of the dicyclohexylammonium salts of 3-caffeoylquinic acid, chlorogenic acid, isomeric dicaffeoylquinic acids and O-glucuronides of apigenin, luteolin and quercetin were formed. The inhibitory activity (**Fig. 2**) of these dicyclohexylammonium salts (degree of inhibition at concentrations 0.1 mg/mL and 0.2 mg/mL were 0.67 and 0.80 respectively) proved to be essentially the same as the activity of ethyl acetate fraction (0.68 and 0.83 respectively). After separating the precipitate from dicyclohexylammonium salts, the filtrate was concentrated and treated with diethyl ether and hexane, whereby a precipitate formed. The degree of inhibition by these substances is twice lower relative to of the ethyl acetate fraction (**Fig. 2**). These results confirm our hypothesis that some of the major components in the extract are potential selective inhibitors of the POP. The powder from the flower of the herb was extracted with two phase system water/ethyl acetate. The ethyl acetate extract from *Flores Tanaceti* (EAFT) obtained by using a two-phase water/ethyl acetate system showed the highest effect (0.85 and 0.97 degree of inhibition) on the postproline-specific enzyme activity (**Fig. 2**).

The crude extract from *T. Vulgare* L. was fractionated by flash chromatography. Some of the fractions showed inhibitory effect of 75-95% on the enzyme activity in the homogenate of MDA-MB-231 cell line.The dependence of the postproline-specific enzyme activity in the cell homogenate on the fraction concentration showing an inhibition rate of 0.95 was investigated. Results were presented in **Fig. 3.**

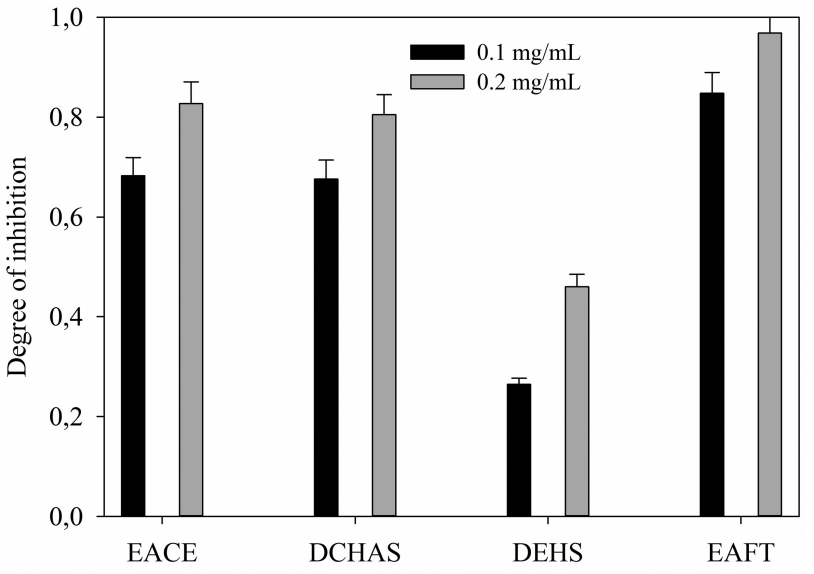

Fig. 2. The inhibition effect of the fractions of T. vulgare on postproline-specific enzyme activity in cell homogenates. EACE – ethyl acetate fraction of the crude extract of tansy; DCHAS – dicyclohexylammonium salts fraction; DEHS – solid substance from diethyl ether/hexane separation; EAFT – ethyl acetate extract from Flores Tanaceti.

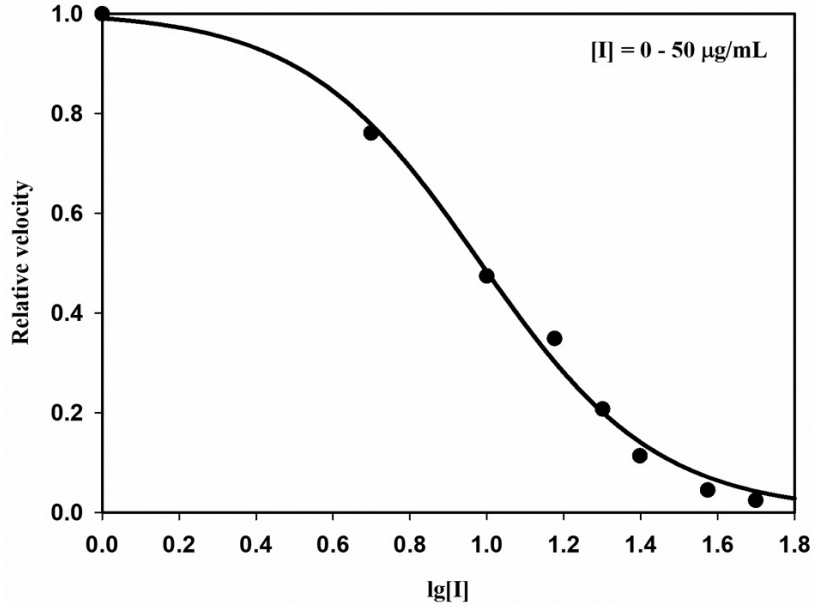

Fig. 3. Relative rate of hydrolysis of Z-Gly-Pro-AMC by homogenate of MDA-MB-231 cells in the presence of different concentrations of the fraction of the highest inhibition activity.

In **Fig. 3**, the dependency of the relative initial rate from the logarithm from concentration of fraction is shown. From the typical sigmoidal dependence obtained, calculated IC_{50} is 10 μg/mL.

Conclusions

The components of the ethyl acetate extracts from the flowers of *T. vulgare L.* demonstrate a high selectivity with respect to the inhibition of proline-specific endopeptidases – enzymes which are known to take part in the genesis and progression of many types of tumors. So, these natural inhibitors could be considered as potential therapeutic agents for the treatment at least of mammary gland carcinoma.

Acknowledgement. This work is financially supported by the National Science Fund of the Bulgarian Ministry of Education and Science, Grant № T02/25 2014.

References

1. **Adolpho, L. O., D. Marin, A. Puigpinos, L. Mendieta, T. Tarragó, A. F. Morel, I. I. Dalcol.** In vitro evaluation of caffeoyl and cinnamoyl derivatives as potential prolyloligopeptidase inhibitors. – *Planta Med.,* **79**, 2013, 1531-1535.
2. **Babkova, K., J. Korabecny, O. Soukup, E. Nepovimova, D. Jun, K. Kuca.** Prolyloligopeptidase and its role in the organism: attention to the most promising and clinically relevant inhibitors. – *Future Med. Chem*. **9**, 2017, 1015-1038.
3. **Baranauskienė, R., R. Kazernavičiūtė, M. Pukalskienė, R. Maždžierienė, P. R. Venskutonis.** Agrorefinery of Tanacetumvulgare L. into valuable products and evaluation of their antioxidant properties and phytochemical composition. – *Ind. Crops Prod.*, **60**, 2014, 113-122.
4. **Dimitrova, M., I. Iliev, D. Tasheva, V. Lozanov, I. Ivanov**. Novel substrates for determination of the fibroblast activation protein-α activity. – *Acta Morphol. Anthropol.*, **24**, 2017, 3-9.
5. **Dos Santos, M. Z., I. I. Dalcol, L. Adolpho, M. Teixidó, T. Tarragó, A. Morel, E. Giralt.** Chemical composition and inhibitory effects of Hypericumbrasiliense and H. connatum on prolyloligopeptidase and acetylcholinesterase activities. – *Med. Chem.*, **12**(**5**), 2016, 457-463.
6. **Gorrell, M. D., J. E. Park.** Fibroblast Activation Protein α. In: *Handbook of Proteolytic Enzymes* (Ed. N. D. Rawlings, G. Salvesen), 3 ed, Academic Press Elsevier, 2013, 3395-3401.
7. **Ito, K., Y. Nakajima, T. Yoshimoto. Prolyloligopeptidase**. **–** In: *Handbook of Proteolytic Enzymes* (Eds. N. D. Rawlings, G. Salvesen), 3 ed, Academic Press Elsevier, 2013, 3360-3364.
8. **Jia, J., T. A. Martin, L. Ye, &W. G. Jiang**. FAP-α (Fibroblast activation protein-α) is involved in the control of human breast cancer cell line growth and motility via the FAK pathway. – *BMC Cell Biol.*, **15**, 2014, 1-16.
9. **Koleckar, V., L. Opletal, E. Brojerova, Z. Rehakova, F. Cervenka, K. Kubikova, L. Jahodar.** Evaluation of natural antioxidants of Leuzea carthamoides as a result of a screening study of 88 plant extracts from the European Asteraceae and Cichoriaceae. – *J. Enzyme Inhib. Med. Chem.,* 23, 2008, 218-224.
10. **Lee, K. H., J. H. Kwak, K. B. Lee, K. S. Song.** Prolyl endopeptidase inhibitors from Caryophylli Flos. – *Arch. Pharmacal. Res.*, **21**, 1998, 207-211.
11. **Marques, M. R., C. Stüker, N. Kichik, T. Tarragó, E. Giralt, A. F. Morel, I. I. Dalcol.** Flavonoids with prolyloligopeptidase inhibitory activity isolated from Scutellaria racemosa Pers. – *Fitoterapia*, **81**, 2010, 552-556.
12. **Misumi, Y., Y. Ikehara**. Dipeptidyl-peptidase IV. In: *Handbook of Proteolytic Enzymes* (Ed. N. D. Rawlings, G. Salvesen), 3 ed, Academic Press Elsevier, 2013, 3374-3379.

13. **Rosenblum, J. S., J. W. Kozarich**. Prolyl peptidases: a serine protease subfamily with high potential for drug discovery. – *Curr. Opin. Chem. Biol.*, 7, 2003, 496-504.
14. **Sabidó, E., T. Tarragó, S. Niessen, B. F. Cravatt, E. Giralt**. Activity-based probes for monitoring postproline protease activity. – *Chem. Biochem.*, **10**(**14**), 2009, 2361-2366.
15. **Vasileva, A., I. Iliev, V. Lozanov, M. Dimitrova, V. Mitev, I. Ivanov.** In vitro study on the antitumor activity of Tanacetumvulgare L. extracts. – *Bulg. Chem. Commun*., **51**, 2019 (in press).
16. **Wilson, C. H., C. A. Abbott.** Expression profiling of dipeptidyl peptidase 8 and 9 in breast and ovarian carcinoma cell lines. – *Int. J. Oncol.*, **41**, 2012, 919-932.
17. **Yazbeck, R., S. E. Jaenisch, C. A. Abbott.** Potential disease biomarkers: dipeptidyl peptidase 4 and fibroblast activation protein. – *Protoplasma*, **255**, 2018, 375-386.
18. **Zheng, W., F. Wang, Y. Zhao, X. Sun, L. Kang, Z. Fan, B. Ma.** Rapid Characterization of Constituents in Tribulusterrestris from Different Habitats by UHPLC/Q-TOF MS. – *J. Am. Soc. Mass. Spectrom.*, **28**, 2017, 2302-2318.

Institute of Experimental Morphology, Pathology and Anthropology with Museum
Bulgarian Anatomical Society

Acta morphologica et anthropologica, 26 (1-2)
Sofia ● 2019

Anthropology and Anatomy

Sex related Differences in the Distribution of Adipose Connective Tissue in Bulgarian Patients Suffering from type 2 Diabetes Mellitus

Atanas G. Baltadjiev, Tzvetanka Petleshkova*

Department of Anatomy, Histology and Embryology, Faculty of Medicine, Medical University-Plovdiv, Bulgaria

* Corresponding author e-mail: dr_atanas@abv.bg

Abstract

Aim: to compare the distribution of adipose connective tissue between 40-60 year old Bulgarian male and female patients with T2DM. Subjects: 217 patients, divided into two groups by sex. Control group: 80 healthy men and women divided into the same groups. Anthropometric parameters: weight, 9 skinfolds, Bioelectrical Impedance Analysis. Calculated indices: BMI, sfTrunk/sfLimbs ratio, skinfolds upper half of body/skinfolds lower half of body ratio, fat mass and subcutaneous fat mass.
Results: The mean values of BMI, % body fat tissue, fat mass and subcutaneous fat mass in female patients were significantly higher than in male patients, but the mean value of visceral fat tissue was significantly higher in male patients. The value of sfTrunk/sfLimbs ratio was greater in male patients than in female patients. These results are a reason for assessing the anthropological status of male patients as worse than that of female patients for the prognostic of disease.

Key words: type 2 Diabetes Mellitus, connective fat tissue, sex related comparison

Introduction

Type 2 Diabetes Mellitus (T2DM) is a long-term metabolic disorder that is characterized by high blood sugar, insulin resistance, and relative lack of insulin. It is really a social problem due to the rapidly growing number of people affected by the disease

worldwide. As of 2015, the estimated 415 million people had diabetes worldwide, with type 2 DM it makes about 90% of the cases. This represents 8.3% of the adult population, with equal rates in both women and men. According to the International Diabetes Federation, the number of diabetes mellitus patients in Europe is expected to increase from 52 millions in 2014 to 68.9 millions by 2035, mostly due to increases in overweight and obesity, unhealthy diet and physical inactivity [7]. Eastern Europe is significantly affected by the disease: Serbia – 13,4%, Bosnia and Herzegovina – 12,6%, Turkey and Romania – 12,5%, Northern Macedonia – 12,1%, Albania – 11,9%. Around 8-9% of the Bulgarian population suffers from this disease.

Conducted surveys were focused exclusively on clarifying the etiology, pathogenesis, clinical course and treatment of the disease. Limited number of studies aimed to clarify the relationship between anthropological parameters determining humans' body constitution, and the differences between both sexes. The fat accumulation in the body of patients with type 2 Diabetes Mellitus occurs primarily in two locations: in the abdomen (central, abdominal, visceral) and subcutaneously (peripheral). Fat accumulation in the abdominal area is commonly associated with increased risk for T2DM [8, 12, 13, 18]. Not many studies have been performed for the sex related distribution of adipose connective tissue. The aim of this study was to compare the distribution of adipose connective tissue between 40-60 year old Bulgarian male and female patients with T2DM.

Materials and Methods

Subjects. Totally of 165 patients aged 40-60 years suffering from type 2 Diabetes Mellitus were involved in the study. They were divided into two groups by sex: 1st group: 40-60 years of age – 92 female patients (mean 52.87±0.56 yrs), 2nd group: 73 male patients (mean 52.29±0.79 yrs). They were diagnosed by a diabetes specialist and recruited from the Clinic of Endocrinology of St. George University Hospital at the Medical University of Plovdiv, Bulgaria. The study period was 2009-2015.

The inclusion criteria were: Bulgarian ethnicity, duration of the disease of not less five years, clinically compensated diabetes at the time of the study. The exclusion criteria were: previous or existing metabolic, oncological and other disorder that could compromise the anthropological study: thyroid related diseases, adrenal glands related diseases, carcinoma, etc.

In the study were involved 80 healthy Bulgarian subjects. The control groups included 40 men at the same age range (51.33±0.93 yrs) and 40 women at the same age range (50.80±1.08 yrs).

An ethical approval was taken for this study. Informed consents were taken from all patients involved in the study.

Methods

Directly measured parameters: body weight, skinfold (sf) thicknesses were measured at 9 locations – sfTriceps, sfBiceps (brachii), sfForearm, sfSubscapular, sfXrib, sfAbdomen, sfSuprailiaca, sfThigh, and sfCalf, using Harpenden Skinfold Calipers (British Indicators Ltd) at standard sites on the right side of the body.

Bioelectrical Impedance analysis (BIA): % body fat tissue and visceral fat tissue were measured with a Body Composition Monitor Tanita BC-532.

Calculated indices: Body mass index (BMI), sfTrunk/sfLimbs ratio, skinfolds upper half of body/skinfolds lower half of body ratio, fat mass and subcutaneous fat mass.

Statistical analysis. Data were analyzed using statistical software SPSS version 15 (SPSS Inc., Chicago, IL). Independent Samples t-Test was used to compare the means of two independent anthropologic parameters in order to determine whether there was statistical evidence that the means were significantly different. The one-way analysis of variance (ANOVA) was used to determine whether there were any significant differences between the means of three or more independent parameters. $P<0.05$ (two tailed) was considered statistically significant.

Results

I. Distribution of adipose connective tissue between female patients and healthy controls.

Significant difference was found between the means of **weight** in the present study. The mean value of female patients was higher than the controls ($p<0.001$). The thicknesses of **sfTriceps, sfThigh and sfCalf** were significantly greater in the healthy controls than in female patients suffering from type 2 Diabetes Mellitus ($p<0.05$), but **sfXrib** was significantly greater in the patients ($p<0.01$), demonstrated in **Table 1**.

Table 1. Anthropological parameters of Bulgarian patients aged 40-60 years with type 2 Diabetes Mellitus compared to healthy controls at the same age.

	Female			**Male**		
Parameters	T2DM mean±sem	Controls mean±sem	P	T2DM mean±sem	Controls mean±sem	P
Weight (kg)	79.65±1.25	69.95±1.83	**<0.001***	84.47±1.38	78.47±1.78	**<0.001***
sf Triceps(mm)	21.94±1.59	28.46±1.85	**<0.05***	10.91±0.60	11.20±0.96	>0.05
sfSubscapular(mm)	28.98±1.42	26.35±1.74	>0.05	23.85±1.42	20.24±1.51	>0.05
sf X rib(mm)	28.68±1.35	22.51±1.50	**<0.01***	22.92±1.26	16.98±1.34	**<0.05***
sfSuprailiaca(mm)	21.68±1.14	23.17±1.62	>0.05	17.83±1.37	20.86±1.60	>0.05
sfAbdomen(mm)	32.06±1.40	34.60±2.03	>0.05	28.68±1.70	33.21±2.10	>0.05
sfBiceps(mm)	12.85±0.76	15.61±1.22	>0.05	7.71±0.47	6.57±0.53	>0.05
sfForearm (mm)	11.59±0.66	12.00±1.19	>0.05	8.20±0.51	7.48±0.60	>0.05
sfThigh(mm)	24.49±1.96	42.47±2.01	**<0.001***	15.08±1.04	20.21±1.89	**<0.05***
sfCalf(mm)	20.21±1.33	27.32±1.59	**<0.01***	10.51±0.86	11.39±0.91	>0.05

sf = skinfold, * statistical significance

Body composition parameters' results, investigated by Bioelectrical Impedance analysis

The values of three parameters: **% body fat tissue, visceral fat tissue and fat mass** were significantly higher in female patients than the healthy controls ($p<0.05$), demonstrated in **Table 2.**

Table 2. Body composition of Bulgarian patients aged 40-60 years with type 2 Diabetes Mellitus.

Parameters	T2DM-female mean±sem	Controls-female mean±sem	P	T2DM-male mean±sem	Controls-male mean±sem	P
BMI	29.04±0.49	26.34±0.51	**<0.001***	31.77±0.51	27.31±0.70	**<0.001***
% body fat tissue	28.71±1.11	24.75±0.86	**<0.05***	42.07±0.99	37.66±0.99	**<0.01***
Visceral fat tissue (kg)	13.79±0.72	11.00±0.55	**<0.05***	11.26±0.40	7.80±0.45	**<0.001***
Fat mass (kg)	24.02±1.30	19.83±1.07	**<0.05***	37.97±1.73	27.48±1.40	**<0.001***
Subcutaneous fat mass (kg)	15.75±0.26	15.65±0.45	>0.05	17.18±0.27	18.68±0.40	**<0.05 ***

* statistical significance

II. Distribution of adipose connective tissue between male patients and healthy controls.

A significant difference was found between the means of **weight,** too. The mean value of male patients with diabetes was significantly higher than the controls ($p<0.001$). The thickness of **sfXrib** in diabetic male patients was significantly higher than the healthy controls ($p<0.05$). The thickness of **sfThigh** in male patients was significantly lower than the controls ($p<0.05$). These results are demonstrated in **Table 1**.

Body composition parameters' results, investigated by Bioelectrical Impedance analysis.

The values of the **% body fat tissue, visceral fat tissue, fat mass** and **subcutaneous fat mass** in male patients with diabetes were significantly higher than the controls ($p<0.05$), demonstrated in **Table 2**.

III. Comparison of some anthropological parameters between female and male Bulgarian patients.

Many statistically significant differences were detected between the measured anthropological parameters in both sexes, demonstrated in **Table 3**.

Table 3. Comparison of some anthropological parameters between female and male Bulgarian patents aged 40-60 years with type 2 Diabetes Mellitus.

	females				males				
Parameters	N	Mean	SEM	SD	N	Mean	SEM	SD	**P**
Weight (kg)	92	79.65	1.25	11.99	73	84.47	1.38	9.49	**<0.01***
sfTriceps(mm)	92	21.94	1.59	15.25	73	10.91	0.60	4.04	**<0.001***
sfSubscapular(mm)	92	28.98	1.42	13.62	73	23.85	1.42	9.62	**<0.01***
sf X rib(mm)	92	28.68	1.35	12.95	73	22.92	1.26	8.52	**<0.01***
sfSuprailiaca (mm)	92	21.68	1.14	10.93	73	17.83	1.37	9.32	**<0.05***
sfAbdomen(mm)	92	32.06	1.40	13.43	73	28.68	1.70	11.51	>0.05
sfBiceps(mm)	92	12.85	0.76	7.29	73	7.71	0.47	3.21	**<0.001***
sfForearm (mm)	92	11.59	0.66	6.33	73	8.20	0.51	3.47	**<0.001***
sfThigh(mm)	92	24.49	1.96	18.80	73	15.08	1.04	7.07	**<0.001***
sfCalf(mm)	92	20.21	1.33	12.76	73	10.51	0.86	5.87	**<0.001***

sf = skinfold, * statistical significance

The mean value of weight in male patients was significantly higher than in female patients ($p<0.01$). The mean values of measured skinfolds were significantly greater in female patients than in male patients, except sf Abdomen. There wasn't detected a significant difference between the compared values ($p>0.05$).

The mean values of **% body fat tissue, fat mass and subcutaneous fat mass** in female patients were significantly higher than in male patients, but the mean value of **visceral fat tissue** was significantly higher in male patients ($p<0.001$), demonstrated in **Table 4**.

IV. Comparison of some indices between female and male patients with type 2 DM.

The **BMI** of male and female patients suffering from diabetes were significantly higher than that of the healthy controls ($p<0.001$), demonstrated in **Table 2**. The mean value of BMI in female patients was significantly higher than in male patients ($p<0.001$), demonstrated in **Table 4**. The values of the **sfTrunk/sfLimbs ratio** and **skinfolds upper half of body/skinfolds lower half of body ratio** were greater in the patients of both sexes compared to healthy controls. The value of **sfTrunk/sfLimbs ratio** was higher in male patients in comparison to female patients. The value of **skinfolds upper half of body/skinfolds lower half of body ratio** in female patients was higher than in male patients, demonstrated in **Table 5.**

Table 4. Comparison of some body composition's parameters between female and male Bulgarian patients aged 40-60 years with type 2 Diabetes Mellitus.

	female				**male**				
Parameters	N	Mean	SEM	SD	N	Mean	SEM	SD	**P**
BMI	92	31.77	0.51	4.89	73	29.04	0.49	3.34	**<0.001***
% body fat tissue	92	42.07	0.99	9.50	73	28.71	1.11	5.97	**<0.001***
Visceral fat tissue (kg)	92	11.26	0.40	3.84	73	13.79	0.72	3.87	**<0.001** *
Fat mass (kg)	92	37.97	1.73	16.59	73	24.02	1.30	6.88	**<0.001** *
Subcutaneous fat mass(kg)	92	17,18	0.27	2.59	73	15.75	0.26	2.85	**<0.001***

* statistical significance

Table 5. Comparison of some indices between female and male patients aged 40-60 years with type 2 Diabetes mellitus.

	females		**males**	
	T2DM	controls	T2DM	controls
sf trunk/sf limbs	1.34	0.85	1.79	1.67
sf upper half of the body/ sf lower half of the body	1.09	0.83	1.07	0.75

Discussion

Analysis of distribution of subcutaneous adipose connective tissue

The mean value of weight was significantly higher in the patients of both sexes than in healthy controls. The differences were very well expressed ($p<0.001$).

Attention should be paid to the distribution of subcutaneous adipose tissue in female patients with T2DM. It was found that in the female patients with T2DM the accumulation of subcutaneous adipose tissue was mostly in torso and less in the limbs. Moreover, the accumulation of adipose tissue consisted predominantly in the upper part of the body compared to the lower, the so-called "apple shaped" body. The thicknesses of sf Triceps, sfThigh and sfCalf were significantly greater in the controls than in female patients [21], but the thickness of sfXrib was significantly greater in female patients. These patients have a worse anthropological status, which would lead to a more severe clinical course of the disease.

Similar tendencies were found by the assessment of distribution of subcutaneous adipose connective tissue in male patients. The thickness of sfXrib was significantly greater in male patients than in controls, but sfThigh was significantly thicker in the controls than in male patients. Attention should be paid that there were found two significant differences only. The body shape constitution "apple" is closely associated with a poor prognostic of the disease [4]. The deposition of adipose connective tissue in the controls of both sexes was predominantly in the limbs and mainly in the lower part of the body, the so-called "pear shaped" body (**table 1 and table 5**).

The mean value of body weight in male patients was significantly greater than in female patients. It can be explained with the sexual dimorphism. Attention should be paid by the comparison of skinfolds between both sexes. The mean values of all 8 measured skinfolds were significantly higher in female patients than in male patients. The exception was sf Abdomen. There wasn't found a significant difference between the mean values of male and female patients ($p>0.05$). Only a tendency was registered, that the value of sfAbdomen in female patients was higher in comparison to male patients (**table 3**). These results defined an unfavourable distribution of subcutaneous adipose connective tissue in female patients compared to the male patients.

Analysis of Body composition parameters' results, investigated by BIA.

It has been found that abdominal obesity, also known as central or visceral obesity, was more closely related to T2DM than the general obesity. The visceral fat was more metabolically active and produced more insulin resistance [5, 16, 19].

Many significant differences were found in the parameters: BMI, % body fat tissue, visceral fat tissue and fat mass. They were significantly greater in female patients with T2DM than in healthy controls. The exception was the accumulation of subcutaneous fat mass. There wasn't detected a significant difference ($p>0.05$). The mean values of above described parameters were significantly greater in male patients than in the healthy controls at the same age, including the parameter subcutaneous fat mass. We have found that the values of following parameters: BMI, %body fat, fat mass and subcutaneous fat mass were significantly higher in female patients than in male patients to comparison between both sexes. Opposite, the mean value of visceral fat tissue was significantly greater in male patients than in female patients at the same age. This parameter is more important than the others, because it is closely related to the insulin resistance [11]. The greater values of visceral fat tissue in male patients determine a worse anthropological status in comparison to female patients.

Analysis of the calculated indices in both sexes patients suffering from type 2 DM.

The mean value of BMI in male and female patients was significantly higher than in healthy controls at the same age and sex ($p<0.05$). The levels of BMI in female patients were significantly higher compared to the male patients ($p<0.001$), (table 2 and table 4). This index demonstrates a total deposition of adipose connective tissue into the human body, but these values had less importance for the prognosis of disease compared to above described parameters [2, 9].

The accumulation of subcutaneous adipose tissue in the patients of both sexes suffering from type 2 Diabetes Mellitus was higher in the torso, than in the limbs. In contrast, the controls exhibited the opposite distribution. The accumulation of subcutaneous adipose tissue was larger in the upper half of the body, than in the lower half. It defined the model of patients' body shape as so-called "apple shaped". The controls exhibited the opposite distribution (**table 5**). The value of the ratio sf trunk/sf limbs was greater in male patients than in female patients. The value of the ratio sf upper half of the body/sf lower half of the body was greater in the female patients than in male patients, but the difference is too thin. These results demonstrated more uneven distribution of adipose connective tissue in male patients than in female patients. The accumulation of fat mass more in the trunk and less in the limbs is significantly and positively associated with a worse glucose metabolism [1, 3, 14, 17]. According to these facts the anthropological status of male patients is defined as worse than that of the female patients. Some researchers confirmed our results and described the importance of intramuscular adipose tissue [15] in patients suffering from T2DM. It is very important to investigate the relationship between the body fat distribution and the complications of the disease too [6, 10, 20].

Conclusion

The values of BMI, % body fat tissue, fat mass and subcutaneous fat mass were significantly greater in female patients than in male patients, but the value of visceral fat tissue was significantly greater in male patients. These data demonstrated the accumulation of connective adipose tissue more subcutaneously, but less viscerally in female patients. It is opposite in the male patients: the accumulation of connective fat tissue is more viscerally, but less subcutaneously. The subcutaneous adipose connective tissue was accumulated predominantly in the torso than in the peripheral part of the body (arms, thighs and lower legs) in the male patients compared to the female.

These results are a reason to assess the anthropological status of male patients as worse than that of female patients for the prognostic of disease. The complex study including anthropometry of adipose connective tissue in patients suffering from T2DM would support the evaluation of the prognosis of the disease.

References

1. **Abbatecola, A. M, F. Lattanzio, L. Spazzafumo, A. M. Molinari, M. Cioffi, R. Canonico**. Adiposity Predicts Cognitive Decline in Older Persons with Diabetes: A 2-Year Follow-Up. – *PLoS ONE*, **5**(**4**), 2010.
2. **Bi, X., Y. T. Loo, C. J. Henry.** Body Fat Measurements in Singaporean Adults Using Four Methods. – *Nutrients,* **10** (**3**), 2018, 303-308.
3. **Choi, S., D. Chung, J. S. Lim, M. Y. Lee, J. Y. Shin.** Relationship between Regional Body Fat Distribution and Diabetes Mellitus: 2008 to 2010 Korean National Health and Nutrition Examination Surveys. – *Diabetes Metab J.*, **41**(**1**), 2017, 51-59.

4. **Fu, J., M. Hofker, C. Wijmenge**. Apple or Pear: Size and Shape Matter. – *Cell Metabolism.*, **21**(**4**), 2015, 507-508.
5. **Hauner, H**. Managing type 2 diabetes mellitus in patients with obesity. – *Treat Endocrinol.,* **3**(**4**), 2004, 223-232.
6. **Heiss, C. J., L. R. Goldberg**. Associations among Visceral Obesity, Type 2 Diabetes, and Dementia. – *J. Obes. Eat Disord.,* 2016; doi: 10.21767/2471-8513.100027
7. IDF. International Diabetes Federation.2016, 21:13. Available at https://www.idf.org/ files.
8. **Janssen, I., P.T. Katzmarzyk, R. Ross.** Waist circumference and not body mass index explains obesity-related health risk. – *Am. J. Clin. Nutr.*, **79**(**3**), 2004, 379-384.
9. **Kalra, S., M. Mercuri, S. S. Anand.** Measures of body fat in South Asian adults. – *Nutr. Diabetes*, **3**, 2013, 1-5.
10. **Kwakernaak, A. J., D.M. Zelle, S. J. L. Bakker, G. Navis**. Central Body Fat Distribution Associates with Unfavorable Renal Hemodynamics Independent of Body Mass Index. – *JASN.*, **24**(**6**), 2013, 987-994.
11. **Kwon, H., D. Kim, J. S. Kim.** Body Fat Distribution and the Risk of Incident Metabolic Syndrome: A Longitudinal Cohort Study. – *Sci. Rep*.,**7**, 2017, doi: 10.1038/s41598-017-09723-y
12. **Meisinger, C., A. Döring, B. Thorand, M. Heier, H. Löwel**. Body fat distribution and risk of type 2 diabetes in the general population: are there differences between men and women? The MONICA/KORA Augsburg cohort study. – *Am. J. Clin. Nutr.*, **84**(**3**), 2006,483-489.
13. **Papaetis, G., P. Papakyriakou, T. N. Panagiotou**. Central obesity, type 2 diabetes and insulin: exploring a pathway full of thorns. – *Arch. Med. Sci.*, **11**(**3**), 2015, 463-482.
14. **Petrofsky, J. S., M. Prowse, E. Lohman**. The Influence of Ageing and Diabetes on Skin and Subcutaneous Fat Thickness in Different Regions of the Body. – *J. Appl. Res.*, **8**(**1**), 2008, 55-61.
15. **Pritchard, J. M., S. Karampatos, K. A. Beattie, L. M. Giangregorio, G. Ioannidis, S. A. Atkinson, L. Thabane, H. Gerstein, Z. Punthakee, J. D. Adachi, A. Papaioannou.** The Relationship between Intramuscular Adipose Tissue, Functional Mobility, and Strength in Postmenopausal Women with and without Type 2 Diabetes. – *J. Aging Res.*, 2015, Article ID 872726.
16. **Sam, S., S. Haffner, M. H. Davidson, R. B. D'Agostino, S. Feinstein, G. Kondos, A. Perez, T. Mazzone.** Relationship of abdominal visceral and subcutaneous adipose tissue with lipoprotein particle number and size in type 2 diabetes. – *Diabetes*, **57**(**8**), 2008, 2022-2027.
17. **Schnijder, M. B., J. M. Dekker, M. Visser, L. M. Bouter, C. D. Stehouwer.** Trunk fat and leg fat have independent and opposite associations with fasting and postload glucose levels. – *Diabetes Care,* **27**, 2004, 372-377.
18 **Snijder, M. B**., **R. M. van Dam, M. Visser, J. C. Seidell.** What aspects of body fat are particularly hazardous and how do we measure them? – *Int. J. Epidemiol.*, **35**(**1**), 2006, 83-92.
19. **Shrestha, O. K., G. L. Shrestha**. Visceral fat versus subcutaneous fat: comparison of their association with type 2 diabetes mellitus. – *JCMC*, **4**(**2**), 2014, 9-12.
20. **Scheuer, S. H., K. Færch, A. Philipsen, M. E. Jørgensen, N. B. Johansen, B. Carstensen, D. R.Witte, I. Andersen, T. Lauritzen, G. S. Andersen.** Abdominal Fat Distribution and Cardiovascular Risk in Men and Women with Different Levels of Glucose Tolerance. – *JCEM,* **100**(**9**), 2015, 3340-3347.
21. **Tafeit, E., R. Möller, T. R. Pieber, K. Sudi, G. Reibnegger**. Differences of subcutaneous adipose tissue topography in type-2 diabetic (NIDDM) women and healthy controls. – *Am. J. Phys. Anthropol.,* **113**(**3**), 2000, 381-388.

Institute of Experimental Morphology, Pathology and Anthropology with Museum
Bulgarian Anatomical Society

Acta morphologica et anthropologica, 26 (1-2)
Sofia ● 2019

Southeuropoid Specifics in the Dermatological Characteristics of the Bulgarian Population from Central Western Bulgaria.

*Nadejda Paraskova[1], Zorka Mitova[2]**

[1] Faculty of Biology, Department of Zoology and Anthropology, Sofia University "St. Kliment Ohridski", Sofia, Bulgaria
[2] Institute of Experimental Morphology, Pathology and Anthropology with Museum, Bulgarian Academy of Sciences, Sofia, Bulgaria

*Corresponding author e-mail: zorkamitova@hotmail.com

The aim of the present study is to make a comparative dermatoglyphic characteristic of eight local populations of Central Western Bulgaria based on five dermatoglyphic traits - Delta index, Index of Cummins, carpal axial triradii (t), images of the hypotenar (Hy), and accessory interdigital triradii (AIT). In the processing and analysis of dermatoglyphic traits, the Cummins and Midlo's method and the Heet's method were used. Based on the analysis of these key traits, the South European and Eastern complexes, the generalized dermatoglyphic distances and the combining polygons were calculated and presented. Results show that in the studied population of Central Western Bulgaria: 1) an increased incidence of t; 2) decreased occurrence of images of Hy and a frequency of AIT and 3) the mean values for some of the dermatoglyphic traits analyzed are in the upper limits of the Eurasian scale, characteristic of the European population with Eastern characteristics.

Key words: South European and Eastern complex, generalized dermatoglyphic distances, combination polygons

Introduction

Dermatoglyphic studies are done in various aspects. The study of the skin relief has its application in both biological and non-biological scientific fields (history, archeology, etc.) [1, 17, 18, 19]. Anthropological studies in dermatoglyphic aspect are successfully applied in the study of individual ethnic, ethnographic and territorial groups of the population [4, 5, 7, 8, 10–14].

The development of the present work was provoked by various historical, archaeological and ethnographic sources that describe the settlement and the subsequent development of the Bulgarian population from the region of Central Western Bulgaria [1, 9, 11, 16].

In addition to the Thracians, Slavs and Proto-Bulgarians, the formation of the Bulgarian nationality also includes smaller ethnic groups such as Pechenegs, Kumans and

others [1]. In the later stages of Bulgarian history, other factors such as the integration, assimilation and amalgamation of separate ethnic groups, mixed marriages in some settlements, as well as the occurrence of settlements, mostly in mountainous areas, with nomadic population, contribute to the development of the Bulgarian nation [1, 3].

The area studied by us is predominantly populated by ethnic Bulgarians. In it, however, many settlements with names of Turkic origin have been described, which gives the researchers the reason to assume that these were settlements of Pechenegs and Yuruks and other nomadic and semi-nomadic communities [1, 6].

With this study of the Bulgarian population of Central Western Bulgaria, we would like to supplement the so-called historical facts about its formation. From an ethnographic point of view, contemporary Bulgarian population is divided into several ethnographic areas. The territory of our research, namely Central Western Bulgaria, is known as the "Shopi" ethnographic area. Anthropological literature reveals dermatoglyphic researches of Bulgarians – Shopi [11], a sample of the Pernik region [16], as well as of Bulgarians from some settlements with Shopish population in the Sofia region [10]. However, the population surveyed in these surveys is concentrated in areas close to Sofia. For this reason, our survey included Bulgarian population from the more extreme regions of the so-called „Big Shopluk", within the territory of Bulgaria.

The aim of the present study is to make a comparative dermatoglyphic characteristic of a local population from different regions of Central Western Bulgaria by analyzing five key ethnic dermatoglyphic traits, whose morphological independence and geographic gradient [4] show territorial differences in the dermatoglyphic picture of different ethnic population groups.

Material and Methods

A Bulgarian population from eight regions of Central Western Bulgaria has been studied (Trudovets, Slivnitsa, Sapareva Banya, Svoge/Iskrets, Kyustendil, Alino, Batanovtsi, Elin Pelin/Buhovo). A total of 1600 individuals of both sexes (800 men and 800 women) – 100 men and 100 women from each area. Dermatoglyphic fingerprints were processed according to the method of Cummins, Midlo [2], modified by Heet, et al widely used in ethnic dermatoglyphics [4]. Five basic dermatoglyphic traits are analyzed – Delta index (DL_{10}), Index of Cummins (Ic), proximal triradii (t), images of the hypotenar (Hy), and accessory interdigital triradii (AIT). The method of Sharma [15] is used to determine proximal triradii. On the basis of the results obtained a comparative-typological analysis was made by Heet's method, with the Eastern (EC) and Southern European complexes (SC) in both sexes [4].

The generalized dermatoglyphical distances (GDD) are calculated and are constructed combining polygons showing the variations of dermatoglyphic traits to the Eurasian scale [4]. Limits of summarized dermatoglyphic distances at territorial level are present in **Table 1**.

Table 1. Limits of generalized dermatoglyphical distances at territorial level (by Heet, 1983).

Category distance	Category limits/men	Category limits/women
very little	0 – 6.4	0 – 5.9
little	6.5 – 10.3	6.0 – 10.1
middle	10.4 – 14.8	10.2 – 15.0
large	14.9 – 18.8	15.1 – 19.4
very large	18.9 – 25.5	19.5 – 26.7

Results and Discussion

Basic dermatoglyphic traits, Eastern and Southern European complexes

In men (**Tabl.2**) from five groups – Trudovets (51,3), Slivnitsa (47,7), Sapareva Banya (52,7) Svoge/Iskrets (52,2) and Batanovtsi (55,2) prevail, although insignificant, Eastern dermatoglyphic features. In the other three groups - Kyustendil (55.5), Alino (52.7) and Elin Pelin/Buhovo (53.7), the Southern dermatoglyphic characteristics are more common.

Table 2. Basic dermatoglyphic traits, Eastern (EC) and Southern European complexes (SC) in men from different regions of Central Western Bulgaria.

Region/sign	**DL_{10}**	**Ic**	**t**	**Hy**	**AIT**	**EC**	**SC**
Trudovets	13,80	8,40	62,00	32,50	17,50	**51,3**	46,2
Slivnitsa	13,00	8,52	64,50	34,00	18,50	**47,7**	47,4
Sapareva banya	13,96	8,45	60,00	31,00	14,50	**52,7**	46,7
Svoge/Iskrets	13,60	8,22	58,00	35,00	11,50	**52,2**	48,4
Kyustendil	12,30	8,61	71,50	30,50	12,50	51,7	**55,5**
Alino	12,50	8,28	58,00	27,00	16,00	50,1	**52,7**
Batanovtsi	13,30	8,74	61,40	23,00	9,00	**55,2**	53,1
Elin Pelin /Buhovo	12,90	8,38	62,20	34,00	6,00	53,4	**53,7**

In women (**Table 3**) there are more pronounced Eastern dermatoglyphic elements in groups of Trudovets (50.6), Sapareva Banya (52.9), Svoge / Iskrets (51.4), Alino (50.4) and Batanovtsi (55.7). The women from Slivnitsa (45.4), Kyustendil (56.0) and Elin Pelin / Buhovo (53.6) have more pronounced Southern elements.

Table 3. Basic dermatoglyphic signs, Eastern (EC) and Southern European complexes (SC) in women from different regions of Central Western Bulgaria.

Region / Traits	**Dl_{10}**	**Ic**	**t**	**Hy**	**AIT**	**EC**	**SC**
Trudovets	13,40	8,60	64,00	28,50	18,50	**50,6**	47,9
Slivnica	12,36	8,74	63,00	36,00	20,50	41,9	**45,4**
Sapareva banya	13,96	8,36	58,50	32,00	13,50	**52,9**	46,9
Svoge/Iskrets	13,80	8,82	57,00	26,00	13,00	**51,4**	46,4
Kyustendil	12,80	8,10	69,00	31,00	14,00	55,2	**56,0**
Alino	13,20	8,38	56,50	28,00	16,00	**50,4**	48,9
Batanovtsi	13,40	8,62	62,00	26,00	8,00	**55,7**	53,0
Elin Pelin/Buhovo	12,60	8,40	60,00	34,00	6,00	51,6	**53,6**

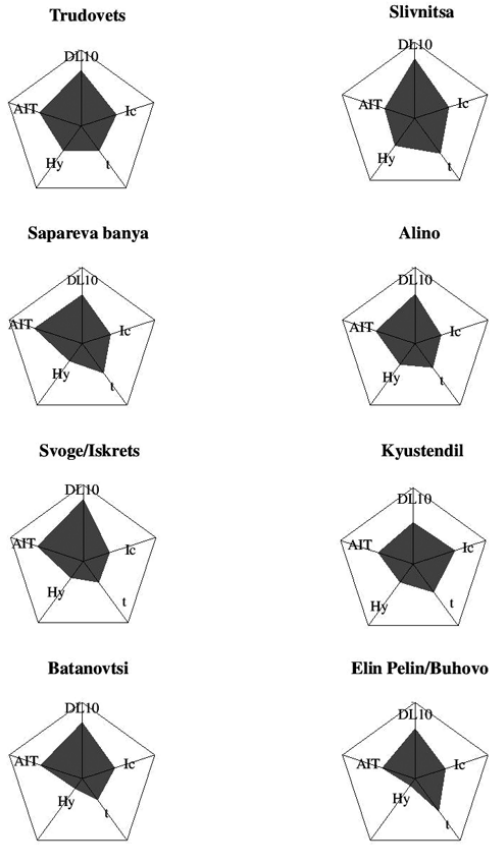

Fig. 1. Combination polygons showing variations in dermatoglyphic signs in males. The radii correspond to the Eurasian scale, assumed to be 100 percent, and their centers show the final Europoide values.

From the tables showing the distribution of Southern European and Eastern traits in men and women from Central West Bulgaria, we can conclude that groups are grouped among the surveyed population as a whole, based on the prevailing dermatoglyphic characteristics. The first group includes the population (men and women) from Trudovets, Sapareva Banya, Svoge/Iskrets and Batanovtsi. This is the group in which for both sexes there is typically a higher frequency of Eastern characteristics. The second group unites the men and women from Kyustendil and Elin Pelin/Buhovo, where the Southern features prevail. However, for Slivnitsa and Alino, there were differences between the two sexes (men and women) regarding the manifestation of the Eastern and Southern dermatoglyphic complexes. The Southern elements (47.7) are characteristic of the Slivnitsa men, while the Eastern ones (45.4) predominate among women. In the Alino population there is a reverse trend – in men have developed Eastern components (52.7), while in women dominate the Southern (50.4). The differences between men and women in these two areas, though insignificant, could be seen as a result of migratory processes.

In order to illustrate the results obtained, combination polygons were constructed, graphically representing the ratios between the five basic dermatoglyphic traits (**Figs 1 and 2**).

From the figures, we see that the men and women examined by us show a tendency for variability in some of the traits, namely axial triradii, hypothenar images, and additional interdigital triradii, which leads to some relatively high South European characteristics in these groups.

When compared to the groups studied by us, with others from Central West Bulgaria, but studied by other authors [10], some regularities were established according to the same methodology (**Fig. 3**).

Among the Bulgarian population, subject of our study, there is a relatively high frequency in proximal triradii and a low frequency incidence of hypotensive imaging. At the same time, in the population surveyed by other authors, there is a reverse trend – low frequency the proximal triradii and high frequency of the images on the hypotenar.

Considering the fact that the survey areas have a different location within the boundaries of an ethnographic area (settlements, around the central city of Sofia and settlements along the periphery), we can conclude that in the outskirts the population is more affected by a number of migration processes, which undoubtedly affect the inheri-

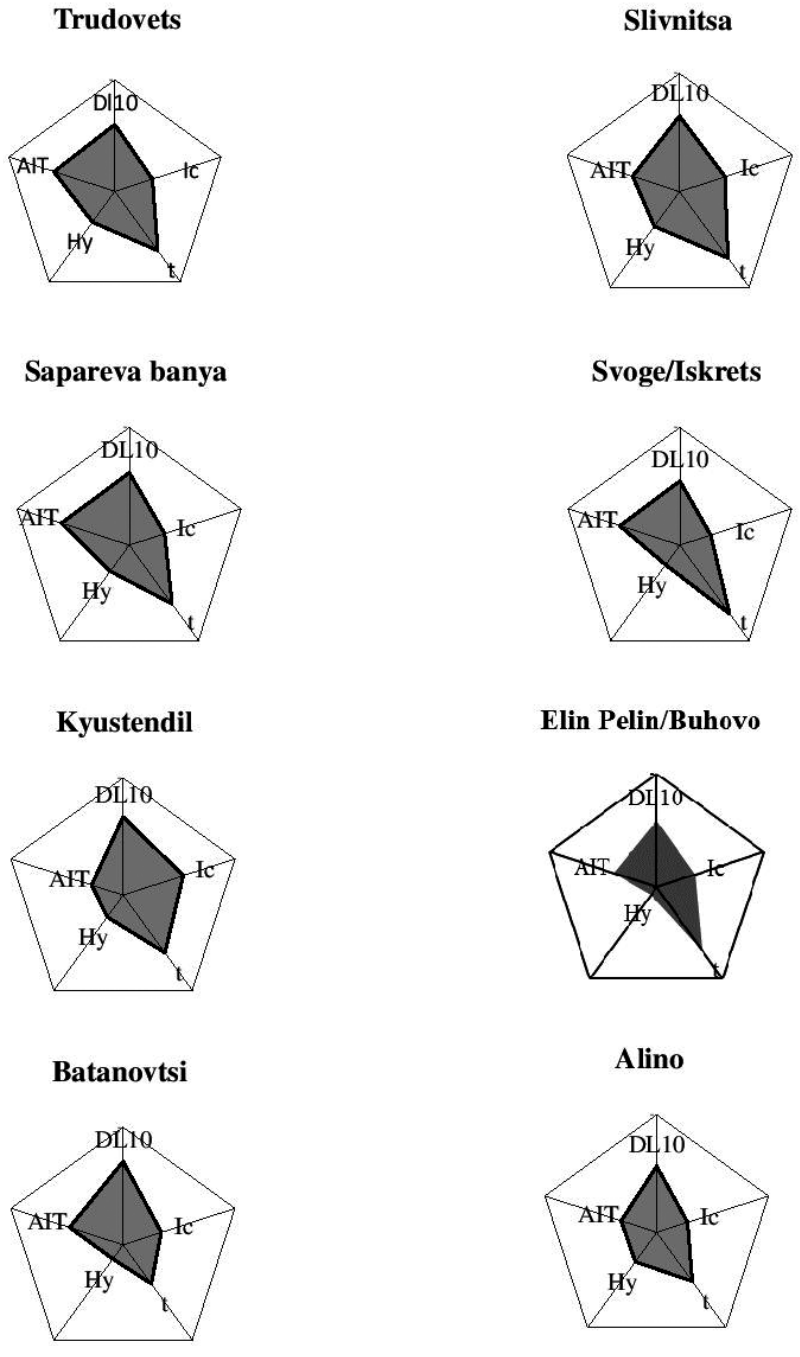

Fig. 2. Combination polygons showing the variations in dermatoglyphic signs in women. The radii correspond to the Eurasian scale, assumed to be 100 percent, and their centers show the final Europoide values.

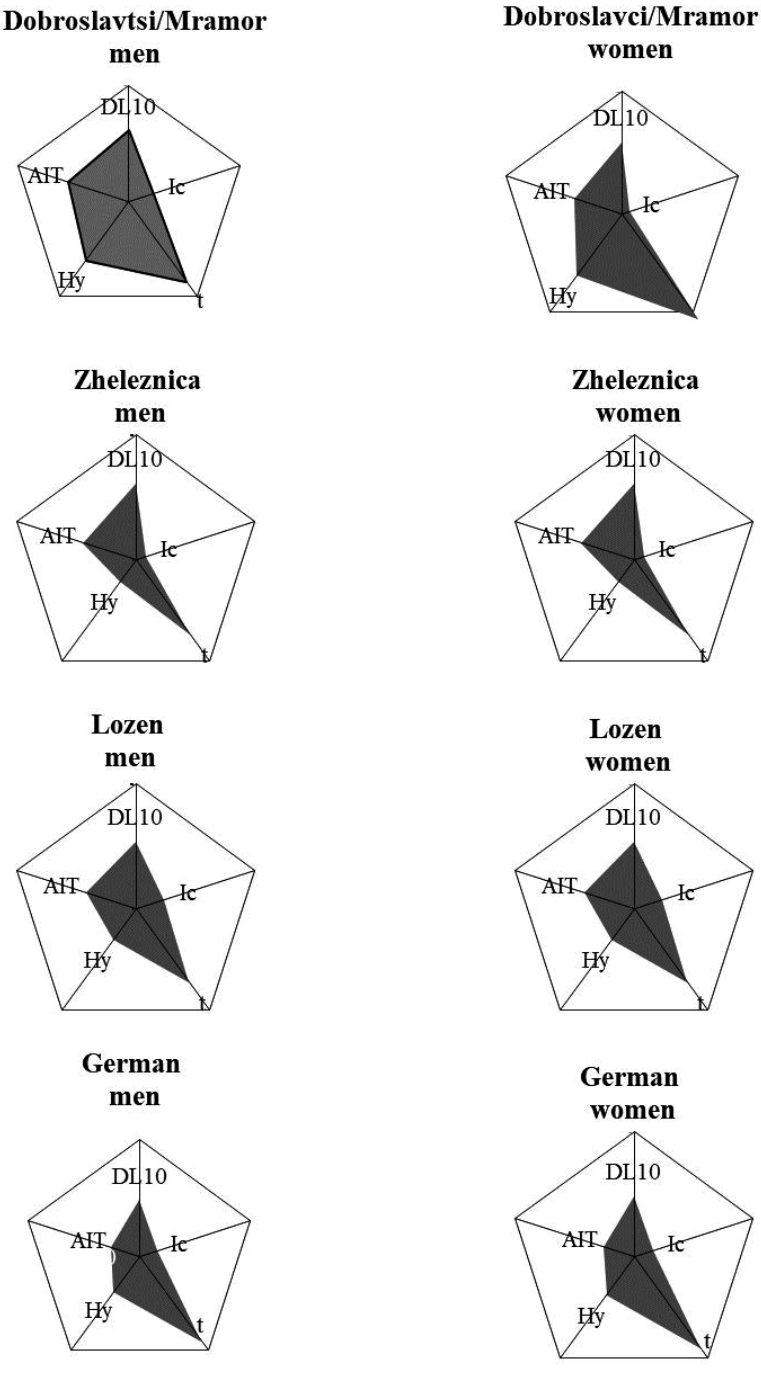

Fig. 3. Combination polygons showing the variations in dermatoglyphic signs in men and women by [10]. The radii correspond to the Eurasian scale, assumed to be 100 percent, and their centers show the final Europoide values.

tance of dermatoglyphic traits. We could say that this combination of dermatoglyphic traits is distinguished as characteristic of the local population.

Generalized dermatoglyphical distances (Tables 4 and 5)

For the studied population of Central West Bulgaria, the generalized dermatoglyphical distances were calculated, showing the mean differences between the five basic dermatoglyphic traits between two groups (limits present in Table 1).

It can be seen that in both genders prevail the average GDD. In male males the aggregate mean GDD ranged from 9.3 to 12.9 (**Table 4**), and in females from 9.0 to 13.6 (**Table 5**).

Table 4. Generalized dermatoglyphical distances (GDD) in the population of Central Western Bulgaria – men: 1 – Trudovets, 2 – Slivnica, 3 – Sapareva banya, 4 – Svoge/Iskrets, 5 – Kyustendil, 6 – Alino, 7 – Batanovtsi, 8 – Elin Pelin/Buhovo.

Region	1	2	3	4	5	6	7	8	GDD
1	–	6,1	3,9	7,5	14,2	10,9	13,1	9,7	**9,3**
2	**6,1**	–	9,3	10,4	10,6	10,8	13,8	7,8	**10,5**
3	**3,9**	9,3	–	7,1	13,1	10,3	11,6	10,9	**10,4**
4	7,5	10,4	7,1	–	15,6	10,9	13,1	8,4	**10,9**
5	14,2	10,6	13,1	**15,6**	–	11,5	14,1	12,2	**12,9**
6	10,9	10,8	10,3	10,9	11,5	–	12,6	12	**11,4**
7	13,1	13,8	11,6	13,1	14,1	12,6	–	11,2	**12,7**
8	9,7	7,8	10,9	8,4	12,2	12	11,2	–	**10,4**

It can be seen also that the group of Trudovets presents the minimal GDD among all groups – with Slivnitsa (6.1) and with Sapareva Banya (3.9) (**Table 4**).

For the men from Kyustendil it was found that they have the maximal GDD from the men of the Svoge/Iskrets region (15.6). In women, however, unlike men, there were no small GDD between the groups (**Table 5**). Among the women from Kyustendil and those from Svoge/Iskrets, there were also large GDD. The same could be explained by the presence of more pronounced Southern features among the Kyustendil population as a whole.

Table 5. Generalized dermatoglyphical distances (GDD) in the population of Central Western Bulgaria – women: 1 – Trudovets, 2 – Slivnica, 3 – Sapareva bania, 4 – Svoge/Iskrets, 5 – Kyustendil, 6 – Alino, 7 – Batanovtsi, 8 – Elin Pelin/Buhovo.

Region	1	2	3	4	5	6	7	8	GDD
1	–	8,7	9,2	8,8	10,3	6,2	6,7	13,4	**9,0**
2	8,7	–	14	14,8	13,3	13	14,5	11,8	**13,6**
3	9,2	14	–	7,3	9,6	6	10	9,1	**9,3**
4	8,8	14,8	7,3	–	15,1	7,4	6,7	14,4	**11,0**
5	10,3	13,3	9,6	**15,1**	–	9,8	13	10,9	**12,0**
6	6,2	13	6	7,4	9,8	–	8,8	10,4	**9,2**
7	6,7	14,5	10	6,7	13	8,8	–	9,2	**10,4**
8	13,4	11,8	9,1	14,4	10,9	10,4	9,2	–	**11,0**

Conclusions

Based on the results obtained, the following conclusions were made:

– In the studied population of Central Western Bulgaria, a characteristic ratio of the traits was found – an increased incidence of carpal axial triradii, decreased occurrence of images of the hypotenar and a frequency of accessory interdigital triradii;

– In the Central Western Bulgaria population, the mean values for some of the dermatoglyphic traits analyzed are in the upper limits of the Eurasian scale, characteristic of the European population with Eastern characteristics.

These results confirm the historical data on population amalgamation and the traces of migration processes in the region.

References

1. **Bozhilov, I., V. Mutafchieva, K. Kosev, A. Pantev**. *History of Bulgaria*. – Sofia, Hristo Botev, 1993, **759**. [in Bulgarian]
2. **Cummins, H., Ch. Midlo.** *Finger prints, palms and soles - introduction to the dermatoglyphics*. – Philadelphia, New York, Dover Publication, 1961, 300.
3. **Georgieva, Tsv.** Space and Spaces of Bulgarians XV-XVII Century. – *MSc Thesis,* University of Sofia, 1999, **343**. [in Bulgarian]
4. **Heet, G.** *Dermatoglyphics of the USSR peoples.* – Moscow*,* Science, 1983, **280**. [in Russian]
5. **Heet, G., I. Shirobokov, I. Slavolubova.** *Dermatoglyphics in Anthropology*. – Saint Petersburg, Nestor History, 2013, **376**. [in Russian]
6. **Kalyonski, A.** *The Yuruks*. – Sofia, Enlightenment, 2011, **470**. [in Bulgarian]
7. **Kavgazova, L.** Anthropological characteristics of a population from the Central Rhodopes. – *J. Anthropol.*, **4,** 2003, 119-123.
8. **Kavgazova, L., R. Stoev.** Dermatogliphic characteristics of a population from Gotse Delchev region (South-Western Bulgaria). – *Acta Morphol. Anthropol.*, **5**, 2000, 115-120.
9. **Kavgazova, L., R. Stoev.** Southeuropoid pequliarities in the dermatogliphic characteristics of population from different parts of Bulgaria. – *J. Anthropol.*, **2**, 1999, 164-171.
10. **Kavgazova, L., R. Stoev.** Dermatoglyphic characteristics of a population from the Sofia region. – *J. Anthropol.*, **3,** 2000, 191-199.
11. **Minkov, Tsv., V. Dimitrova.** Dermatoglyphic characterization of the shopi" population in Bulgaria. – *Ann. Univ. Sofia "St. Kl. Ohridski"*, **1,** (Zool. 82), 1994, 265-275. [in Bulgarian]
12. **Minkov, Tsv., V. Dimitrova, S. Maximova.** Anthropological characterization of Bulgarian population from the region of Strandja according to dermatogliphic data. – *Glasnik ADJ*, **36**, 2001, 123-130.
13. **Nikolova, M.** Heredity of finger dermatoglyphic patterns. – *Biology, Univ. of Plovdiv "P. Hilendarski"*, 29 (**6**), 1991, 215-225. [in Bulgarian]
14. **Nikolova, M., S. Tornjova.** Heredity of finger and palm dermatoglyphic patterns. – *Proceeding of 13 Bartos's symposium on dermatoglyphics*, Smolenice, 31 oct. – 2 nov., 1990, 32-37.
15. **Sharma, A**. *Comparative methodology in dermatoglyphics.* – Delhi, 1964.
16. **Todorov, I.** Anthropological characteristic of a "shopi" population from Pernic region according to dermatoglyphic data. – *MSc Thesis*, University of Sofia, 1994, **41**. [in Bulgarian].
17. **Vassilev, V.** Late medieval necropolis near Nedelko village, Pernik district. – *Archaeol. Discov. and Excavat. for 1975*, 1976, 86. [in Bulgarian]
18. **Vatev, St.** *Anthropology of the Bulgarians*. *Sofia, People's Health Society.* 1939, **123**. [in Bulgarian]
19. **Vatev, St., 1941. Skull measurement in Bulgaria.** - In: *Collection of the Bulgarian Academy of Sciences and Arts*, XXXV-3, Sofia, 257-478. [in Bulgarian]

Institute of Experimental Morphology, Pathology and Anthropology with Museum
Bulgarian Anatomical Society

Acta morphologica et anthropologica, 26 (1-2)
Sofia ● 2019

Anthropological Characteristics of Gagauzes from Kavarna

Racho Stoev

Institute of Experimental Morphology, Pathology and Anthropology with Museum of BAS, Bulgaria, Sofia-1113, Acad. G. Bonchev Str., bl. 25

Corresponding author e-mail: rastesto@abv.bg

Abstract.

The aim of this study is to make an anthropological characterization of an interesting small ethnic group in Bulgaria – the Gagauzes from Kavarna, based on the archives of the Section of Anthropology and Anatomy of IEMPAM-BAS. Data from individual anthropological blanks of 112 males have been processed statistically and analyzed. Based on this characterization the Gagauzes from Kavarna should have been formed as a population in the Balkans. This coincides with the results of the dermatoglyphic and genetic studies in Gagauzes outside Bulgaria.

Key words: Gagauzes, Anthropological characteristics, europoid elements, mongoloid elements, methodics of Michalski

Introduction

The Gagauzes are an interesting ethnic group – Turkic-speaking Orthodox Christians, whose origin is still unclear. They appear on the world scene only in 19th century – before 1868 there is no mention of them. In the beginning of 19-th century they live in the lands of Eastern Bulgaria intermixed with Bulgarians, Greeks, Albanians, Turks, Tartars and Gypsies. After the Russo-Turkish wars of 1806-12 and 1828-29 a great part of them migrate to the Russian Empire (together with Bulgarians and Albanians from the region). These who rested on the Balkans gradually assymilated with Bulgarians and Greeks, but these in Moldova developed proper national identity and received an regional autonomy. Today in Northeastern Bulgaria there exist only a limited number nonassymilated Gagauzes in some localities as Kavarna.

The anthropological studies among them are few. Such ones are carried out first by Pittard [9] in the beginning of 20th century, than after comparable methods with modern ones by Dyachenko in Moldova in 1958, published 1965 [3] and by Pulianos in Bulgaria in 1963, published 1967 [10]. The dermatoglyphic of the Gagauzes in Moldova has been studied by Dolinova [2] and by Segeda [11]. In the last years there are also studies on Y-chromosomal DNA haplogroups, as also on autosomal DNA [12, 4].

The purpose of this work is to make an anthropological characterization of the Gagauzes in Bulgaria based on materials from the scientific archive of IEMPAM-BAS collected in 1982 on an anthropological expedition in Kavarna, under the leadership of P. Boev.

Material and Methods

Individual data on 112 Gagauz-men were analyzed. A standard statistical processing has been made. In some traits it was found significant methodological difference from the standard anthropological methods, which require certain adjustments or exclude these features of analysis. A standard statistical processing was made. An anthropological analysis after methodology of Michalski with some adjustments was made also [5,6,7,8]. These adjustments are an evaluation of the phenotypic presence of the anthropological elements in the intermediary anthropological types, for example AE not to be calculated as 50% a and 50% e, but to pay attention on the anthropological fraction, i.e. Ae = 75% a, 25% e, ae = 50% a, 50% e, aE = 25% a, 75% e and so on. Typological analysis has been made of 109 men only because the lack of eye color in three individual research blanks.

The primary analysis of some anthropologic traits showed a significant deviation in the methodic of their measuring or evaluating from the standard anthropological methods, which necessitated some adjustments or excluding of some traits from analysis.

1. Most cephalometric measurements are close and intermediate to these found by Dyachenko [3] and Poulianos [10]. There is, however great difference in average bizygomatical breadth (132,8 mm) and in its standard deviation (7,8 mm). In reality such values are out of the norms for europoid populations. That's why for the typologic analysis a correction of the bizygomatical breadth has been made according to the formula

   $BBcor = (BB - 132,8) \times 5,1/7,8 + 140,8$, thus the average bizygomatical breadth and its standard deviation has been made equal to the mean of their values after Dyachenko and Poulianos.

2. Doubtful are also the high recorded frequency of epicanthus, of strong protrusions of the cheekbones, of flat face prophile – all of them had to be excluded from further analysis.
3. It seems that dark hair color frequency is overstated and eye color is evaluated by 12 grade scale and not by the standard scale of Martin (16 grades). Thus a connexion of these traits to the standard scales of Martin and Fischer-Saller has been made.
4. The skin color compared with the data of other investigations is decidedly too bright. It apparently is evaluated thus: 3 – white skin, 7 – matte skin, 4-6 intermediate colors, over 8 – swarthy.

Results

The results of the analysis show that the Gagauzes are of average height – 167,3 cm, brachycephals – head index 82,9%, meso- and leptoprosops – morphological facial index 87,8%, leptorrhins – nasal index 66,6%, with straight and curved nose – mean mark after Michalski 67,5, which is higher than straight, hazel eyes, brown hair, well-developed hair on the face and the chest, straight and slightly wavy hair, white and matte skin **(Table 1).**

Table 1. Basic anthropological characteristics of Gagauzes from Kavarna

Anthropological trait	N	M	SD	SE	MIN	MAX
Body height, cm	**110**	**167,3**	**6,9**	**0,7**	**150,4**	**189,0**
Head length, mm	112	185,0	5,8	0,5	170	199
Head breadth, mm	112	153,4	5,8	0,5	138	167
Head height, mm	110	127,1	10,8	1,0	100	165
Head index, %	**112**	**82,9**	**3,4**	**0,3**	**72,6**	**92,2**
Bizygomatic breadth, mm	112	140,8 (132,8)	5,2 (7,8)	0,5 (0,7)	129 (114)	152 (150)
Morphological face height, mm	112	123,5	6,3	0,6	109	140
Morphological facial index, %	**112**	**87,8 (93,3)**	**5,2 (6,7)**	**0,5 (0,6)**	**74,8 (77,5)**	**104,7 (116,4)**
Nasal height, mm	112	55,2	4,5	0,4	44	67
Nasal breadth, mm	112	36,5	2,9	0,3	30	42
Nasal index, %	**112**	**66,6**	**8,0**	**0,8**	**50,8**	**88,6**
Nasal profile after Michalski, 10-100	**112**	**67,5**	**20,6**	**1,9**	**10**	**100**
Eye color after Martin	**109**	**7,3**	**4,1**	**0,4**	**2**	**16**
Hair color after Michalski, 10-70, in parentnesses after Fissher-Saller	**112**	**51,3 /U/**	**12,6**	**1,2**	**20 /M/**	**65 /W-Y/**
Skin color	**111**	**4,0**	**1,7**	**0,2**	**2**	**7**
Face hair	**90**	**3,90**	**0,87**	**0,09**	**2**	**5**
Chest hair	**91**	**3,03**	**1,57**	**0,16**	**0**	**5**
Hair form	**111**	**2,57**	**1,01**	**0,10**	**1**	**5**

According the typological analysis the population of Kavarna's Gagauzes is heterogeneous. Among the individual anthropological types prevail Subnordic – 24%, Dinaric –15%, Northwestern / Atlanto Pontic / – 11%, Finnish and Alpine – 7% each one **(Table 2)**.

Phenotypically prevail Europoid elements / 72.7 % against 27,3% /. The typical for Central end Eastern Asia archimorphic Mongoloid elements (m, z) are only 1.6%, the rest are the protomorphic, which are presented in Europe from antiquity (l, q). Among the Europoid elements Southeuropoid and Northeuropoid elements are almost equally / 47,3% against 52.7% / **(Table 3)**.

Such anthropological structure after Cheboksarov [1] means that the group under study (in this case the Gagauzes) belongs to the Middle European populations, for which is typical the combination of Northerneuropoid (a, y) with Balkanocaucasian (h) and Uralolaponoid (l, q) traits. At the same time, the Mediterranean and Oriental elements (e, k), which show a shift from Central Europe to southeast, are quite pronounced. This coincides with the results of the already mentioned genetic studies, according which Gagauzes belong to the Balkan populations and are most close to Northern Macedonians, to the native inhabitants of Greek Macedonia, to the Bulgarians and Romanians, but in the same time they with Hungarians and Romanians are classified together with West and South Slavs as an "inter-slavic group of populations" [4, 12].

Table 2. Individual typological structure of Gagauzes from Kavarna (classification of Michalski-Henzel)

Anthropological type	Symbol	N	%
Nordic	AA	1	0,9
Armenoid	HH	3	2,8
Teutonish	AY	1	0,9
Egean	AB	1	0,9
Northwestern (atlanto-pontic)	**AE**	**12**	**11,0**
Amoritic	AK	2	1,8
Dinaric	**AH**	**16**	**14,7**
Subnordic	**AL**	**26**	**23,9**
Eurasian	AZ	1	0,9
Finnish	**AQ**	**8**	**7,3**
Rifean	YB	1	0,9
Atlantic	YE	1	0,9
Pseudoalpean	YH	2	1,8
Pseudocromagnoid	YQ	1	0,9
Levantinian	BH	2	1,8
Suboriental	EK	1	0,9
Litoral	EH	3	2,8
Sublaponoid	EL	4	3,7
Southeastern	EQ	2	1,8
Subarmenoid	KH	5	4,6
Western asian	KL	3	2,8
Orientalo-Mongolian	KM	1	0,9
Alpean	**HL**	**8**	**7,3**
Turanian	HM	1	0,9
Anatolian	HZ	1	0,9
Pseudolitoral	HQ	2	1,8
Total		109	100

In bold – anthropological types with significant (over 5%) presence)

Table 3. Phenotypic anthropological structure of Gagauzes from Kavarna (classification of Michalski-Henzel)

Anthropological element	a	y	b	e	k	h	l	m	z	q	Eastern complex	South-europoid complex
%	31,9	2,5	2,3	10,3	6,9	18,8	21,6	0,7	0,9	4,1	27,3	52,7

Conclusion

Based on the analysis above the Gagauzes from Kavarna should have been formed as a population in the Balkans. This coincides with the results of the already mentioned dermatoglyphic and genetic studies in Gagauzes outside Bulgaria.

Acknowledgements: To my friend Lukasz Macuga for the help during the work on this paper.

References

1. **Cheboksarov, N. N.** The Anthropological structure of recent Germans. – *Uchenye Zapiski* MGU, LVIII, 1941, 271-308 [in Russian].
2. **Dolinova, N. A.** Dermatoglyphics of Moldavian population. – *In: Polevye issledovaniya Instituta etnografii AN SSSR*, M., 1978, 174-179 [in Russian].
3. **Dyachenko, V. D.** Anthropological structure of Ukrainian people. – *Naukova dumka, Kiiv*, 1965, 1-151 [in Ukrainian].
4. **Kushniarevich, A., O. Utevska, M. Chuhryaeva, A. Agdzoyan, K. Dibirova, I.Uktveryte, M. Möls, L. Mulahasanovic, A. Pshenichnikov, S. Frolova, A. Shanko, E. Metspalu, M. Reidla, K. Tambets, E. Tamm, S. Koshel, V. Zaporozhchenko, L. Atramentova, V. Kučinskas, O. Davydenko, O. Goncharova, I. Evseeva, M. Churnosov, E. Pocheshchova, B. Yunusbaev, E. Khusnutdinova, D. Marjanović, P. Rudan, S. Rootsi, N.Yankovsky, P. Endicott, A. Kassian, A. Dybo, The Genomic consortium, C. Tyler-Smith, E. Balanovska, M. Metspalu, T. Kivisild, R. Villems, O. Balanovsky.** Genetic heritage of the Balto-Slavic speaking populations: A synthesis of autosomal, mitochondrial and Y-chromosomal data. – *PLoS One*. **10**(**9**) 2015.
5. **Michalski, I.** Anthropological structure of Poland. – *Acta Universitatis Lodziensis*, Lodz, 1949, 1-261 [in Polish].
6. **Michalski, I., T. Henzel.** Principles of human classification after Tadeusz Henzel and Ireneusz Michalski. – *Przegląd Antropologiczny,* **21**, 1-2, 1955 [in Polish].
7. **Orczykowska, Z.** An attempt of Cinstructing an anthropological key on the base of classification of Michalski. – *Przegląd Antropologiczny*, **22**, **1**, 1959, 212-229 [in Polish].
8. **Orczykowska, Z.** Anthropological analysis of Tajiks from Pamir. – *Materiały i Prace Antropologiczne*, **46**, 1959 [in Polish].
9. **Pittard, E.** Contribution to Anthropological Study of Gagauzes. – *Revue Anthropologi Que*, **26** (1916), 419-432 [in French].
10. **Poulianos, A.** Anthropological studies on the Balkans, Athens, 1967 [in Greek].
11. **Segeda, S. P.** The Dermatoglyphics of Ukrainians. – *Ph.D. thesis*, Moscow, 1980 [in Russian].
12. **Varzari, A., V. Kharkov, W. Stephan, V. Dergachev, V. Puzyrev, E. H. Weiss, V. Stepanov.** Searching for the origin of Gagauzes: inferences from Y-chromosome analysis. – *Am. J. Hum. Biol*., **21**, 2009, **3**, 326-36.

Institute of Experimental Morphology, Pathology and Anthropology with Museum
Bulgarian Anatomical Society

Acta morphologica et anthropologica, 26 (1-2)
Sofia ● 2019

Study of Dermatoglyphic Fluctuating Asymmetry in Female Breast Cancer

Galina Yaneva

Department of Biology, Faculty of Pharmacy, Medical University of Varna

* Corresponding author e-mail: galina_yanevaa@abv.bg

Abstract

Dermatoglyphic fluctuating asymmetry patterns are occasionally studied in cancer patients. The present examination covers 82 women with breast cancer and 60 healthy women from the region of Varna, Bulgaria. The dermatoglyphic examinations were performed by the method of Cummins and Midlo and the degree of the fluctuating asymmetry was assessed according to 1-r2 formula and R-L/R+L formula. The comparison of the palmar ridge counts of a-b II, c-d IV and a-d revealed considerably higher fluctuating asymmetry values in breast cancer females than in healthy controls. There were greater correlation coefficient values of the fluctuating asymmetry (1-r2) in the ridge count of the homologous thumbs, forefingers and little fingers of both hands but smaller ones of the third and fourth fingers of both hands in breast cancer females than in healthy controls. These traits could be used within a diagnostic algorithm for breast cancer screening among genetically predisposed female population.

Key words: dermatoglyphics, fluctuating asymmetry, breast cancer, region of Varna

Introduction

Fluctuating asymmetry is defined as random deviations on both sides of the body (limb or organs), with the average values in the population equal on both sides of the body [12, 15]. Fluctuating asymmetry is regarded as a promising measure of the stress experienced by individuals during their development, as well as the interaction between genetic and environmental forces which affect that development [6]. Fluctuating asymmetry is the most sensitive indicator of the ability to cope with stresses during ontogeny [14].

The small, random deviations from perfect symmetry that result from such factors are termed fluctuating asymmetry [11]. 'Fluctuating' refers to a pattern of bilateral variation where variation on the right and left sides is both random and independent. It tends to be small (around 1% of trait size or less). These random departures from bilateral symmetry provide a surprisingly convenient measure of developmental precision: the more precisely each side develops the greater the symmetry. Fluctuating asymmetry is a measure of developmental stability. It is one of many issues at the interface between

biology and medicine that offer valuable information at the whole organism level [11]. Such comprehensive information is a concept familiar to, and frequently used by, biologists, but is often overlooked in medicine [6, 14].

Fluctuating asymmetry is common in morphometric traits and its intensity is determined by the ability of the genotype to create a symmetrical phenotype, despite the intra- and extra-uterine environmental pressures exerted on the embryonal body during its development [5]. The level of fluctuating asymmetry reflects the relative success of developmental homeostasis to block developmental disturbances.

Assessing the developmental stability of individuals or populations by measuring fluctuating asymmetry is a well-established biological concept which has great potential for medical application [10]. The study of the correlations between anthropometric traits (height, palm length, etc.) and dermatoglyphic traits established a drop in the fluctuating asymmetry of finger ridge counts in individuals located in the centre of the distribution curve for morphological traits [4].

Recent biological theoretical treatments pertaining to developmental stability are applied to a range of human health issues such as cancer, genetic diseases, infectious diseases, etc. [14]. Dermatoglyphic fluctuating asymmetry patterns are occasionally studied in cancer patients. There is certain evidence that they could add some essential diagnostic and prognostic information in breast cancer patients, too, and thus contribute to more effective screening and prevention.

The objective of the present study was to comparatively analyze some peculiarities of some dermatoglyphic fluctuating asymmetry patterns in female breast cancer patients and healthy women in terms of the diagnostic significance of this method.

Material and Methods

The present investigation was performed during the period from January 1, 2014 till December 31, 2017. It covered 82 women with clinically, histologically and mammographically confirmed breast cancer as well as 60 healthy women from the region of Varna, Bulgaria. Breast cancer patients were aged between 36 and 80 years while healthy females were aged between 31 and 79 years. All of them were of Bulgarian ethnical origin.

The dermatoglyphic examinations were performed by the basic method of Cummins and Midlo [2]. The degree of the fluctuating asymmetry was assessed by using the ridge count of homologous fingers, palmar ridge counts and three maximal angles according to $1\text{-}r^2$ formula [8, 9] and R-L/R+L formula after the method of univariate ANOVA. Correlation and regression analyses were also applied. Statistical data processing was done by means of SPSS software package, version 19.

Results

Our results were presented in three tables and three figures.

The values of the correlation coefficients of ridge count of homologous fingers and their differences in breast cancer females and healthy controls were compared in **Table 1**. The results from the regression analysis demonstrate statistically significantly higher correlation coefficient values of the fourth fingers of both hands in breast cancer females than in healthy controls only ($p<0.05$) (**Table 1**).

The values of the coefficients of the fluctuating asymmetry (l-r2) of ridge count of homologous fingers and their differences in breast cancer females and healthy controls

were compared in **Table 2**. Correlation coefficient values (r) of the fluctuating asymmetry (l-r2) for the ridge count of the homologous thumbs, forefingers and little fingers are slightly greater while those of the homologous third and fourth fingers of both hands are insignificantly smaller in breast cancer females than in healthy controls (**Table 2**).

The results from univariate ANOVA of three ridge counts concerning the variation type were compared in **Table 3**. There is a statistically significant difference between the intergroup variation and residual (unexplained) variation concerning the b-c ridge count only (**Table 3**).

The results from the comparative analysis of the fluctuating asymmetry patterns in breast cancer females and healthy controls are juxtaposed on **Figure 1, Figure 2** and **Figure 3**. There is a considerable difference in terms of fluctuating asymmetry of the fourth homologous fingers between breast cancer females and healthy controls in favour of the patients only (0,979 versus 0,709) (**Table 2** and **Fig. 1**). There are considerably greater values of a-b II, c-d IV, and a-d palmar ridge counts concerning the fluctuating asymmetry in breast cancer females than in healthy controls (**Fig. 2**). There are relatively small differences between the breast cancer females and healthy controls concerning the fluctuating asymmetry (l-r2) of atd, dat and adt maximal angles (**Fig. 3**).

Table 1. Correlation coefficients (r) of ridge count of homologous fingers in breast cancer females and healthy controls

Left and right hand fingers	Correlation coefficients (r)		
	breast cancer females (n=82)	healthy controls (n=60)	Difference between coefficients
I	0.217	0.327	p>0.05
II	0.370	0.452	p>0.05
III	0.362	0.329	p>0.05
IV	0.593	0.145	**p<0.05**
V	0.387	0.400	p>0.05

Table 2. Fluctuating asymmetry (l-r2) of ridge count of homologous fingers in breast cancer females and healthy controls

Left and right hand fingers	Correlation coefficients (r)		
	breast cancer females (n=82)	healthy controls (n=60)	Difference between coefficients
I	0.953	0.893	+0.060
II	0.863	0.796	+0.067
III	0.869	0.892	-0.023
IV	0.709	0.979	-0.270
V	0.850	0.840	+0.010

Discussion

In the present study, there is a considerably higher fluctuating asymmetry value of the ridge count of the fourth homologous fingers of both hands in breast cancer females than in healthy controls only. The comparison of the palmar ridge counts of a-b II, c-d IV and a-d reveals considerably higher fluctuating asymmetry values in breast cancer females than in healthy controls. There are higher correlation coefficient values of the fluctuating asymmetry ($1\text{-}r^2$) in the ridge count of the homologous thumbs, forefingers

Table 3. Univariate ANOVA of a-b, b-c and c-d ridge counts in breast cancer females and healthy controls

Ridge count	Variation	sum of squares	mean square	F	p
a-b	intergroup	13.6	13.64901	0.17	0.68
	residual (unexplained)	10977.4	78.4102		
b-c	intergroup	3459.4	3459.439	77.134	**0.0001**
	residual (unexplained)	6278.9	44.85		
c-d	intergroup	471.104	471.104	0.68	0.411
	residual (unexplained)	96997.093	692.836		

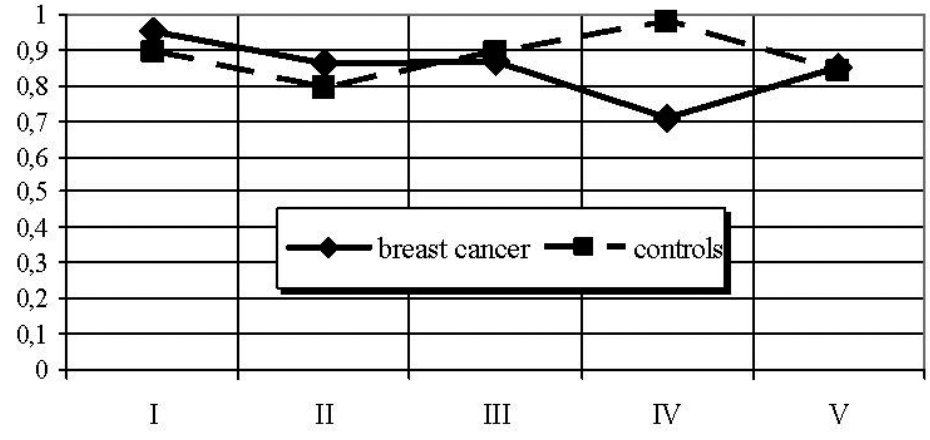

Fig. 1. Fluctuating asymmetry (l-r2) of ridge count of homologous fingers of both hands in breast cancer females and healthy controls

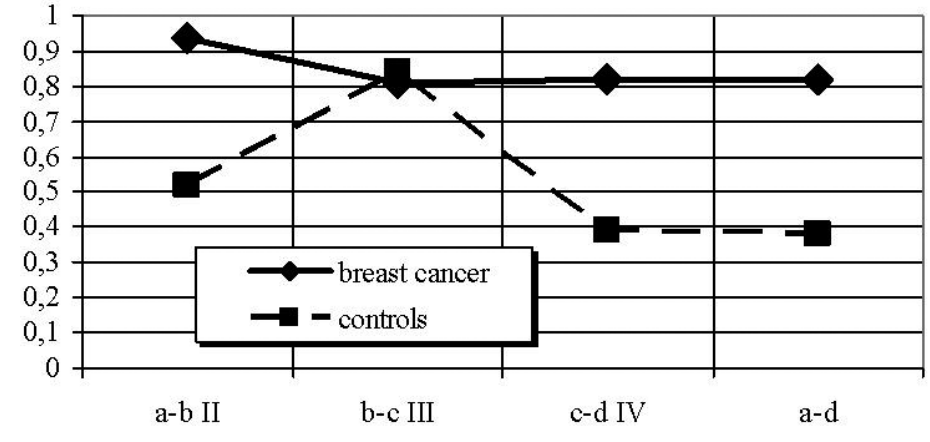

Fig. 2. Fluctuating asymmetry (l-r2) of palmar ridge counts in breast cancer females and healthy controls

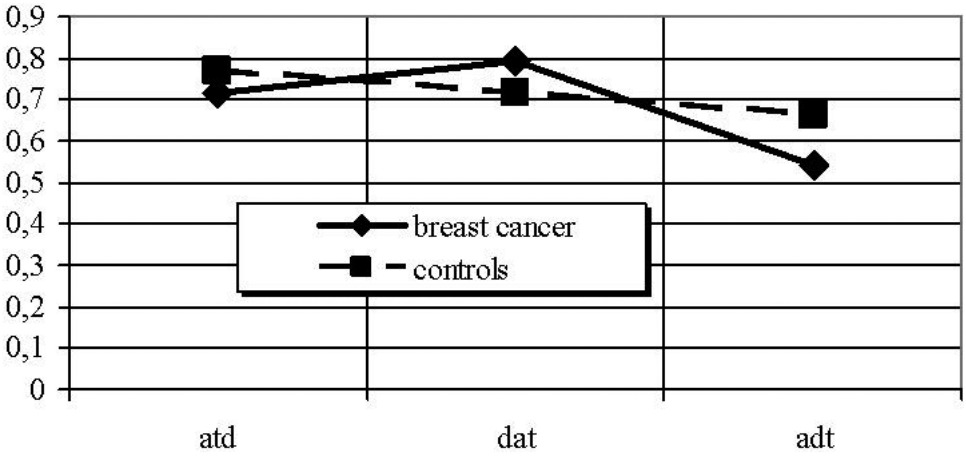

Fig. 3. Fluctuating asymmetry (l-r2) of atd, dat and adt maximal angles in breast cancer females and healthy controls

and little fingers of both hands but smaller ones of the third and fourth fingers of both hands in breast cancer females than in healthy controls.

The fluctuating asymmetry of finger and palmar dermatoglyphics of both hands was compared between 112 breast cancers women and 112 healthy controls in Han ethnic from Ningxia, China [7]. There were statistically significant differences between both groups in terms of the right finger ridge count of the thumb and atd angle ($p<0.05$), the fluctuating asymmetry of the little finger and atd angle ($p<0.01$) as well as in terms of the fluctuating asymmetry of the little finger and the ridge count of the fourth finger ($p<0.05$). There was also a significant difference in radial and ulnar loops ≥ 7 on the distribution of atd angle between these groups.

The fluctuating asymmetry of finger and palmar dermatoglyphic patterns of both hands was comparatively assessed between 100 breast cancer females and 100 healthy controls in India [8]. Fluctuation asymmetry values derived from quantitative parameters such as finger ridge counts, a-b ridge counts and palmar angles were statistically significantly higher in breast cancer females than in healthy controls for the thumb (by 2.01 times), subtotal ridge count (by 2.10 times) and palmar atd angle (by 2.01 times). The following different values of Person's correlation coefficient between both groups for the fluctuating asymmetry were established: thumb – r=0.31 and r=0.79; forefinger – r=0.62 and r=0.77; fourth finger – r=0.71 and r=0.64; subtotal finger ridge count – r=0.66 and r=0.11, and atd angle – r=0.74 and r=0.50. The values of correlation coefficients between both groups for the fluctuating asymmetry ($l\text{-}r^2$) were the following: subtotal finger ridge count – 0.55 versus 0.98; thumb – 0.90 versus 0.36; forefinger – 0.60 versus 0.39, and atd angle – 0.43 versus 0.74.

The relationship between genetic anomalies of different levels and deviations in dermatoglyphic traits of 40 Israeli-Jewish females with cervical cancer and 54 ones with endometrial cancer, on the one hand, and of 874 healthy males and females was comprehensively analyzed [1, 13]. There were statistically significant differences for some dermatoglyphic patterns between cancer patients and the control groups. The indices of fluctuating asymmetry proved more suitable for discrimination, yielding the highest discrimination level between women with cancer and control females.

The environmental and hereditary influence on tumour development using digito-palmar dermatoglyphic traits is assessed in 126 patients of both genders with pituitary tumors

(60 non-functional and 66 functional pituitary tumour patients) in comparison to a control group of 400 phenotypically healthy individuals [3].

Conclusion

Dermatoglyphic fluctuating asymmetry traits deserve further comprehensive and large-scale research in human oncology as they could provide reliable information about the possible effective screening and prevention of the malignant diseases.

References

1. **Bejerano, M., K. Yakovenko, M.B. Katznelson, E. Kobyliansky**. Relationship between genetic anomalies of different levels and deviations in dermatoglyphic traits. Part 7: Dermatoglyphic peculiarities of females with cervical and endometrial carcinoma. – *Z. Morphol. Anthropol*., **83**(**1**), 2001, 75-108.
2. **Cummins, H., C. Midlo**. Finger prints palms and soles. An introduction in dermatoglyphics. Blakinston, Philadelphia, New York: Reprinted Dower, 1961, 319 p.
3. **Gradiser, M., M. Matovinovic Osvatic, D. Dilber, I. Bilic-Curcic**. Assessment of environmental and hereditary influence on development of pituitary tumors using dermatoglyphic traits and their potential as screening markers. – *Int. J. Environ. Res. Public Health*, **13**(**3**), 2016, doi: 10.3390/ijerph13030330.
4. **Kobyliansky, E., G. Livshits**. Anthropometric multivariate structure and dermatoglyphic peculiarities in biochemically and morphologically different heterozygous groups. – *Am. J. Phys. Anthrop*., **70**, 1986, 251-263.
5. **Kobyliansky, E., M. Bejerano, M. B. Katznelson, I. Malkin**. Relationship between genetic anomalies of different levels and deviations in dermatoglyphic traits. – *Stud. Hist. Anthropol*., **4**(2004), 2006, 61-121.
6. **Kowner, R**. Psychological perspective on human developmental stability and fluctuating asymmetry: sources, applications and implications. – *Br. J. Psychol*., **92**(Pt **3**), 2001, 447-469.
7. **Lu, H., Z. H. Huo, P. Gao, J. Chen, T. Li, Z. Y. Shi, L. Peng**. Fluctuating asymmetry of dermatoglyphy in breast cancer patients. – *Acta Anat. Sinica,* **40**(**1**), 2009, 37-40.
8. **Natekar, P. E., F. M. DeSouza**. Fluctuating asymmetry in dermatoglyphics of carcinoma of breast. – *Indian J. Hum. Genet*., **12**(**3**), 2006, 76-81.
9. **Saha, S., D. Loesch, D. Chant, J. Welham, O. El-Saadi, L. Fañanás, B. Mowry, J. McGrath**. Directional and fluctuating asymmetry in finger and a-b ridge counts in psychosis: a case-control study. – *BMC Psychiatry*, **3**, 2003, 1-15.
10. **Scutt, D., J. T. Manning, G. H. Whitehouse, S. J. Leinster**. Fluctuating asymmetry of breasts: Its relationship to breast cancer. – *Imaging*, **10**(**1**), 1998, 19.
11. **Scutt, D., G. A. Lancaster, J. T. Manning**. Breast asymmetry and predisposition to breast cancer. – *Breast Cancer Res.,* **8**(**2**), 2006, R14. doi:10.1186/bcr1388.
12. **Soule, M. E.** Allometric variation. 1. The theory and some consequences. – *Am. Nat*., **120**(**6**), 1982, 751-764.
13. **Tegako, L. I., E. D. Kobyliansky**. Dermatoglyphics in contemporary human scientific cognition. Minsk: Belaruskaya navuka, 2015, 191 p. [in Russian].
14. **Thornhill, R., A. P. Møller**. Developmental stability, disease and medicine. – *Biol. Rev. Camb. Philos. Soc*., **72**(**4**), 1997, 497-548.
15. **Van Valen, L**. A study of fluctuating asymmetry. – *Evolution*, **16**(**2**), 1962, 125-142.

Institute of Experimental Morphology, Pathology and Anthropology with Museum
Bulgarian Anatomical Society

Acta morphologica et anthropologica, 26 (1-2)
Sofia ● 2019

Frontal Sinus Dimensions in the Presence of Persistent Metopic Suture

Silviya Nikolova, Diana Toneva*

Department of Anthropology and Anatomy, Institute of Experimental Morphology, Pathology and Anthropology with Museum, Bulgarian Academy of Sciences, 1113 Sofia, Bulgaria

* Corresponding author e-mail: sil_nikolova@abv.bg

Abstract

The frontal sinus (FS) is an air-filled space and usually appears as two irregularly-shaped cavities separated from each other by a septum. The persisting metopic suture (MS) is considered to be a factor influencing the FS development. In this study we aimed to compare the FS dimensions in metopic (n = 50) and control (n = 75) cranial series and thus to assess the relation between MS persistence and FS pneumatization. All skulls were scanned with industrial μCT system and volumetric images were generated. The total FS width and the height and depth of both FS lobes were measured.
The persistent MS was frequently co-occurred with significantly small and underdeveloped FS. The significant and positive correlations between the FS measurements showed that the FS pneumatization is a spatially-coordinated process and its progress is proportionately expressed in both vertical and horizontal plates of the frontal bone.

Key words: frontal sinus, *metopism*, persistent metopic suture, volumetric imaging, μCT scanning

Introduction

The frontal sinus (FS) is an air-filled space and one of the four paranasal sinuses developed as an expansion of the nasal cavities into the adjacent facial and skull bones. Since both lobes of the FS develop independently, they display a high degree of asymmetry attributed to more rapid development on one side at the expense of the other [21, 22, 23]. Commonly the FS appears as two irregularly-shaped cavities separated from each other by a thin bony septum, although many variations have been reported [28, 32, 34]. Furthermore, the FS has been considered to be unique in each person since its shape differs significantly even in monozygotic twins. Thus, due to its uniqueness, protected location, and frequent radiological documentation, the FS is particularly useful for identification of unknown human remains [22, 23].

The metopic suture (MS) lies between the halves of the fetal frontal bone and usually closes at the first or second postnatal year [29]. Failed fusion of the MS leads to condition known as *metopism*, reported to ranges from 0.8% up to 15% in different population groups [3, 5, 6, 12, 26, 35]. The persisting MS is considered to be a factor influencing the FS development [33]. In this study we aimed to compare the FS dimensions in metopic and control cranial series and thus to assess the relation between the MS persistence and FS pneumatization.

Materials and Methods

Material

The FS was investigated in a total of 125 dry adult male crania distributed into two series: a metopic series including skulls with entirely preserved MS (n = 50) and a control one (n = 75). The skulls belonged to soldiers who died in the Balkan Wars and the First World War, and whose bone remains were preserved in the Military Mausoleum with Ossuary at the National Museum of Military History of Bulgaria.

Methods

The scanning was performed using an industrial μCT system Nikon XT H 225 (Nikon Metrology). In order to compare the FS pneumatization when the MS persisted with normally developed FS, the cases of underpneumatized FS were excluded from the control series. Therefore, before scanning, the non-metopic skulls were inspected for FS development using the real time X-ray visualization. The Inspect-X software was used to adjust the settings. The scanning protocol for all of the specimens was as follows: voltage of 100 kV, a power of 10 W, 100 μA tube current and exposure time of 500 ms. A series of 2000 sequential projections were captured while the object was rotated on 360°. The raw data were reconstructed using the software CT Pro 3D with the same parameters and filters and resolution of 97.5 μm with isotropic voxels. The volumetric rendering, inspection in the three orthogonal plains, and FS measurements were accomplished using VG Studio Max 2.2. The total FS width and the height and depth on both FS lobes were measured on tomograms as linear distances between the outermost points (**Fig. 1**). The supraorbital line, tangential to the upper orbital rims, was used as a baseline for measurement of the FS height.

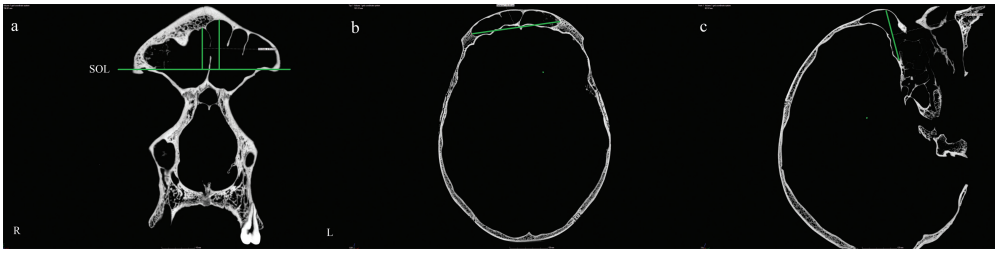

Fig.1. Frontal sinus dimensions: a) Frontal sinus height of right and left lobes measured in the coronal section; b) total frontal sinus width measured in the transversal section; c) frontal sinus depth measured in the sagittal section. Abbreviations: SOL – supraorbital line.

Statistical analyses

The mean, standard deviation (SD), minimum and maximum values were calculated for each measurement in the metopic and control series. The normal distribution of each variable was tested by the Kolmogorov-Smirnov normality test. The statistical significance of intergroup differences was assessed using the independent-samples *t*-test for the normally distributed variables and the Mann-Whiney *U*-test for the non-normally distributed ones. Bilateral differences in the FS height and depth were estimated by the paired *t*-test for the normally distributed variables and the Wilcoxon signed rank test in cases of non-normally distributed ones.

The Pearson bivariate correlation analysis was applied to evaluate the strength and direction of the relationships between the FS measurements. The strength of the correlations was classified according to the absolute values of correlation coefficients as follows: "very weak" (0.00-0.19), "weak" (0.20-0.39), "moderate" (0.40-0.59), "strong" (0.60-0.79), and "very strong" (0.80-1.00). A positive value denoted a positive correlation and a negative one indicated a negative correlation.

The intraobserver reliability was assessed by Intraclass correlation coefficient (ICC). For this purpose, the FSs of 20 randomly selected skulls were measured twice by one observer with a time interval of 4 months. The significance level of all statistical tests was set at $p<0.05$.

Results

The intraobserver reliability for all FS measurements was excellent (≥0.990).

All FS measurements were significantly larger in the control series, except for the depth of the left FS lobe (**Table 1**), which was insignificantly smaller in the metopic skulls. The control series did not show considerable bilateral differences in the FS measurements, whereas in the metopic skulls the depth of the left FS lobe was significantly

Table 1. Comparison between the frontal sinus dimensions in the metopic and control series

Measurements	Metopic series					Control					t-test / Mann-Whitney U-test
	n	mean	SD	min	max	n	mean	SD	min	max	
Frontal sinus width	50	46.57	14.27	19.26	74.50	75	54.19	14.01	30.78	85.67	U = 1394.50 (p = 0.016)*
Frontal sinus height R	37	13.68	6.63	3.52	28.89	75	17.31	8.10	2.69	48.76	U = 1018.50 (p = 0.023)*
Frontal sinus height L	46	14.42	6.23	1.74	27.80	75	17.06	6.50	4.11	36.88	t = -2.206 (p = 0.029)*
Frontal sinus depth R	49	23.70	8.16	10.49	46.23	75	27.16	8.01	5.55	45.03	t = -2.332 (p = 0.021)*
Frontal sinus depth L	50	26.08	7.89	10.08	44.08	75	26.94	8.99	7.40	52.67	t = -0.549 (p = 0.584)

* The significance level was set at $p<0.05$

larger compared to the right one (**Table 2**). In the metopic series, the FS aplasia was observed in 26% (n = 13) as in 8% (n = 4) it was bilateral and in 18% (n = 9) it was unilateral and entirely right-sided.

In both series, all correlations between FS measurements were positive and significant. In the metopic series, the FS width correlated strongly with the height and depth of both FS lobes. Furthermore, strong correlations were observed between the height and depth of right FS lobe as well as between the depths of both FS lobes (**Table 3**). In the control series, the FS width correlated strongly with the heights of both FS lobes. The depths of both FS lobes correlated very strong with one another (**Table 4**).

Table 2. Bilateral differences in the frontal sinus dimensions in the metopic and control series

Measurements	Series	Right					Left					paired t-test / Wilcoxon signed rank test
		n	mean	SD	min	max	n	mean	SD	min	max	
Frontal sinus height	Metopic	37	13.68	6.63	3.52	28.89	37	14.98	6.46	1.74	27.80	t = -1.153 (p = 0.256)
	Control	75	17.31	8.10	2.69	48.76	75	17.06	6.50	4.11	36.88	Z = -0.079 (p = 0.939)
Frontal sinus depth	Metopic	49	23.70	8.16	10.49	46.23	49	26.38	7.67	10.08	44.08	Z = 2.611 (p = 0.009)*
	Control	75	27.16	8.01	5.55	45.03	75	26.94	8.99	7.40	52.67	t = 0.354 (p = 0.724)

The significance level was set at $p<0.05$

Table 3. Correlations between the frontal sinus measurements in the metopic series

	FS width	FS height R	FS height L	FS depth R	FS depth L
FS width	1	0.769*	0.660*	0.767*	0.671*
FS height R		1	0.448*	0.604*	0.385*
FS height L			1	0.452*	0.492*
FS depth R				1	0.686*
FS depth L					1

* The significance level was set at $p<0.05$

Table 4. Correlations between the frontal sinus measurements in the control series

	FS width	FS height R	FS height L	FS depth R	FS depth L
FS width	1	0.730*	0.774*	0.596*	0.546*
FS height R		1	0.682*	0.391*	0.307*
FS height L			1	0.420*	0.391*
FS depth R				1	0.807*
FS depth L					1

* The significance level was set at $p<0.05$

Discussion

It has already been established that metopic skulls possess specific distinctive characteristics in the configuration of the cranium [1, 7, 13, 15-21, 23, 31, 35]. The established greater widths of the forehead and the orbital region could be attributed to the MS persistence, which allows excessive bone growth perpendicular to it [31].The significantly broad and high forehead in the MS series, however, is not related to a greater FS pneumatization. It is known that in metopic skulls both lobes of the FS develop separately on either side since the persistent MS precludes the likelihood of development of the sinus beyond the median plane [8, 28, 21, 23].This entity is useful in clinical practice for differentiation of a persistent MS from a fracture of the frontal bone on a radiograph [4].

The supposed influence of *metopism* on the general FS pneumatization has not been synonymous. It has been suggested that the persistence of MS inhibits the FS pneumatization [10, 27] due to the simultaneous FS development and frontal bone growth. Hence, the bipartite frontal bone and persistent MS could retarded or entirely suppressed the FS pneumatization [30]. The considerably frequent FS underdevelopment in metopic skulls has been established in some previous studies [2, 9, 18, 21, 25, 32, 33], whereas in others such a correlation has not been found [4, 11, 14, 24].

Our previous morphometric investigation performed on digital radiographs revealed a tendency for MS persistence to be frequently related to FS underdevelopment at least at the vertical portion of the frontal bone [21]. The present study is performed with advanced imaging modality allowing comprehensive survey of the FS shape and size. The results confirm previous findings and show that the *metopism* is frequently accompanied by an underdeveloped FS. Furthermore, the significant strong positive correlations between the FH measurements in both series show that the FS pneumatization is a spatially-coordinated process since its progress is proportionately expressed in the vertical and horizontal plates of the frontal bone.

In the metopic series the bilateral FS aplasia is rarer than the unilateral one, which is entirely right-sided. Besides, when the MS persists the FS is considerably smaller. These findings imply that the MS preservation inhibits the FS development. If this is so, it would be expected that the suppressed pneumatization of the vertical portion would be compensated with a hyperpneumatization of the orbital one. Such a tendency, however, is not observed. It has been suggested that the MS probably does not suppress the FS pneumatization itself [18, 21]. Rather, their co-occurrence is an expression or aftereffect of a certain condition during the early developmentand this hypothesis is supported by the present results as well.

It has been supposed that the midface hypoplasia blocks one of the major stimuli for the FS pneumatization, exactly the need to provide a structural bridge between neurocranium and face [32]. Such disorders like Hajdu-Cheney syndrome, cleidocranialdysostosis and pyknodysostosis exibit diminished FS pneumatization [32], as well as MS preservation [16]. The underlying factors causing the common occurrence of *metopism* and FS underdevelopment in non-syndromic individuals, however, are still unclear and are object of further investigations.

Conclusion

The persistent MS was frequently co-occurred with significantly small and underdeveloped FS. Furthermore, the right FS lobe in the metopic series was smaller with considerably decreased horizontal pneumatization, whereas the control series did not show significant bilateral differences in the FS dimensions. The significant positive correlations between the FS measurements showed that the FS pneumatization in both series is a spatially-coordinated process and its progress is proportionately expressed in the vertical and horizontal frontal bone plates.

Acknowledgements: The study was supported by the Bulgarian National Science Fund, Grant number DN01/15-20.12.2016 and Grant number DN11/9-15.12.2017.

References

1. **Ashley-Montagu, M. F.** The Medio-frontal suture and the problem of metopism in the primates. – The Journal of the Royal Anthropological Institute of Great Britain and Ireland, **67**, 1937, 157-201.
2. **Baaten, P. J. , M. Haddad, K. Abi-Nader, A. Abi-Ghosn, A. Al-Kutoubi, A. R. Jurjus .** Incidence of metopism in the Lebanese population. – *Clin. Anat*., **16**, 2003,148-51.
3. **Berry, A. C.** Factors affecting the incidence of non-metrical skeletal variants. – J. Anat., **120**, 1975, 519-535.
4. **Bilgin, S., U. H. Kantarcı, M. Duymus, C. H. Yildirim, B. Ercakmak, G. Orman, C. Gunenc Beser, M. Kaya, M. Gok, A. Akbasak**. Association between frontal sinus development and persistent metopic suture. – *Folia Morphol*.,**72**,2013, 306–310.
5. **Breathnach, A. S**. Frazer‘s anatomy of the human skeleton, London, J. & A. Churchill, 1920, 2th ed., 198-202.
6. **Bryce, T. H.** Osteology and arthrology. – In: *Quain‘s Elements of Anatomy*(Eds. E. A. Schäfer, J. Symington, T. H. Bryce), London: Longmans-Green, 1915, 11th edn.,Vol. IV, Part I, p. 177.
7. **Bryce, T. H.** Observations on metopism. – *J. Anat*., **51**, 1917, 153–166.
8. **Davis, W. B.** Development and anatomy of the nasal accessory sinuses in man. London, WB Saunders Company, 1914, 172 p.
9. **Guerram, A., J. M.Le Minor, S.Renger, G.Bierry**. Brief communication: The size of the human frontal sinuses in adults presenting complete persistence of the metopic suture. – *Am. J. Phys. Anthropol*.,**154**,2014, 621–627.
10. **Hodgson, G.**A text-book of x-ray diagnosis. London, H.K. Lewis,1957,Vol. 1,3rd ed., 419-428.
11. **Hunt, D. R., K. Everest**. Frontal sinus size: Sex, population and metopism affinities. –*Am. J. Phys. Anthropol.*, Abstracts of AAPA poster and podium presentations **114(S32)**, 2001, 82–83.
12. **Keith, A**. Human embryology and morphology. London, Edward Arnold, 1949, 6th ed., 690 p.
13. **Limson, M.** Metopismas found in Filipino skulls. –*Am. J. Phys. Anthropol*., **7**,1924, 317-324.
14. **Marciniak, R., C. Nizankowski**. Metopism and its correlation with the development of the frontal sinuses. – *Acta Radiol*., **51**, 1959, 343-352.
15. **Nikolova, S., D. Toneva.** Frequency of metopic suture in male and female medieval cranial series. – *Acta Morphol. Anthropol*., **19**, 2012, 250–252.
16. **Nikolova, S., D.Toneva,Y. Yordanov, N. Lazarov**. Multiple Wormian bones and their relation with definite pathological conditions in a case of an adult cranium. – *Anthropol. Anz.,* **71**, 2014, 169–190.
17. **Nikolova, S., D. Toneva, I. Georgiev.** A Case of Skeletal Dysplasia in Bone Remains from a Contemporary Male Individual. – *Acta Morphol. Anthropol*., **22**, 2015, 97-107.
18. **Nikolova, S., D. Toneva, I. Georgiev**. A persistent metopic suture – incidence and influence on the frontal sinus development (preliminary data). – *Acta Morphol. Anthropol*., **23**, 2016, 83–90.
19. **Nikolova, S., D. Toneva, I. Georgiev, Y. Yordanov, N. Lazarov**. Two cases of large bregmatic bone along with a persistent metopic suture from necropoles on the northern Black Sea coast of Bulgaria. – *Anthropological Science*, **124**, 2016, 145-153.

20. **Nikolova, S., D. Toneva, I. Georgiev**. Cranial Base Angulation in Metopic and Non-metopic Cranial Series .– *Acta Morphol. Anthropol.,* **24**, 2017, 45-49.
21. **Nikolova, S., D. Toneva, I. Georgiev, N. Lazarov**. Digital radiomorphometric analysis of the frontal sinus and assessment of the relation between persistent metopic suture and frontal sinus development. – *Am. J. Phys.Anthropol*., **165**, 2018, 492-506.
22. **Nikolova, S., D. Toneva, I. Georgiev, A. Dandov, N. Lazarov**. Morphometric analysis of the frontal sinus: application of industrial digital radiography and virtual endocast. – *JOFRI*, **12**, 2018, 31-39.
23 .**Nikolova, S., D. Toneva, I. Georgiev, N. Lazarov**. Relation between metopic suture persistenceand frontal sinus development.– In: *Challenging issues on paranasal sinuses*(Ed. Tang-Chuan Wang), Intech Open, 2018, DOI: 10.5772/intechopen.79376.
24. **Pondé, J. M., R. N.Andrade, J. M.Via, P. Metzger, A. C. Teles**. Anatomical variations of the frontal sinus. - *Int. J. Morphol*., **26**, 2008, 803-808.
25. **Rochlin, D. G., A. Rubaschewa**. The problem of metopism. – *Z. Menschl. Vererb. Konstitutionsl*., **18**, 1934, 339–348 [in German].
26. **Romanes, G. J.** Cunningham‘s Textbook of Anatomy. London, Oxford University Press, 1972, 11th ed., 1012 p.
27. **Samuel, E., G. A. S. Lloyd**. Clinical radiology of the ear, nose and throat. Philadelphia, W.B. Saunders Company, 1978, 2nd ed., 280 p.
28. **Schaeffer, J**. The Embryology, development and anatomy of the nose, paranasal sinuses, nasolacrimal passageways and olfactory organs in man. Philadelphia, P Blakiston’s Son, 1920., 370 p.
29. **Scheuer, L., S. Black.** Developmental juvenile osteology. San Diego, Academic Press, 2000, 102-108.
30. **Schuller, A.** A note on the identification of skull X-Ray pictures of the frontal sinus. – *Med. J. Aust*., **25**, 1943, 554-556.
31. **Schultz, A. H.** The metopic fontanelle, fissure, and suture. – *Dev. Dyn.*, **44**, 1929, 475-499.
32. **Shapiro, R., S. A. Schorr.** A consideration of systemic factors that influence frontal sinus pneumatization. – *Invest. Radiol.*, **15**, 1980, 191-202.
33. **Torgersen, J**. A roentgenological study of the metopic suture. – *Acta Radiol*., **33**, 1950, 1-11.
34. **Yanagisawa, E., H. M. Smith**. Radiographic anatomy of the paranasal sinuses IV. Caldwell View. – *Arch. Otolaryngol*., **87**, 1968, 311-322.
35. **Woo, J-K**. Racial and sexual differences in the frontal curvature and its relation to metopism. – *Am. J. Phys. Anthropol*., **7**, 1949, 215-226.

Institute of Experimental Morphology, Pathology and Anthropology with Museum
Bulgarian Anatomical Society

Acta morphologica et anthropologica, 26 (1-2)
Sofia ● 2019

Morphological Study of Jugular Foramen in Bulgarian Adults

Diana Toneva[1], Silviya Nikolova[1], Dora Zlatareva[2], Vassil Hadjidekov[2]*

[1] Department of Anthropology and Anatomy, Institute of Experimental Morphology, Pathology and Anthropology with Museum, Bulgarian Academy of Sciences, Sofia, Bulgaria
[2] Department of Diagnostic Imaging, Medical University of Sofia, Sofia, Bulgaria

* Corresponding author e-mail: ditoneva@abv.bg

Abstract

The size and shape of jugular foramen (JF) vary widely in different populations. This study aimed to investigate the size of JF in relation to sex and laterality and to establish the incidence of a domed bony roof and complete osseous bridging of the JF in Bulgarian adults. Head computed tomography scans of 148 individuals (66 males and 82 females) were used in the study. Three-dimensional surface models of the skulls were generated from the computed tomography images. The JF measurements were calculated based on the three-dimensional coordinates of definite landmarks located on the JF margin.
The JF differed significantly between males and females in its mediolateral diameter. Bilateral differences were found only in the anteroposterior diameter in males, which was greater on the right side. The domed bony roof was more common in males. The complete osseous bridging of the JF was equally frequent in both sexes.

Key words: jugular foramen, CT, 3D models, sex differences, laterality.

Introduction

The jugular foramen (JF) is a paired bony opening on the cranial base. It is located between the occipital bone and the petrous part of the temporal bone, behind the carotid canal and laterally and anterior to the *foramen magnum*. The JF is transmitted by the inferior petrosal sinus, the glossopharyngeal (IX), vagus (X), and accessory (XI) nerves, the sigmoid sinus becoming the internal jugular vein and some meningeal branches of the occipital and ascending pharyngeal arteries. The JF is conditionally divided into three portions: a smaller anteromedial (petrosal) part, which receives the drainage of the inferior petrosal sinus; a larger posterolateral (sigmoid) portion, which receives the drainage of the sigmoid sinus; and an intermediate (intrajugular) part through which the nerves pass. The structures traversing the foramen are essential for its bony configuration, since these structures develop first and the bone develops secondarily, encircling them [17].

The JF is the most important venous foramen of the skull [32] and the most complex of the foramina through which the cranial nerves pass [17]. It has irregular shape and curved course. In fact, although the JF is referred just as a foramen, it is a canal linking its endocranial to the ectocranial opening [20]. The JF has been previously studied mainly because of its clinical significance. Various congenital, vascular, and tumor lesions can involve the foramen and structures passing through it [27]. The JF could be affected by glomus jugulare tumor, paragangliomas, intracranial meningiomas, schwannomas, metastatic lesions and infiltrative inflammatory processes from surrounding structures [15, 19, 27]. Difficulties in the surgical exposure of this foramen arose from its deep location and the surrounding vital structures, such as the carotid artery, the hypoglossal nerve, the facial nerve and the vertebral artery [15]. The morphology and morphometry of JF are important for neurosurgeons dealing with lesions occupying this region [22]. Besides, morphometric analysis of the JF is crucial for radiologists to predict the chances of preserving nervous and vascular structures intact during surgical interventions [27]. Knowledge of JF dimensions is also important in the diagnosis of JF stenosis or widening [2].

The JF size and shape vary among different skulls and within the same skull from side to side and from its intracranial to extracranial opening [17]. Variations in the JF size have been mainly studied on dry skulls [2, 5, 7, 13, 14, 15, 19, 20, 22, 23, 26, 27, 28, 31, 32]. The JF has been also examined on CT images, but in search of an association between JF side dominance and hand preference [1]. However, medical CT images allow more thorough examination of the JF morphology, providing the possibility for accurate measurements and observation of the foramen from different aspects. Besides, the medical CT is a superior technique to the microsurgical anatomy with dissecting microscope, which also has been used for examination of the JF morphology and especially of its contents [29].

The JF is one of the most variable anatomical structures at the skull base [29]. Its size and shape vary in different populations and sexes [15]. There have been few studies on the sexual dimorphism in the JF size, establishing the presence of sex differences in Brazilians [23] and Poles [32], but absence of such differences in Turks [5]. In addition, some morphological traits of the JF such as dome bony roof and complete osseous bridging could be found with varying frequency among different populations. Since the extreme variations in the JF size and shape could put at risk the neurovascular structures transmitted by the foramen, it is important to know the norm and extremes in the JF morphology in different populations. However, there are no such data reported for the Bulgarian population. Therefore, the present study aimed to investigate the size of jugular foramen (JF) in relation to sex and laterality and to establish the incidence of a domed bony roof and complete osseous bridging of the JF in Bulgarian adults.

Material and Methods

A sample of 148 individuals (66 males and 82 females) was used in the study. The mean age of the males and females was 59.2±17.2 years and 59.3±18.1 years, respectively. All subjects were scanned using a Toshiba Aquilion 64 CT scanner. The scanning protocol was as follows: 32 × 0.5 mm detector configuration, tube voltage of 120 kV, tube current up to 500 mA, exposure time of 0.5 s, and total scan time of 6.5 – 7.0 s. Images were reconstructed with a 512 x 512 reconstruction matrix, 0.5 mm slice thickness and 0.3 mm reconstruction interval using convolution kernel FC81. The study sample did not include individuals with pathological lesions on the skull base. The study was approved by the Ethics Committee at IEMPAM-BAS.

The DICOM series of each individual was imported into the free software 3DSlicer [10], where the bone tissue was segmented using grayscale thresholding (226 – 3071 HU) and a bone mask was created for every image. Subsequently, the bone mask from the whole image stack was converted to a three-dimensional (3D) mask. Based on the outer contours of the mask, a surface 3D model was acquired and exported in PLY format. Afterwards, each 3D model was imported into software MeshLab [6], where the vertebrae were deleted and the skull base was exposed. The same software was used to pick landmarks located on the JF margin. The landmarks were placed on both endo- and ectocranial openings of the JF. Based on the 3D coordinates of these landmarks, the endo- and ectocranial JF measurements were calculated as Euclidean distances (**Fig. 1a-b**). The computation of these distances was performed in the software PAST [12]. The measurements of JF were calculated for both right and left side. The mediolateral diameter of JF (MLD) was measured between the most lateral (JF_{lat}) and the most medial (JF_{med}) point of the JF margin. The anteroposterior diameter (APD) was measured perpendicular to the mediolateral axis, in the widest part of the JF. An index of JF (IJF) was computed between the APD and MLD (IJF=APD/MLD*100) regarding the ecto- and endocranial measurements. Furthermore, ectocranial distances between the most lateral as well as the most medial landmarks of the right and left JF were calculated (**Fig. 1c**). An angle of inclination of the mediolateral axis of the JF (AIJF) toward the line passing through both right and left most lateral JF points was calculated for each side (Fig. 1d). The angle was computed as follows: firstly, a triangle between the most lateral and the most medial points of the JF on the one side and the most lateral point of the JF on the opposite side was constructed; secondly, its sides were reckoned as Euclidian distances; and thirdly, the angle was calculated using the Law of Cosines. In addition, the 3D coordinates of the midsagittal landmarks *basion* and *opisthion* were taken to assess the outlying of the most medial and most lateral points of the JFs from them (**Fig. 1e**).

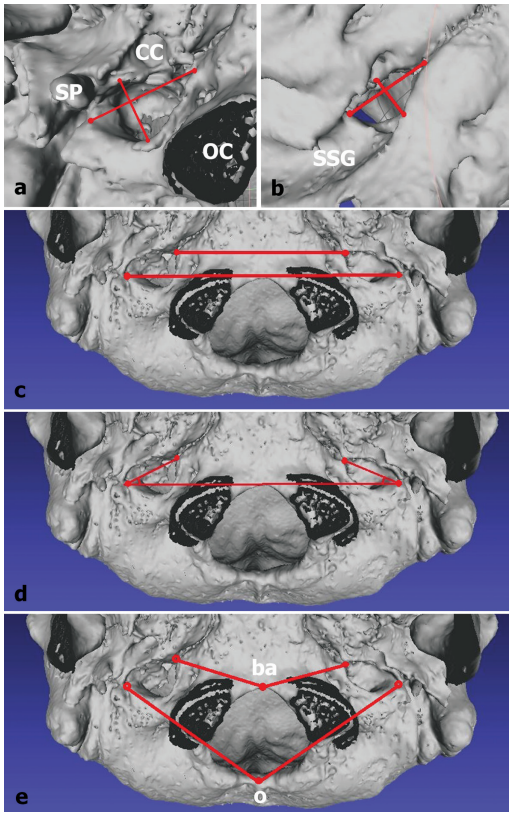

Fig. 1. Measurements: a) ectocranial mediolateral and anteroposterior diameters of the jugular foramen; b) endocranial mediolateral and anteroposterior diameters of the jugular foramen; c) interforaminal distances; d) angle of inclination of the mediolateral axis of the jugular foramen on the right and left side; e) distances from basion (ba) to the medial landmarks of the right and left jugular foramen and from opisthion (o) to the lateral landmarks of the right and left jugular foramen. CC – carotid canal; SP – styloid process, OC – occipital condyle, SSG – sigmoid sinus groove.

The incidence of a domed bony roof (**Fig. 2**) and complete osseous bridging of the JF (**Fig. 3**) was established.

Statistical analsyses

The sex and bilateral differences were evaluated for statistical significance.

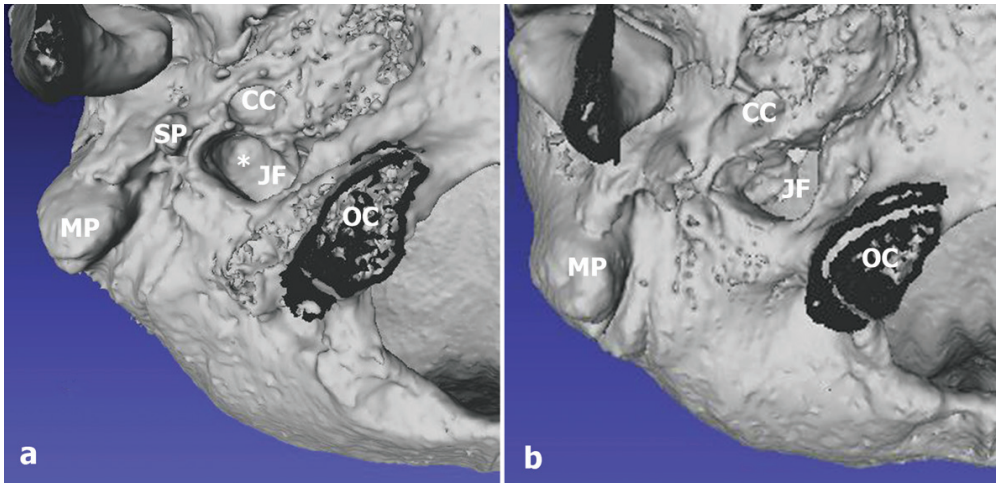

Fig. 2. Domed bony roof of the jugular fossa: a) presence; b) absence. JF – jugular foramen, CC – carotid canal, SP – styloid process, MP – mastoid process, OC – occipital condyle, * – domed bony roof.

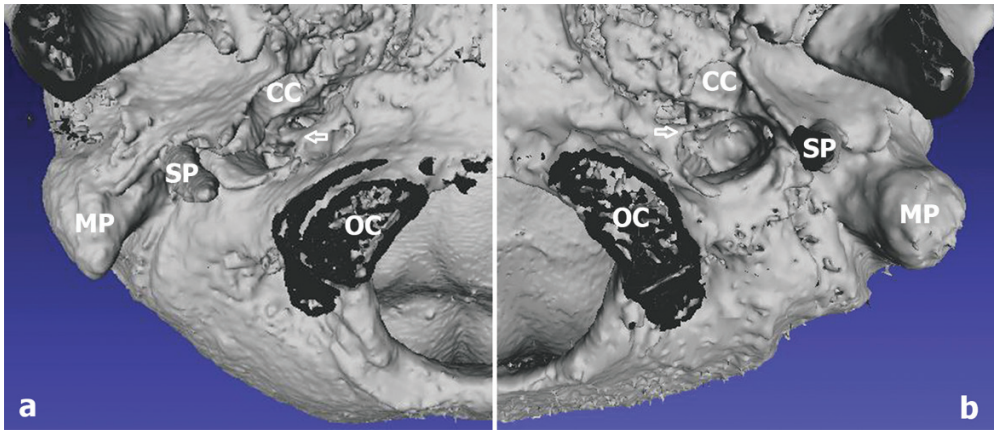

Fig. 3. Complete osseous bridging: a) of the right jugular foramen in a female; b) of the left jugular foramen in a male. CC – carotid canal, SP – styloid process, MP – mastoid process, OC – occipital condyle, ↑ – complete bridging.

The sex differences were assessed using the independent samples t-test. The bilateral differences were estimated by the paired t-test.

Univariate discriminant function analysis was applied to the measurements showing significant sex differences. The sectioning point of the male and female centroids was used as a cut-off value. Applying the discriminant functions, if the resulting score was greater than the cut-off value, it was related to a male and if the score was smaller, it was considered to a female. The leave-one-out cross-validation approach was used to determine the classification accuracy of the discriminant functions. The acceptable level of accuracy was set at 70% [11].

To assess the intraobserver reliability, a sample of 15 skulls was measured twice by one observer. All metric parameters were recalculated and tested by Intraclass correlation coefficient (ICC). According to the ICC values, the reliability was assessed as poor (<0.50), moderate (0.50-0.75), good (0.75-0.90), and excellent (>0.90) [18].

The sex differences in the distribution of domed bony roof and complete osseous bridging of the JF in regard to laterality were assessed using the chi-square test.

For all statistical tests, a value of $p < 0.05$ was accepted as a statistically significant level.

Results

The intraobserver reliability was assessed as excellent for most of the measurements, except for the ectocranial MLD on the left side, endocranial MLD and APD on the left side, and both AIJF, which indicated good reliabilty.

Concerning the ectocranial JF measurements, significant sex differences were found in the MLD on both sides, but not in the APD (**Table 1**). Such differences were also established in the distances between the most lateral and the most medial points of the right and left JFs and in the distances of the JF points to *basion* and *opisthion*. The JFI also showed significant sex differences, but only on the left side, indicating considerably greater APD towards the MLD in females. The right and left AIJF did not show any significant differences between the two sexes. Regarding endocranial JF measurements, they were smaller than the ectocranial ones. Significant sex differences were established only in the MLD on the left side.

In both sexes, the right JF had greater APD than the left one. However, significant bilateral differences were established for the APD only in the male skulls. Such differences were found on both endo- and ectocranial surfaces (**Table 1**). Furthermore, bilateral difference were observed neither in the distances of both JFs to *basion* and *opisthion*, nor in the angle characterizing the inclination of the mediolateral axes of the JFs. Concerning the IJF values on both cranial surfaces, the right JFs were relatively wider than the left ones, especially in males, where bilateral differences were statistically significant.

The univariate discriminant functions including the endo- and ectocranial MLD and the distances between the right and left JFs produced relatively low accuracy rates (**Table 2**). Only the distance between the lateral points of the right and left JFs showed accuracy of nearly 71%. Most of the other studied measurements provided accuracy rates higher than 70%. The highest accuracy of 75.7% was obtained for the discriminant function including the distance from *opisthion* to the most lateral point of the left JF.

A domed jugular fossa indicating the presence of a prominent superior jugular bulb was recorded bilaterally in 27.7% and unilaterally in 43.9% of the skulls. The domed roof was most commonly present bilaterally in males, while in females it was most frequently absent (**Fig. 4**). In unilateral cases, the domed bony roof was more common on the right side in both sexes. The sex differences in the distribution of the domed roof of the jugular fossa regarding the laterality did not achieve statistical significance ($\chi^2(2, N = 148) = 3.26$, $p = .353$).

The presence of a complete osseous bridging of the JF was established in 31.7% (4.7% bilaterally and 27.0% unilaterally) of the skulls. The unilateral bridging in males was observed more frequently on the left side, while in females, it was more common on the ride side (**Fig. 5**). However, the sex differences in the distribution of this feature did not reach statistical significance ($\chi^2(2, N = 47) = 2.02$, $p = .364$).

Table 1. Descriptive statistics of the linear measurements /in mm/ and the angle of jugular foramen /in degrees/ by sex and laterality.

Measurements	Males		Females		Sex differences	Bilateral differences
	Mean	SD	Mean	SD		
MLD_{ecto} (R)	18.21	2.71	16.93	2.35	t = 3.087 (p = 0.002)*	Males: t = 0.812 (p = 0.420) Females: t = 1.187 (p = 0.239)
MLD_{ecto} (L)	17.92	2.09	16.59	2.02	t = 3.899 (p = <0.001)*	
APD_{ecto} (R)	9.70	2.22	9.13	2.03	t = 1.625 (p = 0.106)	Males: t = 3.660 (p = 0.001)* Females: t = 1.878 (p = 0.064)
APD_{ecto} (L)	8.30	1.99	8.47	2.11	t = -0.494 (p = 0.622)	
IJF_{ecto} (R)	54.00	11.55	54.72	12.62	t = -0.358 (p = 0.721)	Males: t = 3.799 (p = <0.001)* Females: t = 1.885 (p = 0.063)
IJF_{ecto} (L)	46.63	12.16	51.04	11.76	t = -2.233 (p = 0.027)*	
MLD_{endo} (R)	14.67	2.10	14.25	2.11	t = 1.184 (p = 0.238)	Males: t = 0.109 (p = 0.913) Females: t = 0.993 (p = 0.323)
MLD_{endo} (L)	14.63	1.70	14.01	1.79	t = 2.142 (p = 0.034)*	
APD_{endo} (R)	7.70	2.45	7.45	2.13	t = 0.657 (p = 0.512)	Males: t = 2.478 (p = 0.016)* Females: t = 1.934 (p = 0.057)
APD_{endo} (L)	6.77	2.05	6.86	1.96	t = -0.267 (p = 0.790)	
IJF_{endo} (R)	52.77	15.99	52.93	15.16	t = -0.060 (p = 0.952)	Males: t = 2.527 (p = 0.014)* Females: t = 1.705 (p = 0.092)
IJF_{endo} (L)	46.65	14.40	49.44	14.42	t = -1.171 (p = 0.244)	
JF_{lat} (R) – JF_{lat} (L)	76.94	4.33	73.01	3.67	t = 5.989 (p = <0.001)*	-
JF_{med} (R) – JF_{med} (L)	45.11	4.38	43.06	3.40	t = 3.208 (p = 0.002)*	-
JF_{lat} (R) – opisthion	52.35	3.43	49.39	2.76	t = 5.817 (p = <0.001)*	Males: t = -1.580 (p = 0.119) Females: t = -1.281 (p = 0.204)
JF_{lat} (L) – opisthion	52.90	2.83	49.72	2.60	t = 7.097 (p = <0.001)*	
JF_{med} (R) – basion	26.70	2.44	24.82	2.01	t = 5.040 (p = <0.001)*	Males: t = 1.251 (p = 0.215) Females: t = 1.102 (p = 0.274)
JF_{med} (L) – basion	26.43	1.98	24.59	2.02	t = 5.570 (p = <0.001)*	
AIJF (R)	27.45	7.10	25.62	6.48	t = 1.634 (p = 0.104)	Males: t = -0.024 (p = 0.981) Females: t = -0.785 (p = 0.435)
AIJF (L)	27.48	7.20	26.27	7.20	t = 1.017 (p = 0.311)	

MLD – mediolateral diameter; **APD** – anteroposterior diameter; **IJF** – index of the jugular foramen; **ecto** – ectocranial; **endo** – endocranial; **JF_{lat}** – the most lateral point of the jugular foramen on the ectocranial side; **JF_{med}** – the most medial point of the foramen on the ectocranial side; **AIJF** – the angle of inclination of the jugular foramen; **R-** right; **L** – left; * – significant at p<0.05.

Table 2. Univariate discriminant functions.

Discriminant functions	Wilks' lambda	Group centroids		Sectioning point	Classification accuracy (%)		
		♂	♀		♂	♀	Overall
0.398 x **MLD_{ecto}(R)** - 6.957	0.939	0.283	-0.228	0.028	62.1	59.8	60.8
0.487 x **MLD_{ecto}(L)** - 8.361	0.906	0.357	-0.288	0.035	54.5	61.0	58.1
0.572 x **MLD_{endo}(L)** - 8.175	0.970	0.196	-0.158	0.019	59.1	58.5	58.8
0.251 x **JF_{lat}(R)–JF_{lat}(L)** - 18.802	0.803	0.549	-0.442	0.054	68.2	73.2	70.9
0.259 x **JF_{med}(R)–JF_{med}(L)** - 11.376	0.934	0.294	-0.237	0.029	59.1	59.8	59.5
0.325 x **JF_{lat}(R)–opisthion** - 16.481	0.812	0.533	-0.429	0.052	68.2	72.0	70.3
0.370 x **JF_{lat}(L)–opisthion** - 18.903	0.743	0.650	-0.523	0.064	75.8	75.6	75.7
0.453 x **JF_{med}(R)–basion** - 11.621	0.846	0.472	-0.380	0.046	62.1	72.0	67.6
0.500 x **JF_{med}(L)–basion** - 12.712	0.825	0.510	-0.411	0.050	69.7	70.7	70.3

MLD_{ecto} – ectocranial mediolateral diameter of the jugular foramen; **MLD_{endo}** – endocranial mediolateral diameter of the jugular foramen; **JF_{lat}** – the most lateral point of the jugular foramen on the ectocranial side; **JF_{med}** – the most medial point of the jugular foramen on the ectocranial side; **R** – right; **L** – left.

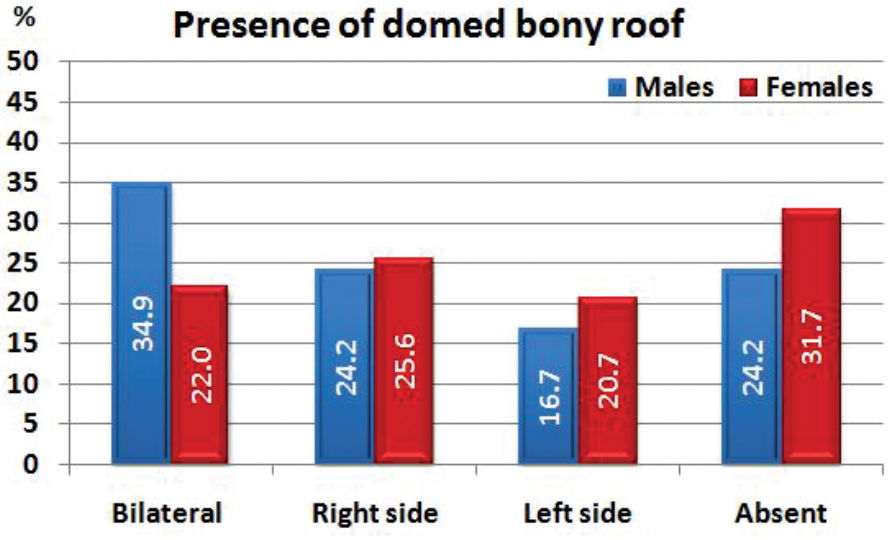

Fig. 4. Frequency of the domed bony roof of the jugular fossa in males and females.

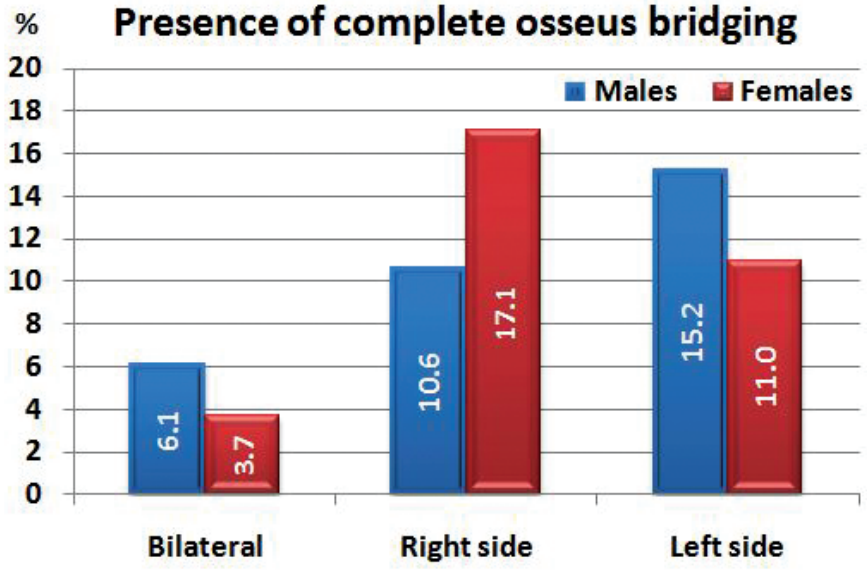

Fig. 5. Frequency of the complete osseous bridging of the jugular foramen in males and females.

Discussion

The JF provides the main venous outflow from the skull [32]. It frequently demonstrates asymmetry [27], which is most prominent in the posterolateral sigmoid portion [17]. The JF size and shape have been related to the size of the internal jugular vein and the presence or absence of a prominent superior bulb [28]. The difference in size of the right and left internal jugular veins is visible in human embryo as early as at the 8th gestation week and probably caused by differences in the pattern of development of the right and left brachiocephalic veins [21]. The variability in JF size from side to side has been also attributed to the difference in size of the sigmoid sinus on the right and left side [17]. The right JF has been frequently found to have larger size [2, 13, 14, 15, 19, 31, 32] with significantly greater measurements of the right JF established in a number of previous studies [5, 7, 20, 22, 26, 28]. Pereira et al. [23] found bilateral differences only in the APD in males, which is observed in our study as well. Significant relationship has been found between sagittal sinus drainage laterality and larger JF size with a statistical association found between the larger JF and the ipsilateral sagittal sinus groove [8]. The larger size of the right foramen have been described with the more common draining of the superior sagittal sinus into the right transverse sinus and the right sigmoid sinus respectivly [4, 8, 16]. Unlike the ectocranial APD, the endocranial diameter has not been established to show such explicite predominance for the right side, which is probably due to the exocranial location of the superior jugular bulb [20]. However, our results show bilateral differences in the WJF in males not only on the ectocranial surface, but also on the endocranial one, which could be related to the size of the sigmoid sinus. The smaller size of the left JF has implied greater susceptibility to compression of the neurovascular structures passing through it [7]. However, the diameters of the JFs from the opposite skull sides have been established to correlate significantly [5, 15], while such correlations have not been found between the JF dimensions on each side [15], suggesting coordinated deveopment of the JFs on the opposite skull sides with regard to the optimal venous otflow.

The sex differences in the JF size have been discussed in few previous studies. Çiçekcibaşi et al. [5] established no sex differences in both JF diameters, whereas Pereira et al. [23] reported significantly greater MLD in males, which is in line with our results. Significant sex differences have been also found in the JF area [32]. According to Das et al. [7], the smaller area of the JF in females might be a risk factor for compression of neurovascular structures passing through it in cases of tumors invading this region. In our study, the right JFs of females have smaller APD than males, while the left ones have slightly greater one, unlike the MLD, which is constatnly greater in males on either side.

The sex differences in the ecto- and ednocranial measurements of the JF have been established to show population specificity. The ectocranial dimensions have demonstrated significant differences between Caucasian males and females, while the endocranial measurements have indicated significant differences between Negroid males and females [20]. In our study, the sex differences on the ectocranial surface are related to the MLD on the right and left sides, while on the endocranial surface, they concern the same measurement but only on the left side.

As far as we know, the discriminating power of the JF measurements in the sex estimation has not been previously studied. The discriminant functions for the JF measurements developed in the present study achive accuracy rates comparebale with those obtained for the *foramen magnum* in the same population [30], suggesting that the measurements of the cranial base foramina are mediocre sex indicators. However, the functions based on dimensions measured between the right and left JFs as well as between

the JF points and midsagittal landmarks, such as *basion* and *opisthion*, achieve higher accuracy results, most of them exeeding 70%, and thus, useful as supportive tools for sex estimation purposes. The sex differences observed in the last-mentioned distances could be explained with the generally larger male skull. The lack of bilateral differences in the measurements between the JF points and midsagittal landmarks as well as between the right and left AIJF indicates the symmetric position of the right and left JFs in the skulls of both sexes.

The presence of a domed bony roof of the JF is related to the presence of a prominent superior jugular bulb [28], while its absence indicates that the bulb is absent or poorly developed [22]. When well-developed, the bulb has rounded upper part which lies in the dome of the jugular fossa [20]. The presence of a domed bony roof on both sides has been the most common reported combination [3, 7, 13, 19, 20, 23, 26, 28] reaching up to 100% in the study of Hossain et al. [14]. However, in some studies, the bilateral absence of domed jugular fossa has been reported as a more common variant [2, 22]. In our study, the domed bony roof is most commonly present bilaterally in males, while it is more frequently absent in females. In cases of unilateral presence of the domed roof, it has been more common on the right side [2, 7, 13, 19, 20], which is confirmed by our results. Besides, no statistically significant sex differences have been reported in the presence of this feature [7], which is established by the present study as well.

Another main morphological trait of the JF is its division by complete osseous bridging. The sigmoid and petrosal parts of the JF are separated by the intrajugular processes of the occipital and temporal bones, which are usually connected by a fibrous bridge, which may occasionally ossify [17]. The bridging of the JF is usually established by the end of fetal development suggesting the existence of genetic factors in the expression of this feature [9]. Some authors found neither sex [9] nor bilateral [9, 28] differences in the incidence of complete JF bridging. However, Kumar et al. [19] observed that it is more frequent on the right side, while Aseta et al. [2] found it more common on the left one. Our observations show that the unilateral bridging in males is more frequent on the left side, while in females, it is more common on the rigth one, although significant sex differences are not established according to this trait. Skrzat et al. [27] noticed that the division of the JF by complete osseous bridging is a rare finding. Notwithstanding, the incidence of complete septation varies in different population groups and has been found between 1% and 24% [7, 13, 15, 22, 23, 31]. In this regard, Hossain et al. [14] reported very high incidence of complete JF septation of 76% on the right and 91% on the left side in Bangladesh skulls. Thus, our results are most close to those of Serbians (24%), reported by Vlajković et al. [31]. In addition, Athavale [3] established that the JF bridging is more common on the endocranial side, which contradicts to our observations.

The variations in JF compartmentalization have been attributed to variability in bone formation around the primitive foramen lacerum posterior [24], which is observed in the early human fetal skull and persists as JF in adults [25]. In this regard, Athavale [3] suggested that JF compartmentalization could be a part of ongoing evolutionary process. However, some compartmentalization patterns can compress the structures passing through the JF and thus could mimic the clinical manifestations of glomus jugulare tumor and cause multiple cranial nerve palsies, i.e. jugular foramen syndrome (Vernet's syndrome). Das et al. [7] observed that the JF bridging is more common in males and put them at a higher risk of these manifestations than females. However, according to our results, this feature is equally frequent in both sexes (males: 31.8%; females: 31.7%), so both Bulgarian males and females could be related to the same risk category.

Altogether, the extreme variations in the JF morphology might put the passing vessels and nerves at risk during surgical procedures in this region [26]. The high vari-

ability in the size and shape of the JF enforces a compulsory preoperative imaging with thorough examination of the foramen morphology to avoid injuries to its content and surrounding structures during surgical operations.

Conclusions

The size of the JF differs significantly between males and females in its MLD. However, the JF dimensions are mediocre sex indicators for forensic purposes. Bilateral differences are found only in the APD in males, since the right JFs have greater size than the left ones. The domed bony roof is more frequently observed in males, while the complete osseous bridging is equally common in both sexes.

Acknowledgements: The study was supported by the Bulgarian National Science Fund, Grant number DN11/9-15.12.2017 and Grant number DN01/15-20.12.2016.

References

1. **Adams, W. M., R. L. Jones, S. V. Chavda, A. L. Pahor.** CT assessment of jugular foramen dominance and its association with hand preference. – *J. Laryngol. Otol.*, **111**, 1997, 290-292.
2. **Aseta, F. B., P. M. Mwachaka, P. I. Mandela, J. Ogeng'o.** Variant Anatomy of the Jugular Foramen: An Osteological Study. – *Acad. Anat. Int.*, **2**(**2**), 2016, 38-43.
3. **Athavale, S. A.** Morphology and compartmentation of the jugular foramen in adult Indian skulls. – *Surg. Radiol. Anat.*, **32**, 2010, 447-453.
4. **Bayaroğulları, H., G. Burakgazi, T. Duman,** Evaluation of dural venous sinuses and confluence of sinuses via MRI venography: anatomy, anatomic variations, and the classification of variations. – *Child's Nervous System*, **34**(**6**), 2018, 1183-1188.
5. **Çiçekcibaşi, A. E., K. A. Murshed, T. Ziylan, M. Şeker, I. Tuncer.** A morphometric evaluation of some importantt boney landmarks on the skull base related to sexes. – *Turk. J. Med. Sci*., **34**, 2004, 37-42.
6. **Cignoni, P., M. Callieri, M. Corsini, M. Dellepiane, F. Ganovelli, G. Ranzuglia.** MeshLab: an open-source mesh processing tool. – *Eurographics*, 2008, 1-8.
7. **Das, S. S., S. Saluja, N. Vasudeva.** Complete morphometric analysis of jugular foramen and its clinical implications. – *J. Craniovertebr. Junction Spine*, **7**(**4**), 2016, 257-264.
8. **Dias, G. J., V. Perumal, C. Smith, J. Cornwal.** The relationship between jugular foramen asymmetry and superior sagittal venous sinus laterality. – *Anthropol. Sci.*, **22**, 2014, 115-120.
9. **Dodo, Y.** A population study of the jugular foramen bridging of the human cranium. – *Am. J. Phys. Anthropol*., **69**, 1986, 15-19.
10. **Fedorov, A., R. Beichel, J. Kalpathy-Cramer, J. Finet, J-C. Fillion-Robin, S. Pujol, C. Bauer, D. Jennings, F. Fennessy, M. Sonka, J. Buatti, S. Aylward, J. V. Miller, S. Pieper, R. Kikinis.** 3D Slicer as an image computing platform for the quantitative imaging network. – *Magn. Reson. Imaging*, **30(9)**, 2012, 1323-1341.
11. **Franklin, D., A. Cardini, A. Flavel, A. Kuliukas.** Estimation of sex from cranial measurements in a Western Australian population. – *Forensic Sci. Int*., **229**, 2013, 158.e1-158.e8.
12. **Hammer, Ø., D. A. T. Harper, P. D. Ryan.** PAST: paleontological statistics software package for education and data analysis. – *Palaeontol. Electron.*, **4**, 2001, 9-18.
13. **Hatiboğlu, M. T., A. Anil.** Structural variations in the jugular foramen of the human skull. – *J. Anat.,* **180**, 1992, 191-196.
14. **Hossain, S. M. A., S. M. M. Hossain, F. A. M. H. Banna.** Variations in the structure of the jugular foramen of human skull. – *Bangladesh Journal of Anatomy*, **10**(**2**), 2012, 45-49.
15. **Idowu, O. E.** The jugular foramen - a morphometric study. – *Folia Morphol.,* **63**, 2004, 419-422.
16. **Joseph, S. C., E. Rizk, R. S. Tubbs.** Dural venous sinuses. – In: *Bergman's Comprehensive Encyclopedia of Human Anatomic Variation* (Eds. R. S. Tubbs, M. M. Shoja, M. Loukas), Wiley Blackwell, 2016, 775-799.

17. **Katsuta, T., A. L. Jr. Rhoton, T. Matsushima.** The jugular foramen: microsurgical anatomy and operative approaches. – *Neurosurgery*, **41**(**1**), 1997, 149-202.
18. **Koo, T. K., M. Y. Li.** A guideline of selecting and reporting intraclass correlation coefficients for reliability research. – *J. Chiropr. Med.*, **15**, 2016, 155-163.
19. **Kumar, A., D. Ritu, M. J. Akhtar, A. Kumar.** Variations in jugular foramen of human skull. – *Asian J. Med. Sci.*, **6**, 2014, 95-98.
20. **Navsa, N., B. Kramer.** A quantitative assessment of the jugular foramen. – *Ann. Anat.*, **180**(**3**), 1998, 269-273.
21. **Padget, D. H.** The development of the cranial venous system in man, from the viewpoint of comparative anatomy. – *Contributions to Embryology*, **36**, 1957, 79-140.
22. **Patel, R., C. D. Mehta.** Morphometric study of jugular foramen at base of the skull in the South Gujarat region. – *IOSR Journal of Dental and Medical Sciences*, **13**, 2014, 58-61.
23. **Pereira, G. A., P. T. Lopes, A. M. Santos.** Morphometric aspects of the jugular foramen in dry skulls of adult individuals in Southern Brazil. – *J. Morphol. Sci.*, **27**, 2010, 3-5.
24. **Shapiro, R.** Compartmentation of jugular foramen. – *J. Neurosurg*., **36**, 1972, 340-343.
25. **Shapiro, R., F. Robinson.** The foramina of middle fossa: A phylogenetic, anatomic and pathologic study. – *Am. J. Roentgenol.*, **101**, 1967, 779-794.
26. **Singla, A., D. Sahni, A. Aggarwal, T. Gupta, H. Kaur.** Morphometric study of the jugular foramen in Northwest Indian population. – *Journal of Postgraduate Medicine, Education and Research*, **46**(**4**), 2012, 165-171.
27. **Skrzat, J., I. Mroz, A. Spulber, J. Walocha.** Morphology, topography and clinical significance of the jugular foramen. – *Folia Med. Crocov.*, **56**(**1**), 2016, 71-80.
28. **Sturrock, R. R.** Variations in the structure of the jugular foramen of the human skull. – *J. Anat.*, **160**(**49**), 1988, 227-230.
29. **Tekdemir, I., E. Tuccar, A. Aslan, A. Elhan, M. Ersoy, H. Deda.** Comprehensive microsurgical anatomy of the jugular foramen and review of terminology. – *J. Clin. Neurosci.*, **8**, 2001, 351-356.
30. **Toneva, D., S. Nikolova, S. Harizanov, I. Georgiev, D. Zlatareva, V. Hadjidekov, A. Dandov, N. Lazarov.** Sex estimation by size and shape of foramen magnum based on CT imaging. – *Leg. Med.*, **35**, 2018, 50-60.
31. **Vlajković, S., L. Vasović, M. Daković-Bjelaković, S. Stanković, J. Popović, R. Čukuranović.** Human bony jugular foramen: Some additional morphological and morphometric features. – *Med. Sci. Monit.*, **16**(**5**), 2010, 140-146.
32. **Wysocki, J., J. Reymond, H. Skarzynski, B. Wrobel.** The size of selected human skull foramina in relation to skull capacity. – *Folia Morphol.*, **66**, 2006, 301-308.

Institute of Experimental Morphology, Pathology and Anthropology with Museum
Bulgarian Anatomical Society

Acta morphologica et anthropologica, 26 (1-2)
Sofia ● 2019

Variant of Brachial Plexus with Unusual Branch of Median Nerve

Ivan Maslarski[1], Pavel Kirilov[1], Galina Yaneva[2]*

[1] Department of Anatomy, histology, pathology and forensic medicine, Faculty of medicine, SU "St. Kliment Ohridski",
[2] Department of Biology, Faculty of Pharmacy, Paraskev Stoyanov Medical University of Varna, Varna, Bulgaria

*Corresponding author e-mail: maslarsky@gmail.com

The variations of Brachial plexus (BP) occur due to several reasons; different interactions of the nerves that make up the BP, the possibility of a different origin from the trunk as well as different location to the brachial artery and other anatomical structures. The frequency of such variations makes this anatomical region quite complicated. Intervention to this region requires specific anaesthetic blockages and a different surgical approach. The current variant of the upper limb was observed during the period from the year 2008 to 2019 – 40 left and 40 right upper limbs in total. In the current case a thin branch coming from the medial cord and thick branch coming from the lateral cord is observed. The thick branch penetrates the facia of coracobrachial muscle, where it moves along with the musculocutaneous nerve. Certain compressions and consecutive pains and traumas in the region of the muscles or the sensitive innervation of the skin in the axillary region in the lateral zone, can also be consequences of traumas and variations in the region of the musculocutaneous nerve.

Key words: brachial plexus, median nerve variations, anaesthetic blockages

Introduction

The brachial plexus is a combination of nerves, which provide motor and sensitive nerves to the upper limb and a small part of the thorax. The brachial plexus also includes adrenergic post ganglionic fibres. In 1884 the first anaesthesia to the upper limb was accomplished by Halstead, using cocaine [2]. The blockage of the brachial plexus (BP) requires a good understanding of the peripheral nervous system as well as parts of the BP. This part of the nervous system is quite variable, taking this into consideration, every variation is worth describing. At the present time the clinical side as well as the so called applied anatomy are both taken into consideration. During anatomical practical exercises with medical students it is imperative to foresee demonstrations and knowledge aiming at the clinical anatomy, the variations of vessels and nerves in the region of the upper limband their practical purposes. Local anaesthetics of the upper limb is a typical example of the practical application of anatomy with available variations.

According to B. Hansen's large scale examination demonstrated that 65.3% of the people have variations in their BP. These variations occur due to several reasons; different interactions of the nerves that make up the BP, the possibility of a different origin from the trunk as well as different location to the brachial artery and other anatomical structures. The frequency of such variations makes this anatomical region quite complicated. Intervention to this region requires specific anaesthetic blockages and a different surgical approach. Such approach requires a correct interpretation of the nerve compressions, whether caused by a tumour or a combination of traumatic events in addition to the variations mentioned above.

Materials and Methods

The cadaver in question describes an interesting version of BP during a routine dissection, with medical students from the Department of Anatomy, histology and pathology, from the Medical Faculty of the Sofia University. The variation has been discovered during practical exercises from regular activities of the Gross anatomy of the Upper limb. The Upper limb belongs to a 78-year old male individual. The Upper limb in question was dissected in advance from the thorax. Fixation is accomplished with formaldehyde.

Results

Fig.1 Brachial plexus with uncommon branch of median nerve; 1 – lateral part of median nerve, 2 – medial part of median nerve, 3 – branch cum musculocutaneous nerve, 4 – ulnar nerve, 5 – median cutaneous nerve, 6 – radial nerve, 7 – axillary nerve, 8 – musculocutaneous nerve.

The current variant of the upper limb is observed during the period from the year 2008 to 2019 – 40 left and 40 right upper limbs in total. In the current case a thin branch coming from the medial cord and thick branch coming from the lateral cord is observed. The thick branch penetrates the facia of coracobrachial muscle, where it moves along with the musculocutaneus nerve. The metric values for the thickness of the nerves are as follows: musculocutaneous nerve – 2 mm; ulnaris nerve – 4 mm; medial part of median nerve – 1 mm, and the lateral part is 2,4 mm; median nerve – 3,4 mm. The length of medial part of median nerve which arises from the medial trunk is 4,5 cm, and those one which arise from the lateral trunk is 9,8 cm. The location of the radial nerve and axillary nerve are in their norm, the same applies for the nerves of the brachial artery (**Fig.1**). The sensitive branch of the medial cutaneous nerve of the arm and the branch of the medial cutaneous nerve of the forearm have a common starting point, from the medial cord.

Discussion

The embryonal development of the BP starts from the 4th week of the embryonic development. The first differentiation occurs from the mesenchymal cells. The primary dorsal nerves form at the level of the medial part towards the distal end of the shoulder bone in the cleft of the muscle forming the arm. During the 32nd day the size of the nerves extends from C5 to Th1 and the 33rd day marks the starting of their fusion and the primary formation of the BP. Between the 39th and 40th day the medial nerve, ulnar nerve and radial nerve reach the level of the arm. The final arrangement of the nerves against each other as well as their location against the blood occurs during 49th or 50th day. During the embryonic development the somites migrate, so they can form the limbs. They carry their own nervous supply, in this way every dermatome and myotome preserve their primary innervation via segments. In this stage of migration of the somites occurs a complex from nearby nerves, which form complex contacts and develop entanglement or a complex model of correspondence between nerves and vesselsin the early stage of fetus. During the growth of the fetus there are changes in the angle in which the future BP will locate, this allows for the development of variations in nerves or vessels in the region of axilarisetregio brachialis.

In normal development BP develops from the front branches of the last four neck nerves and the bigger part of the first pectoral nerve. The combination of the mentioned nerve according to the model is: C5 and C6 join in the superior trunk, C7 separates solely like the medial trunk, whereas C8 and Th1 like the inferior trunk. Each of the three trunks separates in front and rear branch. All posterior branches form the posterior cord. The front branches of the upper and medial trunkform the lateral cord, whereas the front branch of the bottom trunk continues like the medial cord. Consequently, from the proximal to the distal part of the upper limb, develops the radial and axillary nerve from the posterior cord [4]. The lateral cord forms the lateral part of the medial nerve and musculocutaneous nerve.The last cord (medial) forms the medial part of medial nerve, ulnar and cutaneous brachial et antebrachial nerves.

Most frequently the variations arise during the organisation of the lateral cord, this happens either during migration of the somites or during the growth of the fetus and the formation of the neural muscle split. Such observations are supported by various scientists by Miller in 1934 by Sargon in 1995 by Sharma in 2000 by Roy in 2002, and etc. [3]. The variation which is described in our case is the medial nerve to accompany the musculocutaneous nerve, during their transit movement through the coracobrachialis muscle [5]. Rarely the lateral cord penetrates the coracobrachialis muscle and then separates to musculocutaneous and the lateral root of the median nerve. The variations of the lateral cord need to be taken into account during a surgical intervention in the region of axillar and the arm region, in order to avoid compression or trauma of the above described nerves [1].

In the described from us above variation, there can be observed an interesting outline (or location) of the lateral branch of the median nerve, which under normal circumstances originates from the lateral cord and is significantly thinner than the lateral branch of the median nerve. The musculocutaneous nerve penetrates the facia of the coracobrachialis muscle, after which anastomoses with a small branch coming from the median nerve, under the brachial artery (**Fig.2**). The branch of the medial nerve is thin and transit crosses with musculocutaneous nerve towards the distal part of the upper limb. There are no variations in the vessels and more specifically the pathway of posterior humeral circumflex artery and the deep artery of the arm, these often variate when the axillary nerve and musculocutaneous nerve are out of position.

Fig.2. Variant of brachial plexus;1 – lateral part of median nerve, 2 – medial part of median nerve, 3 – branch cum musculocutaneous nerve, 4 – ulnar nerve, 5 – median cutaneous nerve, 6 – radial nerve, 7 – axillary nerve, 8 – musculocutaneous nerve.

Conclusion

The described case in this paper is interesting from the perspective of surgery during reconstruction of the upper limb and the entry in the region of the neck and the shoulder bone or interventions with a shoulder joint. Interest arises also from ananaesthetic perspective, during the formation of a anaesthesia in the region of the BP. Certain compressions and pain and traumas in the region of the muscles or the sensitive innervation of the skin in the armpit in the lateral zone. Certain compressions and consecutive pains and traumas in the region of the muscles or the sensitive innervation of the skin in the armpit in the lateral zone, can also be consequences of traumas and variations in the region of the musculocutaneous nerve. Every variation in the nerve-vessel bundle is of importance, as well as to teach and show to the students, same applies for practical operative work of surgeons in this field.

References

1. **Abhaya, A., J. Khanna, R. Prakash.** Variation of the lateral cord of brachial plexus piercing coracobrachialis muscle. – *J Anat. Soc. India*, **52**(**2**), 2003, 168-170.
2. **Emamhadi, M., S. Yousefzadeh.** Anatomical variations of brachial plexus in adult cadavers. – *Arch. Bone. Joint Surg*., **4**(**3**), 2016, 253-258.
3. **Loukas, M., R. Tubbs, D. Stewart**. An abnormal variation of the brachial plexus with potential clinical significance. – *West Indian Med. J*., **57**(**4**),2008, 403.
4. **Satyanarayana, N., N. Vishwakarma, G. P. Kumar, R. Guha, A.K. Dattal, P. Sunitha.** Rare variations in the formation of median nerve – embryological basis and clinical significance. – *Nepal Med. Coll. J.,* **11**, 2009, (**4**), 287-290.
5. **Uzunq A., S. Bilgic.** Some variations in the formation of the brachial plexus in infants. – *Turkish J. Med. Sci.,* **29**, 1999, 573-577;

Institute of Experimental Morphology, Pathology and Anthropology with Museum
Bulgarian Anatomical Society

Acta morphologica et anthropologica, 26 (1-2)
Sofia ● 2019

A Case of an Uncommon Injury of the Index Finger

*Violeta Nedialkova[1], Georgi P. Georgiev[2], Boycho Landzhov[1], Alexandar Iliev[1]**

[1] Department of Anatomy, Histology and Embryology, Medical University of Sofia, Bulgaria
[2] Department of Orthopaedics and Traumatology, University Hospital Queen Giovanna – ISUL, Medical University of Sofia, Bulgaria

* Corresponding author e-mail: dralexiliev@abv.bg

Herein we present a case of a traumatic injury to the right index finger by an electric screw gun. The screw entered the finger through the medial part of the proximal interphalangeal joint and ended in the middle phalanx, therefore we will discuss bone damage. We point out the approach for immediate treatment, including the use of a screwdriver in order to extract the screw.

Key words: traumatic injury, index finger, surgery

Introduction

The hand is the most commonly injured part of the body. Primary care physicians must routinely manage patients with acute traumatic hand injuries involving retained foreign bodies and puncture wounds. During physical examination, a thorough inspection with comparison to the uninjured hand should be performed. Abnormal positioning, angulation or rotational deformity should be noted and physicians have to document the motor function and to perform tests of tendons and ligaments [3]. If surgical removal of a foreign body or surgical exploration of a wound is decided upon, the procedure must be performed after detailed X-ray analysis, treated with an antibiotic and reviewed multiple times after the manipulation in order to prevent later complications. On the other hand, when foreign bodies have unusual form, like fishhooks, specific techniques are required. Careful evaluation of the surrounding tissue before attempting removal is of great importance and the method depends mainly on the type of foreign body embedded, the location of the injury and the depth of tissue penetration [2].

Case report

A 39-year-old male attended the Emergency Room in the University Hospital "Queen Giovanna" in Sofia with a traumatic injury to his right index finger. The accident hap-

pened when the patient attempted to assemble a wardrobe and instead of attaching a metal screw to a piece of wood, he managed to pierce his finger. The point of entry (**Fig. 1**) was the medial aspect of the proximal interphalangeal joint of the right index finger and the end was on the flexor aspect of the middle phalanx. During X-ray analysis it was observed that the screw pierced through the bone. After local anesthesia was achieved the physician decided to use a screwdriver instead of surgical instruments. The idea was to minimize damage to the collateral tissue by unscrewing the screw and therefore follow the same path that it took during the injury. With minimum effort, the screw came out (**Fig. 2**). A standard procedure was followed afterwards: the wound was washed out, disinfected and bandaged. The patient was let go, treated with antibiotic and reviewed twice after the manipulation, with no more complications.

Fig. 1. **a**) Photograph of the right hand after injury with the screw entering the finger through the medial part of the proximal interphalangeal joint; **b**) Anterior posterior view of the right hand; c) Oblique view of the right hand.

Fig. 2. a) Anterior posterior view of the right hand after screw removal; **b**) Oblique view of the right hand after screw removal; **c**) Photograph presenting the full-length of the screw with the glove patch remaining pierced.

Discussion

The characteristics of simple solutions include brilliance too. The aim of documenting this clinical case was to emphasize on the importance of always seeking the simplest approach in the Emergency Room or any other department, and also in life, which sometimes requires more knowledge and experience than that confined to the

strict medical practice. In managing any injuries of the hand, the basic principles of fracture management are the same whether treatment is closed or open, but special situations require amendments to the well-known methods [1]. It is also of great significance to turn the attention of the specialists to classifying each case as unique and to think of the best way to treat the specific injury, extend their boundaries and eventually use simple and everyday methods. For example, in some cases conservative surgical approach with a "pull and see" policy was adopted successfully. Extraction can be achieved using the mechanical advantage of the lever principle. With this method, while removing the object any movements of sharp edges which will cause secondary damage can be reduced to a minimum [4]. However, trying new methods demands careful examination of the injury, consulting with other specialists and monitoring the patient's condition to determine, whether it has improved or worsened.

References

1. **Corley, F. G. Jr., R. C. Jr. Schenck.** Fractures of the hand. – *Clin. Plast. Surg.,* **23,** 1996, 447-462.
2. **Gammons, M. G., E. Jackson.** Fishhook removal. – *Am. Fam. Physician,* **63,** 2001, 2231-2236.
3. **Cheung, K., A. Hatchell, A. Thoma.** Approach to traumatic hand injuries for primary care physicians. – *Can. Fam. Physician,* **59,** 2013, 614-618.
4. **Rao, G. P., N. S. Rao, P. K. Reddy.** Technique of removal of an impacted sharp object in a penetrating head injury using the lever principle. – *Br. J. Neurosurg.,* **12,** 1998, 569-571.

Institute of Experimental Morphology, Pathology and Anthropology with Museum
Bulgarian Anatomical Society

Acta morphologica et anthropologica, 26 (1-2)
Sofia ● 2019

Review Articles

The Expression of Neuronal Nitric Oxide Synthase in the Kidney and Its Role for Renal Functions

Stancho Stanchev, Boycho Landzhov, Georgi Kotov, Alexandar Iliev*

Department of Anatomy, Histology and Embryology, Medical University of Sofia, Bulgaria

*Corresponding author e-mail: stanchev_1989@abv.bg

The present work reviews the distribution of neuronal nitric oxide synthase in the kidney and its role in various renal functions. A review of the literature shows that most authors have focused on the endothelial isoform as the primary source of nitric oxide production in kidneys. Nowadays, there is convincing evidence that renal neuronal nitric oxide synthase plays a role in the control of the regulatory mechanisms of the kidney such as tubuloglomerular feedback mechanism and pressure natriuresis. It seems that the increased immunoreactivity of neuronal nitric oxide synthase in both renal cortex and medulla has renoprotective role under hypertension and weakens the development of target organ damage.

Key words: neuronal nitric oxide synthase (nNOS), kidney, spontaneously hypertensive rats (SHR), Wistar rats

Nitric oxide (NO) is a signaling molecule, which takes part in the regulation of various renal functions – maintenance of glomerular and medullary hemodynamics, sodium homeostasis, renin production, influence on the renal sympathetic activity. It is synthesized by the three isoforms of the enzyme nitric oxide synthase (NOS), which are all expressed in the kidney [7, 13]. Endothelial NOS (eNOS) is found mainly in the intrarenal vascular endothelium, the cells of the collecting ducts and distal tubular segments [11], while inducible NOS (iNOS) is usually expressed under pathological conditions [5]. There is convincing evidence that neuronal nitric oxide synthase (nNOS) has a primary role for the maintenance of blood pressure and vascular tone. This isoform is mainly expressed in macula densa cells, cells of the thick ascending limb of the loop of Henle, Bowman's capsule, cells of the collecting ducts and efferent arterioles [11]. Indeed, nNOS is responsible for various regulatory functions depending on its localization in the renal structure. For example, in the inner medulla, nNOS participates in the longterm regulation of blood pressure – the selective inhibition of the isoform in rats

on high salt diet results in arterial hypertension [12]. On the other hand, macula densa-derived NO is associated with regulation of the tubuloglomerular feedback (TGF) and renin production [11, 12]. Several hypotheses suggest the effects of macula densa-derived NO – 1. it influences macula densa cells and acts as an autacoid; 2. NO affects the juxtaglomerular mesangial cells; 3. NO reaches the afferent arteriole via diffusion process and induces vasodilatation [17]. The final effect of macula densa-derived NO is to attenuate TGF. Many hormones and molecules such as prostaglandins and angiotensin II influence the TGF sensitivity. For example, angiotensin II enhances TGF, while the atrial natriuretic peptide attenuates this autoregulatory mechanism [17]. It seems that the salt intake, intracellular pH, angiotensin II and the protein inhibitor of nNOS are important regulatory factors for nNOS activity and renin production [18, 21]. The influence of salt intake on nNOS expression in macula densa cells shows contradictory results. Some studies have shown increased nNOS activity in rats on low salt diet [20]. On the other hand, an increased NO production has been described in macula densa cells on high salt intake [23]. The activity of nNOS depends on the intracellular pH and is most prominent at pH 8 [22]. The protein inhibitor of nNOS is mainly expressed in the endothelial cells of the glomerular capillary tufts, the cells of the collecting ducts, but it is not found in macula densa cells [18].

The decrease of average blood pressure together with the increased renal blood flow and glomerular filtration rate during pregnancy are usually associated with higher levels of NO. The observed hemodynamic changes can be explained by increased activity of nNOS [2]. Undoubtedly, this isoform is important for normal pregnancy, but the mechanisms that affect the renal hemodynamics are still misunderstood. The short-term use of a selective inhibitor of nNOS in non-pregnant rats doesn't cause significant changes in the renal hemodynamics, while in pregnant rats it is accompanied by a 25% decrease in glomerular filtration rate and 60% increase in intrarenal vascular resistance [1]. In addition, the short-term selective inhibition of nNOS doesn't lead to changes in average blood pressure, while chronic inhibition provokes arterial hypertension [4].

The altered NO production may have a crucial role in the development of renal morphological changes in various pathological conditions that lead to end stage kidney disease. Many studies have demonstrated reduced plasma NO levels in patients with chronic kidney disease compared to control groups. The mechanism for the decreased production of NO is still poorly understood, but factors such as decreased l-arginine levels and accumulation of NOS inhibitors have been discussed [16].

Over the years, most researches have focused on the role of eNOS in the maintenance of blood pressure and the regulation of various renal functions. In addition, the altered production of NO is usually associated with changes in systemic blood pressure and the deficiency of NO is a possible mechanism for the development of arterial hypertension [8]. The application of NOS inhibitors in healthy rats causes hypertension and chronic kidney damage [3]. Some authors have studied the influence of the selective inhibition of nNOS by 7-nitroindazole (7-NI) on blood pressure, glomerular filtration rate and TGF. The results show that the acute application of 7-NI doesn't affect blood pressure, but it increases TGF. An elevated blood pressure and intensive TGF are observed in the treated rats after one week. The chronic inhibiton of nNOS for four weeks is associated with pronounced hypertension in the experimental group rats compared to control animals. This data indicates that the altered production of NO by nNOS may have a significant role in the development of arterial hypertension [15]. There is limited and contradictory information regarding the changes in the expression of renal nNOS under hypertensive conditions. The spontaneously hypertensive rat (SHR) is a good experimental model for demonstration of the consequences of prolonged untreated essential hypertension [24]. In this strain, the primarily enhanced TGF has been discussed

in the pathogenesis of elevated blood pressure. The main function of the macula densa-derived NO is to attenuate this autoregulatory mechanism and the changes in the expression of nNOS may play a crucial role in the progress of hypertension in SHR. Some authors have established a higher activity of the constitutive isoforms of renal NOS – eNOS and nNOS in SHR compared to Wistar rats [9, 14]. Some studies have described higher expression of nNOS in macula densa cells together with NADPH-oxidase. The increased activity of NADPH-oxidase is associated with production of superoxide ions, which further react with NO and decrease its bioavailability. The authors conclude that nNOS expression is closely associated with the balance between NO and superoxide ions [21]. In addition,the reduction of superoxide ions leads to vasodilatation of the afferent arterioles in SHR, while such effect is not observed in Wistar rats [10].

Fernandez et al. [6] have studied the expression of nNOS in age-matched Wistar rats and SHR. It was found that the immunoreactivity of nNOS is high positive in the inner papillary region and lacking in the outer medulla in the normotensive group. In the renal cortex, the isoform was mainly found in macula densa cells, as well as the parietal and visceral layers of Bowman's capsule. In SHR, the inner medulla showed a higher immunoreactivity and positive expression of the isoform was found in the outer medulla [6]. Our previous study also demonstrated a higher expression of nNOS in the renal medulla and the structural elements of the renal corpuscles in SHR compared to normotensive Wistar rats [19]. The increased expression of NOS in both renal cortex and medulla is associated with compensatory changes in TGF and pressure natriuresis [11]. These findings suggest that nNOS plays a renoprotective role in arterial hypertension and influences the development of hypertensive structural alterations such as glomerulosclerosis, and tubulointerstitial fibrosis, described by the term hypertensive nephrosclerosis.

References

1. **Abram, S. R., B. T. Alexander, W. A. Bennett, J. P. Granger.** Role of neuronal nitric oxide synthase in mediating renal hemodynamic changes during pregnancy. – *Am. J. Physiol. Regul. Integr. Comp. Physiol.,* **281,** 2001, R1390-R1393.
2. **Alexander, B. T., M. T. Miller, S. Kassab, J. Novak, J. F. Reckelhoff, W. C. Kruckeberg, J. P. Granger.** Differential expression of renal nitric oxide synthase isoforms during pregnancy in rats. – *Hypertension*, **33,** 1999, 435–439.
3. **Baylis, C., B. Mitruka, A. Deng.** Chronic blockade of nitric oxide synthesis in the rat produces systemic hypertension and glomerular damage. – *J. Clin. Invest.,* **90,** 1992, 278-281.
4. **Braam, B.** Renal endothelial and macula densa NOS: integrated response to changes in extracellular fluid volume. – *Am. J. Physiol.,* **276,** 1999, R1551-R1561.
5. **Choi, J. Y., S. A. Nam, D. C. Jin, J. Kim, J. H. Cha.** Expression and cellular localization of inducible nitric oxide synthase in lipopolysaccharide-treated rat kidneys. – *J. Histochem. Cytochem.,* **60**, 2012, 301-315.
6. **Fernandez, A. P., J. Serrano, S. Castro, F. J. Salazar, J. C. López, J. Rodrigo, E. Nava.** Distribution of nitric oxide synthases and nitrotyrosine in the kidney of spontaneously hypertensive rats. – *J. Hypertens.,* **21,** 2003**,** 2375-2388.
7. **Grzelec-Mojzesowicz, M., J. Sadowski.** Renal tissue NO and intrarenal hemodynamics during experimental variations of NO content in anaesthetized rats. – *J. Physiol. Pharmacol.,* **58,** 2007, 149-163.
8. **Gu, X., G. A. Herrera.** Expression of eNOS in kidneys from hypertensive patients. – *Int. J. Nephrol. Renovasc. Dis.,* **3,** 2010, 11-19.
9. **Hayakawa, H., L. Raij.** Nitric oxide synthase activity and renal injury in genetic hypertension. – *Hypertension*, **31**, 1998, 266-270.

10. **Ichihara, A., M. Hayashi, N. Hirota, T. Saruta.** Superoxide inhibits neuronal nitric oxide synthase influences on afferent arterioles in spontaneously hypertensive rats. – *Hypertension,* **37,** 2001, 630-634.
11. **Lee, J.** Nitric oxide in the kidney: its physiological role and pathophysiological implications. – *Electrolyte Blood Press.,* **6,** 2008, 27-34.
12. **Mattson, D. L., T. G. Bellehumeur.** Neural nitric oxide synthase in the renal medulla and blood pressure regulation. – *Hypertension,* **28,** 1996, 297-303.
13. **Mount, P. F., D. A. Power.** Nitric oxide in the kidney: functions and regulation of synthesis. – *Acta Physiol.,* **187**, 2006, 433-446.
14. **Nava, E., M. T. Llinás, J. D. Gonzalez, F. J. Salazar.** Nitric oxide synthase activity in renal cortex and medulla of normotensive and spontaneously hypertensive rats. – *Am. J. Hypertens.,* **9**, 1996, 1236-1239.
15. **Ollerstam, A., J. Pittner, A. E. Persson, C. Thorup.** Increased blood pressure in rats after long-term inhibition of the neuronal isoform of nitric oxide synthase. – *J. Clin. Invest.,* **99**, 1997, 2212-2218.
16. **Reddy, Y. S., V. S. Kiranmayi, A. R. Bitla, G. S. Krishna, P. V. Rao, V. Sivakumar**. Nitric oxide status in patients with chronic kidney disease. – *Indian J. Nephrol*., **25,** 2015, 287-291.
17. **Ren, Y. L., J. L. Garvin, O. A. Carretero.** Role of macula densa nitric oxide and cGMP in the regulation of tubuloglomerular feedback. – *Kidney Int.,* **58**, 2000, 2053-2060.
18. **Roczniak, A., D. Z. Levine, K. D. Burns.** Localization of protein inhibitor of neuronal nitric oxide synthase in rat kidney. – *Am. J. Physiol. Renal. Physiol.,* **278**, 2000, F702-F707.
19. **Stanchev, S., A. Iliev, L. Malinova, B. Landzhov, W. Ovtscharoff.** Light microscopic and ultrastructural kidney changes in spontaneously hypertensive rats. – *Compt. Rend. Acad. Bulg. Sci.,* 2018, (in press).
20. **Tojo, A., M. Kimoto, C. S. Wilcox.** Renal expression of constitutive NOS and DDAH separate effects of salt intake and angiotensin. – *Kidney Int.,* **58,** 2000, 2075-2083.
21. **Tojo, A., M. L. Onozato, T. Fujita.** Role of macula densa neuronal nitric oxide synthase in renal diseases. – *Med. Mol. Morphol.,* **39**, 2006, 2-7.
22. **Wilcox, C. S.** The kidney: physiology and pathophysiology. New York, Raven Press, 2000.
23. **Wilcox, C. S., W. L. Welch.** TGF and nitric oxide: effects of salt intake and salt-sensitive hypertension. – *Kidney Int.,* **55**, 1996, S9-S13.
24. **Zhou, X., E. D. Frohlich.** Analogy of cardiac and renal complications in essential hypertension and aged SHR or L-NAME/SHR. – *Med. Chem.,* **3**, 2007, 61-65.

Institute of Experimental Morphology, Pathology and Anthropology with Museum
Bulgarian Anatomical Society

Acta morphologica et anthropologica, 26 (1-2)
Sofia ● 2019

Influence of Economic and Social factors on the Body Dimensions in Newborns

I. Yankova Pandourska, R. Stoev, Y. Zhecheva, A. Dimitrova*

Institute of Experimental Morphology, Pathology and Anthropology with Museum, Bulgarian Academy of Sciences, 1113 Sofia, Bulgaria

* Corresponding author e-mail: anthropologyvaila@gmail.com

Abstract

The anthropological characteristic of the population of each country is a biological reflection of the specificity of the living conditions during its historical development and at present days. The physical development of newborns, children and adolescents is an important indicator for the influence of various biological and socio-economic factors on the growing child's organism still in the mother's womb. The aim of the current review is to summarize the available data for the impact of economic and social factors on the physical development of newborns.

Key words: newborns, socio-economic factors, secular trend, mothers, seasonal variations

Introduction

The physical development of newborns, children and adolescents is a reflection of the influence of a variety of biological and socio-economic factors on the growing infant's organism still in the mother's womb. The low standard of life, hardships in war time, economic crises, disrupted ecological balance, as well as other natural and social disasters render strong negative influence on the basic morphological parameters of newborns [7, 12, 53]. As an important indicator of their health status are widely accepted body weight and body length at birth. Because of their sensitivity to socio-economic influences these anthropometric characteristics often are used also as markers of living standards [6]. Other widely used indicators characterizing socio-economic status are also the percentage of newborns with low (under 2500 g) and very low (under 1500 g) birth weight, as well as the average number of liveborn children [54, 57, 60].

The influence of the environmental factors on the development of the newborn is not direct but mediated by the mother. This determines the fact, that newborn's anthropometric measurements (especially body weight) are indicators of economic wellbeing and quality of life of the mothers during the pregnancy [59]. The influence of unfavorable social factors on the pregnant woman leads to decrease of the mean body weight of the newborns with 150-200 g [39].

In Bulgaria the greater part of the newborns' studies are concerned mostly on their anthropometric characteristic and the influence of parental factor on the physical development of children [13, 14, 19, 30, 40, 47, 61]. The tendencies of some anthropometric parameters in newborns from Plovdiv for a period of 56 years are evaluated by Dimitrov [12]. Taking into account the socio-economic changes in Bulgaria he found an increase in the percentage of newborns with higher body weight with improvement of living conditions and the socio-economic situation in the country.

Significant differences in newborns body dimensions are observed in children born to mothers living in different climate-geographic regions [23, 37]. Today it is known that the grade of intrauterine development of the child depends of the long-term (historical) adaptation of the mother to the temperature, humidity and the barometric characteristics of the life place [16, 22, 52, 56]. On the territory of Bulgaria five climatic areas can be distinguished, which suggests that there could be differences in the anthropometric dimensions of children, born in different regions of the country. As far as we know, investigations on the dependency of basic anthropometric characteristics of newborns from the climate-geographic factors in our country have not been carried out.

The variability of stature, body weight and other anthopometric characteristics of neonates are studied in interpopulation aspect. This variability is determined by many factors, which include genetic, racial and ecological specificity of the population [38, 56, 57]. The changes in the newborns' sizes from different regions and countries are important indicator of living standard, health and socio-economic status of the particular population.

The aim of the current review is to summarize available data for the impact of economic and social factors on the physical development of newborns.

Influence of economic and social factors on the body dimensions in newborns and secular trends

The anthropological characteristic of the population of each country is a specific biological reflection of the specificity of socio-economic conditions of life during its historical development and at present days. By comparison of anthropological data of newborns, children and adolescents from different generations and regions, the specifics of their growth and maturation during the different periods of time and in different living conditions are revealed.

A secular tendency (negative or positive) of human growth and development is indicator of the incessantly changing conditions of life. The secular changes are much more expressed in social groups and populations which suffer from delay in their socio-economic progress. According to a number of authors the changes in birth weight are slight in developed countries, while in developing ones the newborns' weight is strongly affected by maternal nutrition. Similarly in the countries, where the population has low socio-economic status more children with low birth weight are born [5, 7, 17, 21, 26]. As mentioned above the body dimensions of the newborns and especially the body weight are an indirect indicator of the quality of life and social status of the mother. The difficulty in its implementation lies in the fact that the quality of life, unlike the income-based life standard, is determined by a whole complex of socio-cultural characteristics [27]. The reaction of representatives of different societies to the same event can be significantly different. This coincides with the opinion that birth weight reflects the interaction of many processes and phenomena, the contribution of which can be different [58]. The studies of long-term (intergenerational) changes in the medico-anthropological status of newborns allow the assessment of the general biological processes in children growth and development on the one hand, and on the other - serve

to assess the influence of social and economic factors on the newborns' sizes during different time periods.

Many studies on secular changes in the growth and development of newborns, children and adolescents exist in global plane for the last 10-15 years [7, 16, 23, 33, 41, 45], but in Bulgaria they are relatively scarce [19, 30, 51, 61]. After the 1980s, until the beginning of the 21st century a retardation and even halt of the acceleration processes are established [5, 61]. This means that either living conditions have stopped their improvement or that they have already allowed the full expression of the genetic potential [5]. In recent years a new tendency of increase of the newborns' body dimensions is observed. In parallel with the increase in the percentage of the children born with weight over 3500 g increases also the part of the newborns with body weight under 2500 g. This trend is also observed in countries as USA, England, Japan, Bosnia and Herzegovina [33, 41].

The physical development and the basic body dimensions of the newborns are closely related to the general health status of the children and affect the individual's health throughout life. For this reason, knowing the peculiarities of the physical development during the neonatal period and the factors which determine it are of great social and scientific importance.

Anthropometric dimensions of newborns to single and to married mothers. Influence of the duration of pregnancy

Children born to single mothers and women without registered marriage lag in body weight in comparison with newborns from families. This fact is valid for populations of developing (economically underdeveloped) countries but also for developed and well-developed countries [2, 21, 24, 51]. According to the widespread point of view the cause of this dependence is the lower quality of life of women which bear children without marriage. According to the conception of evolutional medicine [8], the absence of man's support during the pregnancy leads to stress in the mother and as a consequence of this the duration of pregnancy is shortened and children with low birth weight are born (Krueger's hypothesis). The shortened duration of the pregnancy is interpreted as one of the mechanisms which decrease the mother's contribution to the child. Regardless of the evident interest of the scientific society, the researches in this field are still scarce.

The newborn body measures are an important indicator for the health status of the individual in the next ontogenetic stages [3, 44]. Therefore, the monitoring of the state of children, born to non-married mothers as a group with specific body weight at birth is important. In Bulgaria, the frequency of such births is near 60% for previous years according to National Statistical Institute's (NSI) data. In 2016 this frequency is 58,6% – second place in the European Union (average percentage in the EU – 42,6%, other Balkan countries – 27,8%, USA – 39,8% and Russia – 21,1%) [10].

Body dimensions of children, born to women of different age groups

During the ontogenetic stages, genetic and environmental factors cause different in force influence on the organism. Their effect is the strongest during the intrauterine period when the embryo is especially sensitive to mutagen factors and to different external and internal influences. The basic factors influencing the growth and development of the child's organism during this period are number of fetuses, genotype, age and basic body dimensions of the mother, birth order, season of birth, nutrition, education and profession of the parents, living conditions, urbanization, etc. [19, 25, 42, 43, 49].

The existence of a relation between parental age (mostly mother's age) and the indicators of newborns' physical development is treated by number of authors [9, 34, 35]. They established that in mothers under the age of 15 and those over 35 years there is a greater likelihood to give birth to children with lower body weight. In a number of studies a tendency of increasing the body length and weight of the newborns with advancing of maternal age is described [11, 13, 20, 47, 51].

In many Eastern European countries a relatively high proportion of women giving birth in a very young age is registered. In Bulgaria in 2016 there are 39,9 living births per 1000 women aged 15-19 years according to NSI. This is the highest value in EU (average 11,0 o/oo), in the Balkans (24,7 o/oo) and twice higher in comparison with USA (22,3 o/oo) or Russia (18,4 o/oo) [10].

The births in very young age have a negative effect on the body of the mother and the child. In teenage pregnancy direct biological competition between the two organisms – of the mother and the fetus is possible to appear [36]. This is the one of the reasons for the higher percent of births of infants with low birth weight (below 2500 g) by mothers under the age of 18 years [1, 2, 19, 31]. On the other hand, in Bulgaria, as well as in Europe and Russia, there is an increase of the average mother's age at first birth. In Bulgaria it is 27 years (in Sofia it rises up to 29,8 years) according to NSI data in 2016. Only in 2015, it was 26,0 years, which was minimum for EU (average 28,9 years), subminimum for the Balkans (including Moldova) and near the level in USA (26,4 years) and Russia (25,3 years). The mean age of mothers at birth also increases. In 2016 in Bulgaria it is 27,6 years – minimal in EU (average 30,6 years), subminimum in the Balkans (including Moldova) and about a year lower than the average age at birth in Russia (28,4 years) and USA (28,7 years) [10].

At the same time the medico-anthropological characteristics of children, born to mothers over the age of 30 years rest insufficiently studied.

Seasonal variations in newborns' dimensions from different socio-economic groups

The rate of intrauterine development of the fetus depends on the long-term adaptation of the mother to the natural and environmental conditions in which she lives [22, 56]. The influence of the climatic factors on the body dimensions at birth in the Russian population is analyzed by Vershubskaya et al. [52], but a number of questions remain unclear. One of them is the influence of the birth season in the groups of contemporary population [4, 50]. These authors described differences in newborns body weight from Northern and Southern hemispheres, depending on seasonality. Miklashevskaya [29] found lower body weight in children, living in hot climate regions in comparison with those from the moderate climatic areas. Some authors consider that these differences are due to fluctuations of vitamin D production under the influence of changes in ultraviolet radiation [28, 46, 55].

The relation between birth season and anthropometric characteristics (stature, body weight) and newborns health is a subject of many studies [15, 18]. Significant differences are established in children born in different climatic-geographic regions and altitudes [32, 48]. In Bulgaria studies on the impact of the climatic-geographic factors and seasonality on newborns growth and development are scarce [31].

Conclusions

Perinatal and environmental factors (socio-economic, climate-geographic and others) have a great influence on the processes of growth, development and maturation of

the infant's organism. From their complex influence the realization of individual genetic potential for growth and development is determined to a great extent.

References

1. **Afriyie, J., B. Kweku, E. A. Asiamah, S. T. Boateng.** Low birth weight among adolescents at Cape Coast metropolitan hospital of Ghana. – *Int. J. Reprod. Contracept. Obstet. Gynecol.*, **5**(**12**), 2016, 4242-4247.
2. **Amosu, A. M., A. M. Degun.** Impact of maternal nutrition on birth weight of babies. – *Biomed. Res.*, **25**, 2014, 75-78.
3. **Barker, D. J., C. Osmond, T. J. Forsen, K. L. Thornburg, E. Kajantie, J. G. Eriksson.** Fetal and childhood growth and asthma in adult life. – *Acta Paediatr*, **102**, 2013, 732-738.
4. **Bobak, M., A. Gjonca.** The seasonality of live birth is strongly influenced by socio-demographic factors. – *Hum. Reprod.*, **16**(**7**), 2001, 1512-1517.
5. **Bodzsar, E. B., C. Susanne.** Secular growth changes in Europe. – Eötvös University Press, Budapest, 1998, 1-381.
6. **Brainerd, E.** Reassessing the standard of living in the Soviet Union: An analysis using archival and anthropometric data. – *JEH*, **70**(**1**), 2010, 83-117.
7. **Bralić, I., U. Rodin, J. Vrdoljak, D. Plavec, V. Čapkun.** Secular birth weight changes in liveborn infants before, during, and after the 1991-1995 homeland war in Croatia. – *Croat Med J.*, **47**, 2006, 305-312.
8. **Brüne, M., Z. Hochberg**. Evolutionary medicine – the quest for a better understanding of health, disease and prevention. – *BMC Medicine*, **11**, 2013, 116.
9. **Da Silva, A. A., V. M. Simoes, M. A. Barbieri, H. Bettiol, F. Lamy-Filho, L. C. Coimbra.** Young maternal age and preterm birth. – *Paediatr. Perinat. Epidemiol.*, **17**, 2003, 332-339.
10. **Demoskop Weekly**, 2018. [in Russian] Available at: http://www.demoscope.ru/weekly/2018/0795/index.php
11. **Dimitrov, I., T. Zahariev.** Influence of some natural and social factors on physical development of newborns. – *Obstetrics and Gynecology*, XIV, **2**, 1975, 119-125. [in Bulgarian].
12. **Dimitrov, I.** Accelerative changes in some anthropometric indices of newborn infants in Plovdiv during the period from 1939 to 1995. – *Folia Med*, XXXIX, **1**, 1997, 80-84.
13. **Dundova, R.** Longitudinal growth study of children aged 0-3 years. PhD thesis, Sofia, 1978, 1-158. [in Bulgarian].
14. **Dundova, R., D. Kalaikov, B. Zahariev.** Influence of some medico-social factors on the physical development of children in Bulgaria up to 3 years of age. II. Influence of education, social group, visit nurseries and the number of children in the family. – *Pediatriya*, **1**, 1991, 79-83. [in Bulgarian].
15. **Felix, R., A. Day, G. Nita, A. Forouhi, K. Ken, A. B. Ong, J. R. B. Perry.** Season of birth is associated with birth weight, pubertal timing, adult body size and educational attainment: a UK Biobank study. – *Heliyon*, **1**(**2**), 2015, Article No: e00031.
16. **Godina, E.,** Dynamics of the processes of human growth and development: spatial-time aspects. Abstract Doctor of Biological Sciences, Moskva, 2001. [in Russian].
17. **Hata, J., T. Ninomiya, Y. Hirakawa, M. Nagata, N. Mukai, S. Gotoh, M. Fukuhara, , F. Ikeda, K. Shikata, D. Yoshida, K. Yonemoto, M. Kamouchi, T. Kitazono, Y. Kiyohara.** Secular trends in cardiovascular disease and its risk factors in Japanese: Half century data from the Hisayama study (1961-2009). – *Circulation,* **128**(**11**), 2013, 1198-1205.
18. **Hughes, M. M., J. Katz, L. C. Mullany, S. K. Khatry, S. C. LeClerq, G. L. Darmstadt, J. M. Tielsch.** Seasonality of birth outcomes in rural Sarlahi District, Nepal: a population-based prospective cohort. – *BMC Pregnancy Childbirth*, **14**, 2014, 310.
19. **Ivanova-Pandourska, I. Y.,** Anthropological characteristics of newborns from Sofia at the beginning of the 21st century. PhD thesis, Sofia, 2005, **199** [in Bulgarian].
20. **Kornafel, D**. Maternal age and birth weight of newborns. – *Studia Antropologiczne*, III, **1823**, 1996, 5-14 [in Polish].
21. **Koupilova, I., K. Rahu, M. Rahu, H. Karro, D. A. Leon.** Social determinants of birth weight and length of gestation in Estonia during the transition to democracy. – *Int. J. Epidemiol.*, **29**(**1**), 2000, 118-124.

22. **Kozlov, A., V. Nuvano, G. Vershubsky.** Changes in Soviet and post-Soviet Indigenous diets in Chukotka. – *Études Inuit Studies*, **31**(**1-2**), 2007, 103-119.
23. **Kozlov, A. I., G. G. Vershubskaya, D. V. Lisitzin.** Long-term changes of anthropometric indicators of children in some ethnic groups, RF. – *Pediatriya*, **87**(**3**), 2009, 63-66 [in Russian].
24. **Kozlov, A., G. Vershubskaya.** Newborn body mass in groups with different degree of urbanization in Perm territory. – *Perm Medical Journal*, **30**(**1**), 2013, 109-113. [in Russian]
25. **Kramer, M. S., R. Kakuma.** Energy and protein intake in pregnancy (Cochrane database of systematic reviews). The Cochrane Library, Issue 4, 2003, pages CD000032. https://doi.org/10.1002/14651858.CD000032.
26. **Lissner, L., K. Mehlig, A. Sjöberg, J. Chaplin, A. Niklasson, KAlbertsson-Wikland.** Secular trends in weight, height and BMI in young Swedes: the 'Grow up Gothenburg' studies. – *Acta Paediatr.*, **102**(**3**), 2013, 314-317.
27. **Marmot, M., R. G. Wilkinson.** Social Determinants of Health. Oxford, Oxford University Press; 2005, 376.
28. **McGrath, J. J., D, Keeping, S. Saha, D. C. Chant, D. E. Lieberman, M. O'Callaghan.** Seasonal fluctuations in birth weight and neonatal limb length: does prenatal vit. D influence neonatal size and shape? – *Early Hum. Dev.*, **81**, 2005, 609-618.
29. **Miklashevskaya, N.** Growth processes in children and adolescents of different ethno-territorial groups of the USSR. PhD thesis, Moscow, 1985, 389 c. [in Russian].
30. **Mladenova, S.** Anthropological characteristics of growth and development of children and adolescents from the Smolyan region in contemporary living conditions. PhD thesis, Plovdiv, 2003 [in Bulgarian].
31. **Mladenova, S.** Influence of some factors on the main indicators of newborns physical development in Smolyan region (1980-2008). – *Anniversary book «Biological Sciences for a Better Future»*, Plovdiv University, 2012, 171-185. [in Bulgarian].
32. **Mueller, C., H. J. Buettner, J. M. Hodgson, S. Marsch, A. P. Perruchoud, H. Roskamm, F. J. Neumann.** Inflammation and long-term mortality after non-ST elevation acute coronary syndrome treated with a very early invasive strategy in 1042 consecutive patients. – *Circulation*, **105**, 2002, 1412–1415.
33. **Oken, E.** Secular trends in birth weight. – *In: Recent Advances in Growth Research: Nutritional, Molecular and Endocrine Perspectives* (Eds. M.W. Gillman, P.D. Gluckman, R.G. Rosenfeld), Nestle Nutr Inst Workshop Ser., Nestec Ltd., Vevey/S. Karger AG., Basel, 71, 2013, 103-114. https://doi.org/10.1159/000342576
34. **Pavlov, Y., N. Slavov, F. Pandurski, N. Danova.** Length and body weight of the newborns after 36 gestational weeks – indicators in maternal age over 30 years. – *Obstetrics and Gynecology*, XXVII, **1**, 1988, 45-49. [in Bulgarian].
35. **Rousham, E., M. Gracey.** Factors affecting birthweight of rural Australian Aborigines. – *Ann. Hum. Biol.*, **29**(**4**), 2002, 363-372.
36. **School, T. O., T. P. Stein, W. K. Smith.** Leptin and maternal growth during adolescent pregnancy. – *Am. J. Clin. Nutr.*, **72**, 2000, 1542-1547.
37. **Schumacher, R. E., S. M. Donn, S. M. Kovarik, D. A. Amato.** The impact of gestational age on dysmaturity/postmaturity. – *J. Perinatol.*, **9**(**4**), 1990, 401-406.
38. **Singh, D. K.** Affecting pre-weaning relative growth rate in Black Bengal kids. – *IVJ,* **79**(**9**), 2002, 948-951.
39. **Spencer, N., S. Logan.** Social influences on birth weight. – *J Epidemiol. Community Health*, **56**(**5**), 2002, 326-327.
40. **Stanimirova, N., L. Peneva, Tz. Baltova.** Physical and pubertal development of Bulgarian children from 0 to 18 years of age. Norms and standard curves. – Sofia, 2007, p. 118 [in Bulgarian].
41. **Takemoto, Y., E. Ota, D. Yoneoka, R. Mori, S. Takeda.** Japanese secular trends in birthweight and the prevalence of low birthweight infants during the last three decades: A population based study. – *Sci. Rep.*, 6, 2016, 31396. doi: 10.1038/srep31396.
42. **Tanner, J. M.** Interaction of heredity and environmental factors in controlling growth. In: *Education and Physical Growth* (Ed. J.M. Tanner), 2nd Edition, London, Hodder and Stoughton, 1978, 90-114.
43. **Taylor, C. M., J. Golding, A. M. Emond.** Adverse effects of maternal lead levels on birth outcomes in the ALSPAC study: a prospective birth cohort study. – *BJOG*, **122**(**3**), 2015, 322-328, doi: 10.1111/1471-0528.12756.

44. **Thornburg, K. L., N. Marshall.** The placenta is the center of the chronic disease universe. – *Am. J. Obstet. Gynecol*., **213**(**40**), 2015, 14-20.
45. **Tretyak, A., E. Godina, L. Zadorozhnaya.** Secular Trends of Sizes at Birth in Russian Infants Born between 1987 and 2002. – *J. Physiol. Anthropol. Appl. Human Sci*, **24**(**4**), 2005, 403-406.
46. **Tustin, K., J. Gross, H. Hayne.** Maternal exposure to first-trimester sunshine is associated with increased birth weight in human infants. – *Dev. Psychobiol.*, **45**(**4**), 2004, 221-230.
47. **Tzirovski, M.** Medical-anthropological study of children from breastfeeding periods and early childhood. PhD thesis, Plovdiv, 1987, p. 298 [in Bulgarian].
48. **Ulijaszek, S.** Secular trend in birthweight among the Purari delta population, Papua New Guinea. – *Ann. Hum. Biol.*, **28**(**3**), 2001, 246-255.
49. **Underwood, J.H.** Sex ratio of live births in Micronesia. – *Am. J. Hum. Biol.*, **7**, 1995 431-435.
50. **Vershubskaya, G. G., A. I. Kozlov.** Approaches to the study of the newborns body dimensions: Scientific schools and „unsolved puzzles". – *Nov. research*, **1**(**18**), 2009, 51-65. [in Russian].
51. **Voigt, M., G. Heineck, V**. **Hesse.** The relationship between maternal characteristics, birth weight and pre-term delivery: evidence from Germany at the end of the 20th century. – *Econ. Hum. Biol.*, **2**, 2004, 265-280.
52. **Vershubskaya, G. G., A. I. Kozlov, Y. A. Kastkina.** Climate and size of the Russian newborns. – *Perm Medical Journal*, XXXIII, №3, 2016, 82-88. [in Russian].
53. **Voorhost, F. J., L. M. Bonter, P. D. Bezemer, P. H. J. Kurver.** Maternal characteristics and expected birth weight. – *Eur. J. Obstet. Gynecol. Reprod. Biol.*, **50**, 1993, 115-122.
54. **Ward, W. P.** Birth weight and economic growth, 2nd edition. – *University of Chicago Press,* Chicago, IL, US, 1993, 240.
55. **Weiler, H., S. Fitzpatrick-Wong, R. Veitch, H. Kovacs, J. Schellenberg, U. McCloy, C. K. Yuen.** Vitamin D deficiency and whole-body and femur bone mass relative to weight in healthy newborns. – *CMAJ,* **172**(**6**), 2005, 757-761.
56. **Wells, J. C., T. J. Cole**. Birth weight and environmental heat load: a between-population analysis. – *Am. J. Phys. Anthropol.*, **119**(**3**), 2002, 276-282.
57. **Wells, J. C. K., M. S. Fewtrell.** Measuring body composition. – *Arch. Dis. Child.*, **91**(**7**), 2006, 612-617.
58. **Wilcox, M. A., S. J. Smith, I. R. Johnson, P. V. Maynard, C. E. Chilvers.** The effect of social deprivation on birthweight, excluding physiological and pathological effects. – *Br. J. Obstet. Gynaecol.,* **102**(**11**), 1995, 918-924.
59. **WHO.** World Health Statistic 1980. – WHO, Geneva, 1980
60. **WHO.** Multicentre Growth Reference Study Group, WHO Child Growth Standards: Length/height-for-age, weight-for-age, weight-for-length, weight-for-height and body mass index-for-age: Methods and development. – WHO, Geneva, 2006.
61. **Yankova, I., Y. Zhecheva.** Secular changes in basic anthropometrical features of neonates and children in early childhood from Sofia. – *Acta morphol. anthropol.*, **19**, 2012, 279-283.

Guidelines for Authors

Acta morphologica et anthropologica is an open access peer review journal and publishes original articles, short communications, reviews, letters to the Editors. The aim of the journal is to provide a forum for cytological, histological, anatomical and anthropological research community in life sciences, including cell biology, immunobiology, pathology, neurobiology, environmental and toxicological research, reproductive biology, pharmacology, physical development and medical anthropology, paleoanthropology, anatomy, paleoanatomy, etc.

Contact details and submission

Manuscripts should be in English with total length not exceeding 10 standard pages, line-spacing 1.5, justified with 2.5 cm margins. The authors are advised to use Times New Roman, 12 pt throughout the text. Pages should be numbered at the bottom right corner of the page. Manuscript submission is electronic only. The manuscripts should be sent to**: iempam@bas.bg and ygluhcheva@hotmail.com**

All correspondence, including notification for Editor's decision, requests for revision, is sent by e-mail. After acceptance of the manuscript a hard copy should be sent to Editorial Office address:

Institute of Experimental Morphology, Pathology and Anthropology with Museum
Bulgarian Academy of Sciences
Editorial Office of Acta morphologica et anthropologica
Acad. Georgi Bonchev Str., Bl. 25
1113 Sofia, Bulgaria

Article structure

The article should be arranged under the following headings: Introduction, Material and Methods, Results, Discussion, Conclusion, Acknowledgements and References.
Title page – includes:

- **Title** - concise and informative;
- **Author(s)' names and affiliations** – indicate the given name(s) and family name(s) of all authors. Present the authors' affiliation addresses below the names. Indicate all affiliations with a lower-case superscript after the author's name and in front of the appropriate address. Provide the full postal address information for each affiliation, including the country name.
- **Corresponding author** – clearly indicate who will handle the correspondence for refereeing, publication and post-publication. An e-mail should be provided.
- **Abstract** – state briefly the aim of the work, the principal results and major conclusions and should not exceed 150 words. References and uncommon, or non-standard abbreviations should be avoided.
- **Key words** – provide up to 5 key words. Avoid general, plural and multiple concepts. The key words will be used for indexing purposes.

Introduction – state the objectives of the work and provide an adequate background, avoiding a detailed literature survey or summary of the results.

Material and Methods – provide sufficient detail to allow the work to be reproduced. Methods already published should be indicated as a reference: only relevant modifications should be described.

Results – results should be clear and concise.

Discussion – should explore the significance of the results in the work, not repeat them. A combined *Results and Discussion* section is often appropriate. Avoid extensive citation and discussion of published literature.

Conclusions – the main conclusions of the study should be presented in a short section.

Acknowledgements – list here those individuals who provided help during the research and the funding sources.

Units – please use the International System of Units (SI).

Math formulae – please submit math equations as editable text, not as images.

Electronic artwork – number the tables and illustrations according to their sequence in the text. Provide captions for them on a separate page at the end of the manuscript. The proper place of each figure in the text should be indicated in the left margin of the corresponding page. **All illustrations (photos, graphs and diagrams)** should be referred to as "figures" and given in abbreviation "Fig.", and numbered in Arabic numerals in order of its mentioning in the manuscript. They should be provided in grayscale as JPEG or TIFF format, minimum 300 dpi. The illustrations should be submitted as separate files.

References – they should be listed in alphabetical order, indicated in the text by giving the corresponding numbers in parentheses. The "References" should be typed on a separate sheet. The names of authors should be arranged alphabetically according to family names. In the reference list titles of works, published in languages with non-Latin alphabet, should be translated, original language must be indicated at the end of reference (e.g., [in Bulgarian]). Articles should include the name(s) of author(s), followed by the full title of the article or book cited, the standard abbreviation of the journal (according to British Union Catalogue), the volume number, the year of publication and the pages cited, for books - the city of publication and publisher. In case of more than one author, the initials of the second, third, etc. authors precede their family names.

For articles: Davidoff, M. S., R. Middendorff, G. Enikolopov, D. Riethmacher, A. F. Holstein, D. Muller. Progenitor cells of the testosterone-producing Leydig cells revealed. – *J. Cell Biol.,* **167**, 2004, 935-944.

Book article or chapter: Rodriguez, C. M., J. L. Kirby, B. T. Hinton. The development of the epididymis. – In: *The Epididymis - from molecules to clinical practice* (Eds. B. Robaire, B. T. Hinton), New York, Kluwer Academic Plenum Publisher, 2002, 251-269.

Electronic books: **Gray, H.** *Anatomy of the human body* (Ed. W.H.Lewis), 20th edition, NY, 2000. Available at http://www.Bartleby.com.

PhD thesis: **Padberg, G**. Facioscapulohumeral diseases. *PhD thesis*, Leiden University, 1982, 130 p.

Website: National survey schoolchildren report. National Centre of Public Health and Analyses, 2014. Available at http://ncphp.government.bg/files

Page charges

Manuscript publication is free of charges.

Ethics in publishing

Before sending the manuscript the authors must make sure that it meets the Ethical guidelines for journal publication of Acta morphologica et anthropologica.

Human and animal rights

If the work involves the use of human subjects, the authors should ensure that work has been carried out in accordance with *The Code of Ethics of the World Medical Association* (Declaration of Helsinski). The authors should include a statement in the manuscript that informed consent was obtained for experimentation with human subjects. The privacy rights of human subjects must always be observed.
All animal experiments should comply with the *ARRIVE guidelines* and should be carried out in accordance with the U.K. Animals (Scientific procedures) Act, 1986 and the associated guidelines *EU Directive 2010/63/EU* for animal experiments, or the National Institutes of Health guide for the care and use of Laboratory animals (NIH Publications No. 8023, revised 1978) and the authors should clearly indicate in the manuscript that such guidelines have been followed.

Submission declaration

Submission of the manuscript implies that the work described has not been published previously, is not considered under publication elsewhere, that its publication is approved by all authors, and that if accepted, it will not be published elsewhere in the same form, in English or in any other language, including electronically, without the informed consent of the copyright-holder.

Contributors

The statement that all authors approve the final article should be included in the disclosure.

Copyright

Upon acceptance of an article, the authors will be asked to complete a "Journal Publishing Agreement". An e-mail will be sent to the corresponding author with the Journal Publishing Agreement Form or a link to the online version of this agreement.

Peer review

This journal operates a single blind review process. All contributions will be initially assessed by the Editor for suitability for the journal. All suitable papers are then sent to two independent expert reviewers to assess the scientific quality of the paper. The Editor is responsible for the final decision regarding acceptance or rejection of articles.

After acceptance

Proof correction

The corresponding author will receive proofs by e-mail in PDF format and will be requested to return it with any corrections within a week.

Offprints

The journal provides free access to all papers in each volume that can be downloaded from the following website: http://www.iempam.bas.bg/journals/acta.html